THE PLASMA PHYSICS OF SHOCK ACCELERATION

FRANK C. JONES

Laboratory for High Energy Astrophysics, NASA/Goddard Space Flight Center, Greenbelt, MD 20771, U.S.A.

and

DONALD C. ELLISON

Department of Physics, North Carolina State University, Raleigh, NC 27695–8202, U.S.A.

(Received January 7, 1991)

Abstract. The notion that plasma shocks in astrophysical settings can and do accelerate charged particles to high energies is not a new one. However, in recent years considerable progress has been achieved in understanding the role particle acceleration plays both in astrophysics and in the shock process itself. In this paper we briefly review the history and theory of shock acceleration, paying particular attention to theories of parallel shocks which include the backreaction of accelerated particles on the shock structure. We discuss in detail the work that computer simulations, both plasma and Monte Carlo, are playing in revealing how thermal ions interact with shocks and how particle acceleration appears to be an inevitable and necessary part of the basic plasma physics that governs collisionless shocks. We briefly describe some of the outstanding problems that still confront theorists and observers in this field.

1. Introduction

One of the most striking aspects of the tenuous plasmas common in astrophysics is that they often contain particle populations which are not in thermodynamic equilibrium. Nonthermal populations, often with power-law distributions, are observed either directly or by inference (i.e., from radiative properties) in most low-density environments. The most exceptional example of this is the galactic cosmic-ray distribution which extends from MeV energies to above 10^{20} eV! The highest energy cosmic rays are, by far, the most energetic particles known in the Universe, and energies this high have not occurred elsewhere since the temperature in the early universe dropped below $\sim 10^{24}$ K (about 10^{-28} s after the Big Bang). In a low-density environment, particles 'scatter collisionlessly' against magnetic turbulence rather than against other particles and the scattering can be nearly elastic in the plasma frame. Particles are forced to equilibrate with the collective body of particles held together by the nearly frozen-in magnetic field rather than with each other, and individual particle energies can become extremely large. Nonthermal particle distributions can develop and persist for long times.

Tenuous astrophysical plasmas differ from laboratory plasmas in another important way; in most environments where energetic populations are observed, typical sound speeds are considerably less than easily obtainable bulk flow velocities, and shocks are expected to develop. In fact, *shocks are associated with most energetic particle populations seen in astrophysics*. The exceptions include pulsar magnetospheres, the aurorae, and sites where magnetic reconnection occurs (although shocks may be important in recon-

Space Science Reviews **58:** 259–346, 1991.

nection as well). The dominance of collective field-particle processes means that, unlike terrestrial shocks, the dissipation mechanism in astrophysical shocks is almost always collisionless. In the heliosphere, collisionless shocks are directly observable with spacecraft and they have received considereable attention. In every case where direct observations has been made, shocks are seen to accelerate particles, often to power-law distributions. Observations of heliospheric shocks, along with a great deal of theoretical and simulation work, also show that field-particle interactions control the shock dissipation and structure. Furthermore, initial results from large-scale plasma simulations suggest that not only is particle acceleration likely to accompany collisionless shocks, but that the injection and acceleration of ambient particles may even be *essential* for dissipation in quasi-parallel shocks and high Mach number quasi-perpendicular shocks*. The plasma physics of shock dissipation and particle acceleration seem to be intimately related.

The promise of shock acceleration as a 'universal' acceleration mechanism has prompted a great deal of work in he past decade or so and we refer readers to several reviews for a full theoretical and observational background, including source references (Toptyghin, 1980; Axford, 1981; Drury, 1983; Völk, 1984, 1987; Forman and Webb, 1985; Scholer, 1985; Blandford and Eichler, 1987; Berezhko and Krymskii, 1988; Onsager and Thomsen, 1991). In this review, we give a critical discussion of several important aspects of shock acceleration theory including hydrodynamic analytic methods, computer simulations, and particle acceleration in oblique shocks.

In the remainder of this section we list, starting from the Earth and moving outward, energetic particle populations and the evidence for associated shock waves. In Section 2 we give a brief history of the notion that astrophysical shocks could be responsible for producing high-energy particles, starting with a 'pre-history' in the 1940's and continuing through the beginning of the 'Modern Era' of the 1970's. In Section 3 we review the test particle theories of shock acceleration including the diffusion-convection equation approach and the individual particle approach. Section 4 takes up the nonlinear aspects of shock acceleration, namely the way in which the accelerated particles produce (or help to produce) the turbulence that is necessary for diffusive shock acceleration† to work and the way in which the accelerated particles can modify the shock structure itself when their pressure becomes dynamically important. In Section 5 we discuss some of the problems that are peculiar to acceleration in oblique and quasi-perpendicular shocks, primarly the complexities that develop in the shock structure itself.

Section 6 contains the 'main message' of this review. In this section we discuss the work that is being carried out by many workers, including the present authors, in studying the process of shock formation and particle acceleration with computer simu-

* We use the term quasi-parallel to mean shocks with normals within approximately 45° of the magnetic field direction while quasi-perpendicular means shocks with normals greater than 45° to the magnetic field direction. The term oblique will be applied to any shock which is not strictly parallel or perpendicular.

† In most cases, the terms diffusive shock acceleration and first-order Fermi shock acceleration are used interchangeably. The only situations where a distinction needs to be made are those, such as thermal particle injection and relativistic shocks, where the diffusion approximation is not appropriate.

lations. Here we argue that, invaluable as past analytic work has been, it is only through the highly nonlinear work of computer simulation (strongly coupled to space observations) that the real secret of the plasma physics of shock acceleration is being revealed. This secret is, we believe, that not only is the acceleration of particles to strongly non-thermal energies an inevitable product of a plasma shock, it is in many cases *an essential part of the shock formation process itself*. For high Mach number shocks at least, accelerating particles to superthermal energies is the primary dissipation process that is necessary for the shock to exist. If the acceleration of charged particles by plasma shocks did not exist the shocks would have had to invent it. The paper ends with brief conclusions in Section 7.

1.1. Astrophysical shock waves

1.1.1. *The Earth's Bow Shock*

The Earth's bow shock region offers our best laboratory for studying collisionless plasmas and shocks and a great deal has been learned here since the advent of *in situ* spacecraft observations. Perhaps most importantly, the discovery of the bow shock proved that collisionless shocks do, in fact, exist (Sonett and Abrams, 1963; Ness *et al.*, 1964). The upstream (or foreshock) region of the bow shock contains energetic particles, as well as a great deal of magnetic wave activity. The different geometric shock configurations (from quasi-perpendicular to quasi-parallel) show quite different particle and magnetic field behavior. Energetic particles observed upstream of the quasi-perpendicular bow shock have been modeled successfully by assuming that some fraction of the incoming solar wind 'reflects' off the steep magnetic field gradient (e.g., Sonnerup, 1969; Ipavich *et al.*, 1988). The so-called diffuse ion population observed near the quasi-parallel bow shock is modeled extremely well by assuming that the solar wind is shock accelerated as predicted by the first-order Fermi mechanism (see Edmiston *et al.*, 1982; Lee, 1982; and Ellison and Möbius, 1987, and references therein) which we discuss in detail below. In general, bow shock observations and modeling clearly show that collisionless shocks can accelerate particles, that the acceleration process is intimately associated with magnetic field activity, and that models of the process of injection and acceleration at both the quasi-perpendicular and quasi-parallel shock are reasonably close to reality. Of course, other particle populations which are not shock accelerated may be present, as is the case when magnetospheric particles leak out into the foreshock region (e.g., Scholer *et al.*, 1981), but these populations have properties, such as charge state and a burst-like time signature, which make them clearly distinguishable from the shock associated energetic particles (see Möbius *et al.*, 1986; Fuselier *et al.*, 1991). Of particular importance is the observation that thermal solar wind ions can be directly injected and accelerated at the quasi-parallel shock (Ellison *et al.*, 1990b); no separate superthermal seed population of ions is necessary for Fermi acceleration to work. The actual details of injection are, however, still uncertain and may involve stochastic processes in the turbulent shock layer (e.g., Gosling *et al.*, 1989).

1.1.2. *Solar Flares and Interplanetary Traveling Shocks*

Solar flares and interplanetary traveling shocks represent two more cases where shocks and associated energetic particles have been observed or inferred. Solar flare explosions most likely result when magnetic field energy, stored in the twisted surface fields, is suddenly released presumably via magnetic reconnection. Energetic particles and shocks (as evidenced by various emissions including type II radio observations; e.g., Cane and Reames, 1988, and references therein) are produced in the corona and these shocks are believed to further accelerate ions and electrons to extremely high energies (see Forman *et al.*, 1986; and Chupp, 1990, for reviews). Solar energetic particle (SEP) events have been divided into impulsive (duration $\lesssim 1$ hr) and gradual (duration > 1 hr) flares. Besides timing, the two classes show distinct differences in electron spectral shapes, electron to proton ratios, abundances of heavy elements, and other characteristics (see report on solar flare workshop held at the University of Tasmania, January 24–26, 1990, by B. Klecker, *EOS*, p. 1102, September 25, 1990). Stochastic (i.e., second-order Fermi) and shock acceleration are the most likely processes for accelerating flare particles after the initial energy deposition. Gamma-ray emission, believed produced by energetic ions in the solar corona, and bremsstrahlung emission, believed produced by relativistic electrons, have been successfully modeled using stochastic acceleration in the high Alfvén velocity magnetic field close to the exploding flare loop (Miller and Ramaty, 1989; Hua *et al.*, 1989). On the other hand, spectra of energetic particles seen in space can often be fit extremely well with first-order Fermi acceleration. Ellison and Ramaty (1985) show that simple test-particle Fermi acceleration can match electron, proton, and alpha particle spectral shapes extending from 100 keV to 100 MeV (100 MeV nucl^{-1} for alphas) with reasonable coronal shock compression ratios. Recently, Lockwood *et al.* (1990a, b) compare proton spectra from 20 MeV to 10 GeV obtained by the IMP spacecraft and the worldwide network of neutron monitors to stochastic and first-order Fermi acceleration predictions and conclude that these spectra are consistent with Fermi acceleration.

The interplanetary travelling shocks (IPSs), which also result from solar flares and travel out past the Earth, have been directly observed by a number of spacecraft. In general, fast quasi-parallel IPSs are seen to be efficient particle accelerators which, because of their large size, can accelerate thermal solar wind ions to energies above 2 MeV (e.g., Gosling *et al.*, 1981; Cane *et al.*, 1990), well above energies seen in the diffuse ion population at the Earth's bow shock (see Lee, 1983; and Lee and Ryan, 1986, for theoretical discussions). The large shock radius of IPSs (compared to the small Earth bow shock) allows a power-law spectrum to develop which is consistent with the predictions of first-order Fermi acceleration. Recent work by Reames (1990), Cane and Reames (1988), and Cane *et al.* (1988) has shown that a consistent picture of the acceleration and transport of particles can be found in which large 'solar proton events' are dominated by material accelerated directly from the solar wind by the traveling shock. This is true of both high- and low-energy particles and is consistent with previous detailed studies of a single large interplanetary event (i.e., Kennel *et al.*, 1984, 1986). Quasi-perpendicular IPSs are also observed to accelerate particles and this has been

modeled with shock drift acceleration theory (see Armstrong *et al.*, 1985, for a review and references to relevant observations). While strong intensity enhancements are often observed at quasi-perpendicular IPSs, and debate on the relative importance of Fermi versus shock drift acceleration continues, we feel that observations generally show that quasi-parallel IPSs are more efficient and produce higher energy particles (e.g., Reinhard *et al.*, 1983; Sanderson *et al.*, 1983). As with the Earth's bow shock, quasi-parallel IPS observations are, in general, consistent with first-order Fermi acceleration in the turbulent magnetic fields near the shock while shock drift acceleration, which occurs when a particle gains energy by drifting in the induced electric field along the shock surface, may well explain particle acceleration when the shock is quasi-perpendicular.

1.1.3. *Cometary Shocks*

Cometary shocks have been observed by spacecraft at Comet Halley and possibly at comet Giacobini–Zinner. Comet Halley shows clear evidence for particle acceleration at the plasma shock formed when outgassed material is ionized in the solar wind. The accelerated populations have been analyzed with models containing a combination of first- and second-order Fermi acceleration (e.g., Gombosi *et al.*, 1989). The evidence for a shock and associated particle acceleration is less convincing in Giacobini–Znner (Tranquille *et al.*, 1986), but energetic ions are seen and ion flow deflection may indicate a shock (Hynds *et al.*, 1986).

1.1.4. *Corotating Interaction Regions*

Corotating interaction regions consist of a pair of forward and reverse shocks formed when a fast solar wind stream overtakes a slower solar wind stream. These shock pairs have been observed by spacecraft and energetic particles are associated with them. Fisk and Lee (1980) have shown that the energetic particles can be understood in terms of Fermi acceleration combined with adiabatic losses.

All of the shocks we have discussed thus far, with the sole exception of solar corona shocks, have been directly observed by spacecraft. Furthermore, the indirect evidence for corona shocks is extremely convincing. As we move outward from the Sun, the evidence for shocks and accompanying particle acceleration becomes much less direct. However, in all the cases we will discuss, shock acceleration remains a likely mode of particle acceleration given the state of current observations.

1.1.5. *Solar Wind Termination Shock*

A solar wind termination shock is expected to form when the ram pressure of the supersonic solar wind drops to the value of the interstellar thermal pressure. When pressure balance occurs, the highly supersonic solar wind will be decelerated in a strong shock. Original estimates of the position of this shock were relatively close in (< 50 AU) but the termination shock has not yet been crossed by the Pioneer and Voyager spacecraft which have reached ~ 50 AU. The solar wind is weak compared to the winds of more massive hot stars which may contribute to the production of galactic cosmic rays or at least serve as injectors providing energetic seed particles which are later

accelerated to cosmic-ray energies (e.g., Shapiro, 1990). The solar wind termination shock may also be responsible for accelerating the so-called *anomalous component* of cosmic rays. These particles are believed to originate as neutral interstellar atoms which enter the heliosphere and are subsequently ionized and accelerated at the nearly perpendicular termination shock (e.g., Pesses *et al.*, 1981; Jokipii and Kóta, 1990).

1.1.6. *Shocks Near Stellar Size Compact Objects*

Shocks near stellar size compact objects such as accretion shocks onto X-ray binaries or pulsar wind termination shocks represent an increasingly speculative environment where shock acceleration may occur. X-ray binaries are believed to be star systems where at least one of the stars is a neutron star. Ultrahigh energy (UHE) gamma radiation up to 10^{16} eV has been reported from several X-ray binaries (e.g., Samorski and Stamm, 1983; Lloyd-Evans *et al.*, 1983) and this has been explained by energetic ions interacting with matter within the binary system (e.g., Eichler and Vestrand, 1985). For 10^{16} eV gamma rays to be produced, ions with at least 10^{17} eV must be accelerated. While no acceleration mechanism has been proposed which can easily explain these high energies and which does not have formidable difficulties, shock acceleration has been suggested (e.g., Kazanas and Ellison, 1986b), as have pulsar mechanisms (e.g., Chanmugam and Brecher, 1985). Hillas and Johnson (1990) give a good discussion of the difficulties various acceleration mechanisms have producing such energies in these systems. Recently, neutral particles have been reported from Cygnus X-3 at $\sim 10^{18}$ eV (Cassiday *et al.*, 1989). These may be neutrons, resulting from collisions with UHE protons accelerated near the neutron star and ambient nucleons or even photons. If these observations are confirmed, they would clearly indicate particle acceleration to nearly maximum cosmic-ray energies in compact X-ray binaries (see Hillas, 1984a, b) and these energetic particles may be the result of shock acceleration. A cautionary note on these high-energy gamma-ray observations must be made. As this paper is being written, no source, other than the Crab nebula, is currently being detected in gamma rays above 10^{12} eV (see proceedings of the ICRR Symposium on the Astrophysical Aspects of the Most Energetic Cosmic Rays, Kofu, Japan, 1990).

While pulsar wind termination shocks have not been observed and no clear relationship exists between particle acceleration or UHE radiation from such shocks, pulsars are believed to emit highly relativistic $e^- - e^+$ winds (Rees and Gunn, 1974; Kennel and Coroniti, 1984) which might, upon interaction with the supernova remnant, produce highly relativistic shocks. Recent work (e.g., Gaisser *et al.*, 1987; Harding and Gaisser, 1990) assumes that the first-order Fermi mechanism produces energetic particles at these shocks, and expected γ-ray fluxes have been calculated. However, if Fermi acceleration does occur, the relativistic theory must be used in these extremely high-speed shocks (e.g., Peacock, 1981; Kirk and Schneider, 1987a, b; Ellison *et al.*, 1990a).

1.1.7. *Supernova Remnants and Galactic Cosmic Rays*

Supernova remnants (SNRs) are currently believed to be the primary sources of galactic cosmic rays having energies below $\sim 10^{14-15}$ eV. SNRs have the necessary power and the Fermi shock acceleration mechanism can provide the observed spectrum (see Axford, 1981, for a review). In addition, even though SNRs are far removed from *in situ* observation they nevertheless show clear evidence for shock acceleration. Relativistic electrons are believed responsible for the radio synchrotron emission seen in shell-like SNRs. In some cases, the radio emission forms a thin shell-like structure which is believed to coincide with the outward moving blast wave. Radio spectral indexes have been measured for about 200 SNRs and they show a mean value near 0.5 (i.e., $S_\nu \sim \nu^{-0.5}$) with a relatively small spread ($\sim \pm 0.2$), implying an underlying electron spectrum with energy power-law exponent ~ -2 (e.g., Clark and Caswell, 1976; Green, 1984; see Reynolds, 1988, for a review). This power-law index is very close to the inferred source spectrum of galactic cosmic rays, and is part of the circumstantial evidence linking SNRs with the production of cosmic rays. However, as the above average implies, many remnants show radio spectra flatter than an E^{-2} electron spectrum would produce, and other effects, such as adiabatic compression of pre-existing cosmic-ray electrons in large (i.e., old) remnants where radiative cooling allows large compression ratios, may be important.

Many SNRs are also observed in X-rays. The X-ray emission is believed to be produced by hot ($\sim 10^7$ K) shock-heated gas and is further evidence that the blast wave shock is real. In some examples such as Tycho's SNR, the radio and X-ray profiles are extremely similar, providing further circumstantial evidence that the relativistic electrons and the hot gas are produced together, presumably by the expanding shock.

The cosmic rays with energies above 10^{15-16} eV are not easily explained by current acceleration mechanisms (Lagage and Cesarsky, 1983). These high-energy particles contain a tiny fraction of the energy so power requirements are small, however, the acceleration time for first-order Fermi acceleration becomes longer than the remnant age as energies surpass $\sim 10^{14}$ eV. It has been suggested that shock acceleration times can be significantly shortened in quasi-perpendicular shocks (Jokipii, 1987; Ostrowski, 1988) and since most of the surface area of a SNR can be expected to be quasi-perpendicular rather than quasi-parallel, this may overcome acceleration time limits.

As just mentioned, cosmic rays below $\sim 10^{14}$ eV show a power-law spectrum with index (after adjustment for energy-dependent escape from the galaxy) of ~ 2. Just such a power law comes naturally from the simplest form of Fermi shock acceleration and this, coupled with the fact that spectra $\sim E^{-2}$ are seen in other sources, has led to much of the initial excitement over shock acceleration. Above $\sim 10^{15}$ eV, however, the observed cosmic-ray distribution steepens to $\sim E^{-3}$ and maintains a good power law to $\sim 10^{19}$ eV. While much speculation has been made concerning the source of these highest-energy particles, their origin remains one of the great unsolved mysteries in astrophysics.

1.1.8. *The Galactic Wind Termination Shock*

The galactic wind termination shock is analogous to the solar wind termination shock and should result when the supersonic galactic halo outflow, produced by supernova explosions, comes into pressure balance with the intergalactic medium. Because of its extremely large size, the termination shock may be able to accelerate particles to the highest cosmic-ray energies (i.e., above 10^{19} eV) and models of this process have been presented (Jokipii and Morfill, 1985). However, the very existence of the shock is still being debated and critical parameters for acceleration are completely unknown and unlikely to be found in the conceivable future.

1.1.9. *Shocks Associated with Active Galactic Nuclei*

Active galactic nuclei (AGNs) and quasars move our frame of reference even further beyond the solar system. However, unlike the purely speculative galactic wind termination shock, AGNs are known to produce strongly non-thermal particle populations and conditions are such that shocks are likely to occur. While most of the work on AGN emission has focused on accretion disks which produce mainly thermal radiation, it seems fair to say that the broad-band emission generally seen in these objects (AGNs emit roughly equal energy per decade, i.e., per $d \log_{10} E$, from radio to X-ray and sometimes γ-ray energies) argues for an accelerated particle component. It is also likely that shocks will form in the strongly supersonic flows expected near the massive black hole either inside of the accretion disk or possibly outside the disk in a nearly spherical shock if little angular momentum is present (e.g., Blandford and McKee, 1977; Mészáros and Ostriker, 1983). In any case, strong broad-band radiation over many (10–12) energy decades suggests that quasi-thermal accretion disks cannot be responsible for all of the emission, and first-order Fermi particle acceleration in accretion shocks has been suggested as a way of converting the gravitation potential energy into energetic ions and then, through particle-particle collisions, into radiation (Kazanas and Ellison, 1986a; Zdziarski, 1986). We note that there seems to be no conceptual difficulty in having both an accretion disk and shocks producing energetic particles in the central engine.

1.1.10. *Extra-Galactic Radio Jets*

Extra-galactic radio jets offer another possible location of particle acceleration in shocks (see Begelman *et al.*, 1984, for a review). The observed superluminal motion in some jets clearly implies that highly supersonic flows exist in these sources and it is likely that strong shocks will form at the working surface between the jet and the intergalactic medium (e.g., Witzel *et al.*, 1988). The sharp near-infrared cutoffs seen in the continuous spectra of some jets have been modeled with first-order Fermi shock acceleration limited by synchrotron and photon interactions (Biermann and Strittmatter, 1987). The shock models appear to be consistent with the spectral observations and suggest that jets may be capable of accelerating nuclei to the highest cosmic-ray energies (e.g., Hillas, 1984b).

The above list confirms our assertion that a vast array of astrophysical environments are likely sources of collisionless shocks. In what follows, we present some of the

evidence supporting the contention that shocks naturally produce energetic particles with high efficiencies.

2. Brief Historical Review

2.1. Early ideas on shock acceleration

Although the current interest in plasma shocks as accelerators of charged particles dates back to 1977, the idea that shocks could be a source of energetic particles is considerably older than that. Even though many of the early notions about the detailed mechanism of shock acceleration have not turned out to be viable, some of these ideas have shown a surprising durability and play an important role in current theories.

– Darwin. Perhaps the earliest suggestion that shock waves were responsible for accelerating cosmic rays came from Sir Charles Darwin (1949). Starting with a discussion of the pitting of marine propellers by cavitation in the water, Darwin noted that hydrodynamics could lead to regimes where a few particles could be accelerated to extreme energy. He then applied this idea to turbulence in the solar atmosphere and from this to the suggestion that cosmic rays might be accelerated by this process. He pointed out that the solar surface manifested such phenomena as flares and prominences and that 'from some of them will spurt out spray, which occasionally will have very high velocities indeed'. Darwin suggested that even if this process could not produce the cosmic rays directly it could act as the injector to Fermi's (1949, 1954) statistical acceleration mechanism.

This notion of a hydrodynamic wave steepening until it breaks and spews out a froth of energetic particles clearly prefigures the ideas set out some eleven years later by Colgate and Johnson (1960). It should be noted that in this paper, Darwin pointed out the phenomenon of 'equipartition of velocity rather than energy' that is characteristic of such shock processes. This concept is, today, an important ingredient of current shock acceleration ideas as it leads to a preferred injection of heavy nuclei into the accelerator.

– Parker (1958a) noted that the turbulent gas motions of the galactic disk and halo were approximately Mach one when the pressure of the cosmic rays was included in computing the speed of sound (the Mach number is the ratio of the fluid flow speed to the local sound speed). He proposed that this was no accident, rather it was an example of a self-regulating system: if the cosmic-ray energy density were too low the motions would steepen into shock waves which would accelerate more cosmic rays. On the other hand when the cosmic-ray energy density is high enough to make the motions Mach one the shocks fade and there is no more acceleration. This was named the 'Mach One Effect'. In Parker's work, however, the shocks were considered to be the moving irregularities that produced second-order Fermi acceleration. Parker (1961) also suggested that particles reflecting off a parallel shock could generate plasma waves via the firehose instability in an upstream precursor. These waves would then convect back into the shock and help provide dissipation. We show below that this idea has received considereable support from recent plasma simulation work.

– Colgate and Johnson (1960) proposed that cosmic rays are the last fraction of the atmosphere of a star that has undergone a supernova explosion. The shock travelling upward through an ever decreasing density would achieve relativistic velocities and impart high energies to the last particles that were shocked. In their model the energy spectrum depended on the density versus radius function of the exploding star, this being derived from the equations of radiative-hydrodynamic stability and produced a differential spectrum that was an inverse power law. The power-law exponent they found was equal to -3, somewhat steeper than observed but considering the complexity of the derivation it was, perhaps, closer to observation than one might have imagined.

– Hoyle (1960) considered the case in which a considerable portion of the momentum and energy of a gas through which a shock is passing is carried by relativistic particles. He pointed out that in this situation the ratio of specific heats, γ, can approach a value of $\frac{4}{3}$ and the compression ratio can approach 7 rather than $\frac{5}{3}$ and 4, respectively, for a nonrelativistic gas. The increased compression can result in a large increase in particle energy and he gives an example of the cosmic-ray gas in which a 23-fold increase in particle energy results for a shock speed of 10^8 cm s^{-1}. This appears to be essentially the 'cosmic-ray dominated' shock of the two-fluid approach to shock acceleration that we will discuss in Section 4.2.

– Schatzman (1963) considered particles traversing a shock and was able to deduce that a power-law energy spectrum would result. He found that on one traversal of the gyro-orbit the magnetic moment was approximately conserved (as did Parker, numerically; see above) and when scattering was added, he obtained a power-law spectrum, but not with the simple exponent obtained in later work.

– Fisk (1971) was first to note that a shock propagating through a diffusive medium would accelerate particles by scattering the particles with converging scattering centers. However, he applied this approach to a particular class of events observed at travelling interplanetary shocks, hence, the generality of the method was not noticed. Also, Fisk did not obtain the, now well-known, result that the spectrum of the accelerated particles depends on the shock's compression ratio, r, as

$$N \sim p^{-\sigma}, \tag{2.1}$$

where N is the particle density in space and scalar momentum, p, and $\sigma = (r + 2)/(r - 1)$ is the spectral index.

2.2. 'Modern era' of shock acceleration

The important breakthrough in understanding shock acceleration occurred in 1977–1978 when a series of independent papers showed how a power-law momentum spectrum of accelerated particles results from very general properties of a plasma shock travelling through a medium in which energetic particles were diffusing (Axford *et al.*, 1977; Krymsky, 1977; Bell, 1978a, b; Blandford and Ostriker, 1978). These papers showed that the steady-state power-law spectrum that resulted was:

– independent of the injection spectrum, provided the injection spectrum was steeper than the resultant spectrum shown above (i.e., Equation (2.1)),

– independent of the details of the scattering process as long as the distribution function of the accelerated particles could be considered isotropic to first order, and

– independent of the shock geometry if the diffusion scale was smaller than any curvature of the shock front but larger than the shock thickness.

The property that gave this process a wide appeal was the fact that, with the simplest assumptions, the particle spectrum depended only on the compression ratio of the shock and most astrophysical shocks, since they are strong, have compression ratios that are constrained to a rather narrow range of values near $r = 4$ (assuming $\gamma = \frac{5}{3}$). For shocks with Mach numbers greater than 4 say, $3.4 < r < 4$ and $2 < \sigma < 2.3$ (Figure 2.1). A

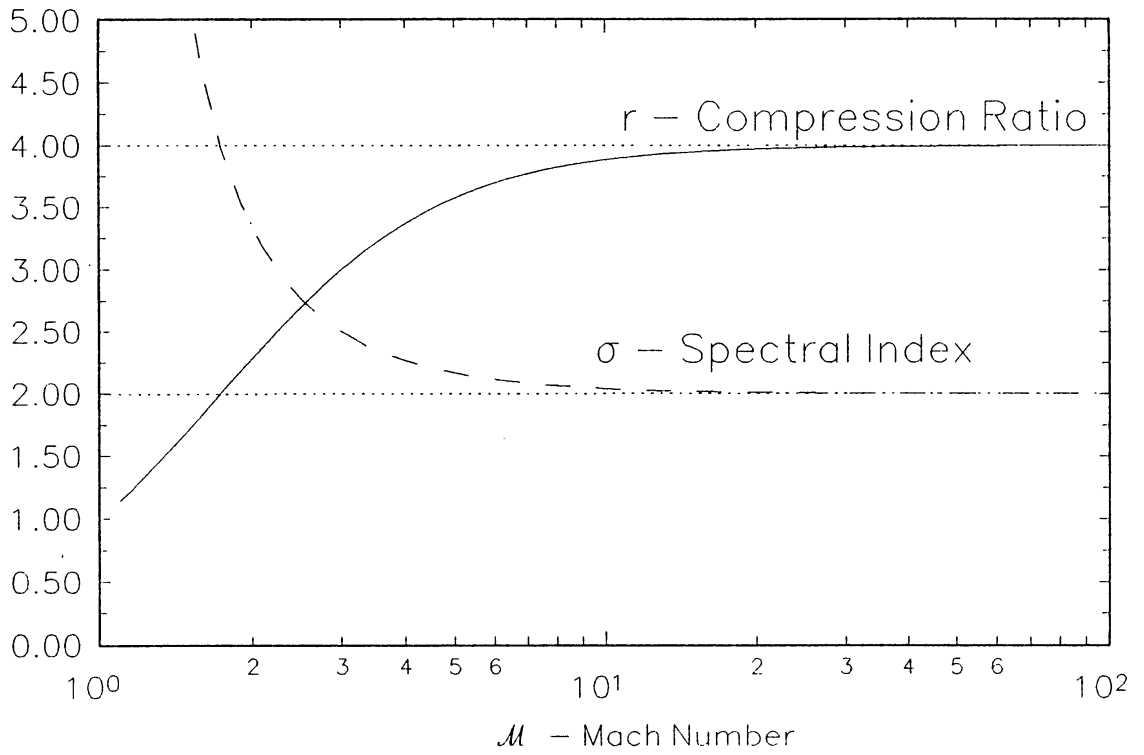

Fig. 2.1. A plot of the compression ratio, r, and the spectral index, σ, versus the Mach number, $\mathcal{M}$, for a simple gas shock in a monatomic, non-relativistic gas with $\gamma_g = \frac{5}{3}$.

spectral index of $\sigma \simeq 2$ is characteristic of energetic particle spectra observed in a wide range of astrophysical environments and, in particular, closely fits the inferred source spectrum of galactic cosmic rays for energies below approximately 10^{15} eV. The dependence of r and σ on Mach number are shown in Figure 2.1 for a shock in a gas with a ratio of specific heats, $\gamma = \frac{5}{3}$. The approach of Axford *et al.* (1977), Krymsky (1977), and Blandford and Ostriker (1978) was to obtain the accelerated particle distribution function by solving the simple one-dimensional diffusion-convection equation with a flow discontinuity representing the shock transition. They obtained power-law momentum spectra whose exponent depended only on the velocity jump across the shock. Bell (1978a, b), on the other hand, employed an equivalent individual particle kinetic approach to obtain the distribution function. In addition, Bell went further and derived the upstream diffusion coefficient from the Alfvén wave generation produced

by the counter streaming of the accelerated particles. In this sense, Bell's work was the first 'self-consistent' treatment of the scattering process in shock acceleration.

3. Test Particle Theories of Shock Acceleration

Much, but not all, of the work done on the theory of shock acceleration in the late 1970's employed the test particle approach in which the plasma shock was taken as a 'given' phenomenon and certain selected or 'test' particles were allowed to interact with it. The test particles can be represented by their distribution function, and their collective interaction with the flowing plasma can be described by the diffusion-convection equation. On the other hand, the test particles can be described as individual particles and one can investigate the details of how each particle interacts with the shock over a period of time. In either case, the distinguishing characteristic is that the particles are *test* particles; they are acted on by the plasma but they do not react back to modify the plasma flow or shock in any way.

As we shall see, the two methods give essentially the same results so we may consider them to be equivalent. What they do not do is show the way in which the accelerated particles themselves enter into the plasma physics of the shock process itself. In some cases, it will turn out that the acceleration of some fraction of the plasma to superthermal energies will be an important, if not the primary, dissipative mechanism responsible for producing the shock. It should not be surprising for the dissipative process in a *collisionless* shock, where charged particles interact via long-range, collective plasma processes, not to result in an immediate thermalization of the free energy. Rather, the energy would be given to a few of the particles by an acceleration process and only later would this energy be thermalized by the much slower particle-particle collision process.

3.1. General orientation, coordinate system, etc.

Before taking a more detailed look at shock acceleration theories we should take a brief look at the basic notion of a plasma shock; what it is and how it is described. We shall examine a simple set of equations that describe a shock and agree on a basic coordinate system that will be employed in the remainder of this paper.

3.1.1. *Basic Coordinate System*

In Figure 3.1 we show the simplest picture of a shock that one could draw; the shock is viewed in its own rest frame, a fluid flows in from the left with a velocity u_1 out to the right with a velocity u_2. (We will sometimes use the word velocity where the directionless word speed would be more rigorously correct, however, the distinction will usually be unnecessary and no confusion should arise from this practice.) The flow is from the $-x$-direction and proceeds in the $+x$-direction. At $x = 0$ the flow speed changes abruptly (a shock) from u_1 to a slower speed, u_2, and then continues to $x = +\infty$ (in the remainder of this paper we shall adhere to the convention that the subscript 1 shall refer to quantities measured aysmptoticly upstream and 2 to those measured asymptoticly downstream). The only coordinate of interest is the x-coordinate and

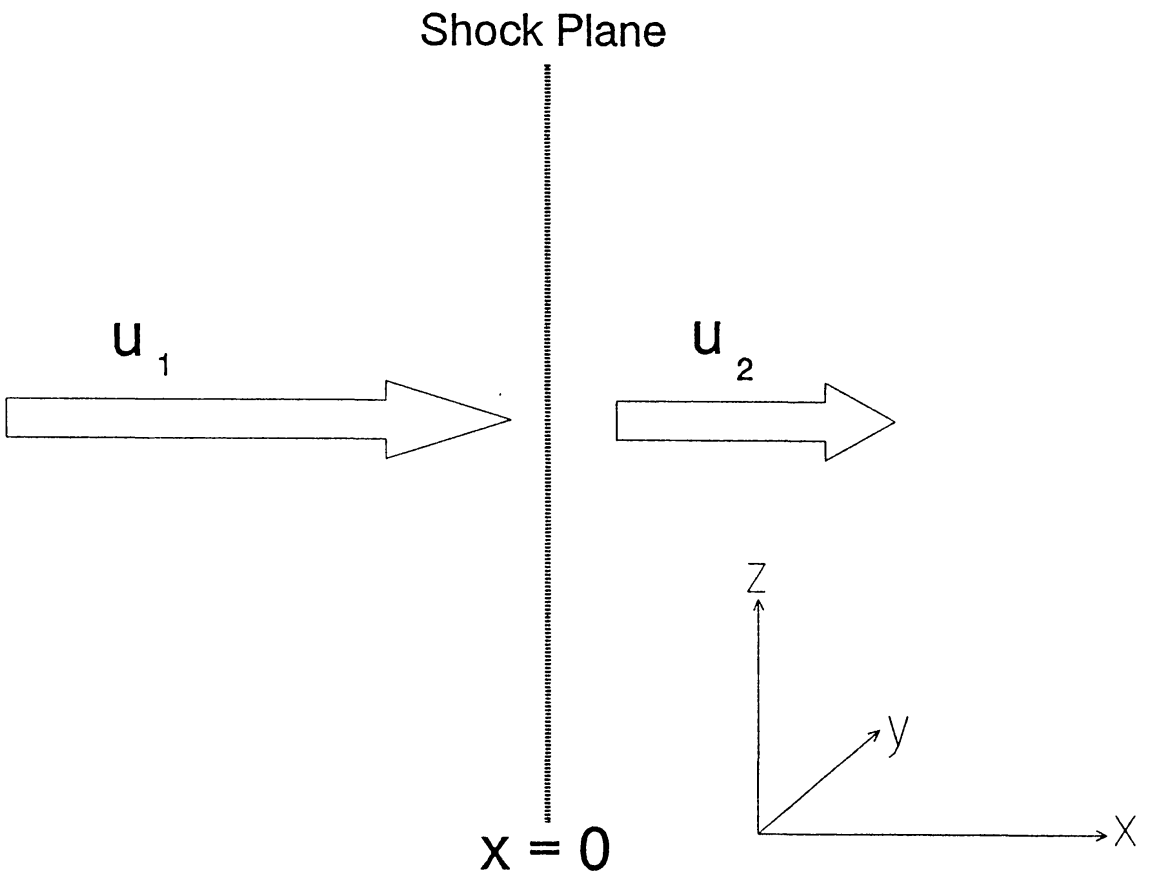

Fig. 3.1. The basic coordinate system that will be used in this paper. Plasma flows in from $x = -\infty$ with velocity u_1 and passes through the shock, which is stationary in this frame, at $x = 0$. Plasma leaves the shock with velocity u_2 and flows to $x = +\infty$.

though we shall later expand this simple scheme to include oblique flows and magnetic fields it will remain true that *all variation will be in the x-direction only*, the shock will thus constitute an infinite plane normal to the x-axis. This will essentially limit us to a consideration of one-dimensional shock models and though we will not treat higher-dimensional models directly, we will note those areas where such considerations could change or affect the results.

3.1.2. *Rankine–Hugoniot Relations*

In a simple, steady-state hydrodynamic picture of a plasma shock, the state of ionization of the gas is irrelevant and we may therefore think of it as a simple fluid; we may write three equations that describe the conservation of the flux of mass, momentum, and energy as the fluid moves along the x-axis.

$$\frac{\partial(\rho u)}{\partial x} = 0 \quad \text{mass flux}, \tag{3.1}$$

$$\frac{\partial}{\partial x}(\rho u^2 + P) = 0 \quad \text{momentum flux}, \tag{3.2}$$

$$\frac{\partial}{\partial x}\left(\frac{1}{2}\rho u^3 + \frac{\gamma_g}{\gamma_g - 1} uP\right) = 0 \quad \text{energy flux}, \tag{3.3}$$

where ρ is the mass density, P is the pressure of the gas, and γ_g is the ratio of specific heats ($= \frac{5}{3}$ for a monoatomic, non-relativistic gas).

Since these equations are all total derivatives it is trivial to integrate them from $x = -\infty$ to a running value of x to obtain the conditions that must hold between the upstream values of flow speed, density, and pressure and those values at a point downstream. We obtain

$$[\rho u]_1^x = 0, \tag{3.4}$$

$$[\rho_1 u_1 u + P]_1^x = 0, \tag{3.5}$$

$$\left[\rho_1 u_1 \frac{1}{2}u^2 + \frac{\gamma_g}{\gamma_g - 1} uP\right]_1^x = 0, \tag{3.6}$$

where $[A]_1^2 \equiv A_2 - A_1$ and it should be noted that Equation (3.4) allows us to replace the quantity ρu with the constant value $\rho_1 u_1$ anywhere we choose.

These equations always have the trivial solution that nothing changes at all; there is no transition from one state to another. On the other hand, Equations (3.4) to (3.6) are second-order, algebraic equations and should have only one other solution. In other words there can be no smooth transitions via intermediate states between the asymptotic upstream state and the asymptotic downstream state because these two asymptotic states are the only ones that conserve the flux of mass, momentum, and energy.

Had we included the diffusion of momentum and energy by viscosity we would have obtained, instead of simple algebraic equations, a set of first-order differential equations that could have been integrated smoothly from one asymptotic state to another. As it stands, we must describe the transition as a discontiuous jump from one state to another, i.e., a shock. This demonstrates the point that a shock must be described as a mathematical discontinuity only if one does not include in the physical picture the dissipative mechanism of entropy production that is required to go from the upstream state to the downstream state.

Even if dissipation is included so that a smooth description of the transition is possible, the above algebraic equations *still hold* for the asymptotic upstream and downstream states (all gradients are assumed to vanish there). These equations are called the Rankine–Hugoniot (R-H) relations for a simple shock and, given the upstream conditions, they may be solved for the downstream flow velocity, density, and pressure. Introducing the compression ratio, $r \equiv u_1/u_2 = \rho_2/\rho_1$*, and the upstream Mach number, $\mathcal{M}_1^2 = \rho_1 u_1^2/(\gamma_g P_1)$, we have the expressions (e.g., Ferraro and Plumpton,

* Note that $u_1/u_2 = \rho_2/\rho_1$ only for nonrelativistic flows. In relativistic shocks, the Lorentz factor for the upstream and downstream flows must be included and we have $\gamma_1\rho_1 u_1 = \gamma_2\rho_2 u_2$ (e.g., Heavens and Drury, 1988). The density ratio $\rho_2/\rho_1 \to \infty$ in highly relativistic shocks, while u_1/u_2 remains finite. Since particle acceleration depends on scattering between the converging flows, u_1/u_2 is the relevant parameter for shock acceleration.

1966, p. 96)

$$r = \frac{(\gamma_g + 1)\mathcal{M}_1^2}{(\gamma_g - 1)\mathcal{M}_1^2 + 2},$$

$$P_2 = P_1\left[1 + \gamma_g \mathcal{M}_1^2\left(1 - \frac{1}{r}\right)\right], \tag{3.7}$$

$$= P_1 \frac{2\gamma_g \mathcal{M}_1^2 - (\gamma_g - 1)}{\gamma_g + 1},$$

where the trivial $r = 1$ solution has been factored out.

We note that for incoming flow speeds that are just at the sound speed (i.e., $\mathcal{M}_1 = 1$), $r = 1$ and $P_2 = P_1$; there is no shock. It would appear that for $\mathcal{M}_1 < 1$ we could have an expansion shock with $r < 1$ and $P_2 < P_1$, it can be shown that such a transition would involve a *decrease* of entropy rather than an increase so such transitions are ruled out by the second law of thermodynamics.

If we consider the opposite extreme, i.e., $\mathcal{M}_1 \to \infty$, the pressure ratio, P_2/P_1, grows without limit but the compression ratio approaches the limiting value $(\gamma_g + 1)/(\gamma_g - 1) = 4$ for a monatomic, nonrelativistic gas with $\gamma_g = \frac{5}{3}$. As mentioned above, this limit implies accelerated spectra with $\sigma \gtrsim 2$. Spectra $\sim p^{-2}$ are marginally divergent in energy density and this fact will play an important role in the nonlinear acceleration theories that we discuss below.

3.1.3. *Coordinate System for Oblique Shocks*

We have not yet discussed the role a magnetic field would play in the shock process. Since an ionized gas or plasma has a high conductivity any magnetic field would be tied to the plasma (i.e., 'frozen-in') and would, in general, contribute to the dynamics of the shock. In a strictly parallel shock where both the magnetic field and the plasma flow are directed along the x-direction, the field's only role is to support the Alfvén waves that act as the glue between the plasma and the energetic particles that are being accelerated. In oblique shocks (we define oblique to be all shocks with an angle between the upstream magnetic field and the shock normal greater than 0°, i.e., $\theta_{Bn} > 0°$), the magnetic field takes a more active role and influences both the shock jump conditions and particle acceleration. Although most of the discussion in this paper will concern parallel or nearly parallel shocks, we will discuss the oblique case to some extent so we present here the reference frames and quantities that will be used in that discussion. In all cases, we assume that the upstream flow speed is directed along the x-axis.

In Figure 3.2 we show the appropriate coordinates for an oblique shock viewed in the normal incidence (NI) frame. In this frame the shock is at rest, as before, and the fluid flows in from the left antiparallel to the shock normal. The magnetic field, however, is not along the normal and changes its direction as it moves through the shock. In addition to contributing an isotropic pressure, $B^2/(8\pi)$, the magnetic field also con-

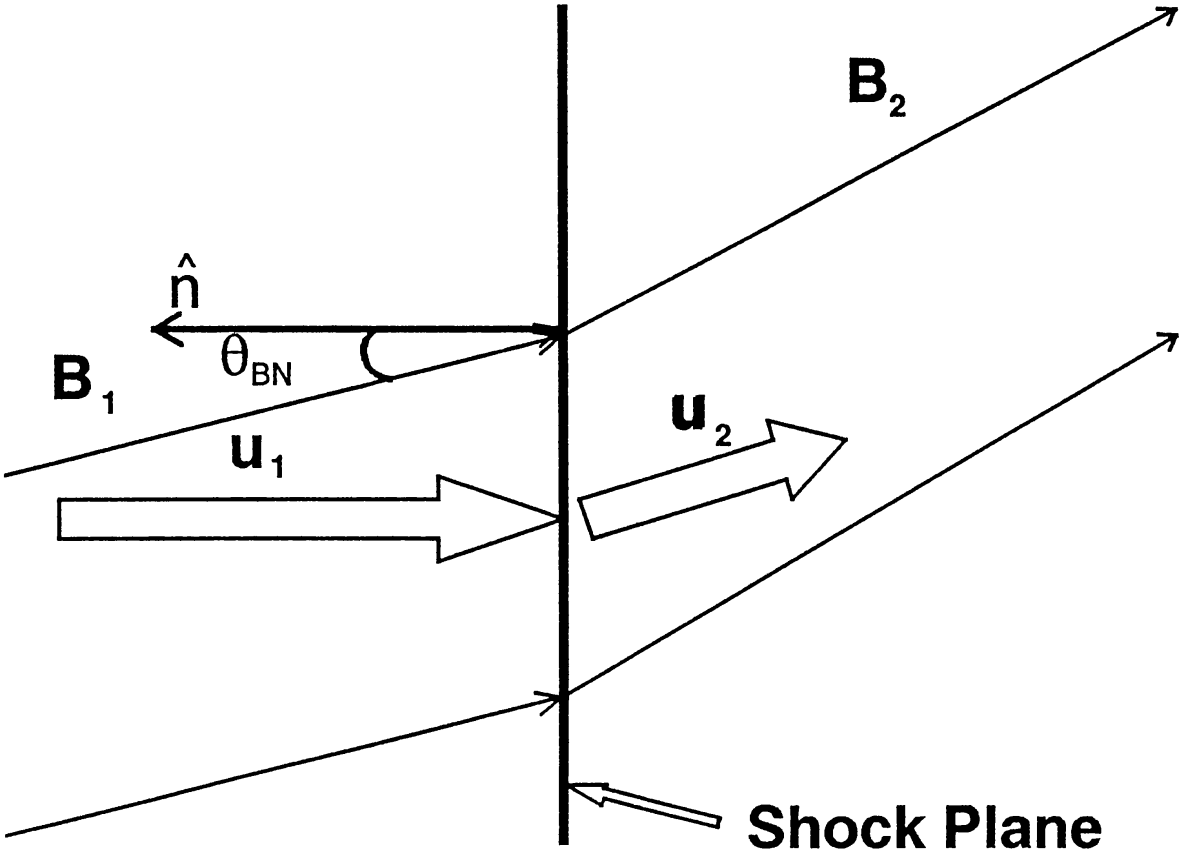

Fig. 3.2. The Normal Incidence (NI) frame; plasma flows in parallel to the shock normal and leaves, in general, at an angle.

tributes a tension in the amount $B^2/(4\pi)$ along the field direction. This means that the plasma can convect y and z components of momentum in the x-direction. This adds two more components to the momentum flux conservation equation but adds five new quantities (u_y, u_z, B_x, B_y, and B_z). Fortunately, Maxwell's equations provide the other three equations that are needed; $\nabla \cdot \mathbf{B} = 0$ and $\nabla \times (\mathbf{u} \times \mathbf{B}) = 0$.

Needless to say, the magneto-hydrodynamic form of the jump conditions is considerably more complicated than the Rankine–Hugoniot equations that apply to a simple fluid. A clear derivation of these equations may be found in Boyd and Sanderson (1969) or in Decker (1988), we will therefore only present them here for future reference. If we define the unit vector $\hat{\mathbf{n}}$ in the direction of the shock normal (i.e., the negative x-direction), we may write the jump conditions in vector form as:

$$[\rho \mathbf{u} \cdot \hat{\mathbf{n}}]_1^2 = 0\,, \tag{3.8}$$

$$[\rho \mathbf{u}(\mathbf{u} \cdot \hat{\mathbf{n}}) + (P + B^2/8\pi)\hat{\mathbf{n}} - (\mathbf{B} \cdot \hat{\mathbf{n}})\mathbf{B}/4\pi]_1^2 = 0\,, \tag{3.9}$$

$$\left[\mathbf{u} \cdot \hat{\mathbf{n}} \left\{\frac{1}{2}\rho u^2 + \frac{\gamma_g}{\gamma_g - 1} P + \frac{B^2}{4\pi}\right\} - \frac{(\mathbf{B} \cdot \hat{\mathbf{n}})(\mathbf{B} \cdot \mathbf{u})}{4\pi}\right]_1^2 = 0\,, \tag{3.10}$$

$$[\mathbf{B} \cdot \hat{\mathbf{n}}]_1^2 = 0\,, \tag{3.11}$$

$$[\hat{\mathbf{n}} \times (\mathbf{u} \times \mathbf{B})]_1^2 = 0\,. \tag{3.12}$$

With no loss of generality we may rotate our coordinate system so that $B_{y1} = 0$. Then it can be shown (Kantrowitz and Petschek, 1966) from the above set of equations that $B_{y2} = u_{y2} = 0$. If **B**, **u**, and $\hat{\mathbf{n}}$ are coplanar upstream from the shock then **B**, **u**, and $\hat{\mathbf{n}}$ remain in the same plane (the coplanarity plane) downstream from the shock. An important property of oblique shocks is that, when viewed in the NI frame, an electric field is produced by the motion of the plasma across the magnetic field. This field is given by

$$\mathbf{E} = -\frac{\mathbf{u} \times \mathbf{B}}{c}, \tag{3.13}$$

and will play an important role in the so-called 'shock drift' acceleration of particles in oblique shocks (see Section 5.3).

There are some cases in which it is easier to work in a frame in which this electric field does not appear. Such a frame, called the deHoffman–Teller frame (deHoffman and Teller, 1950), can be obtained by an observer moving with respect to the NI frame with a velocity, V_{HT}, parallel to the shock plane. This velocity is given by

$$\frac{\mathbf{V}_{\mathrm{HT}} \times \mathbf{B}}{c} = -\mathbf{E} = \frac{\mathbf{u} \times \mathbf{B}}{c} \tag{3.14}$$

or

$$V_{\mathrm{HT}z} = \frac{u_{\mathrm{NI}} B_z}{B_x}. \tag{3.15}$$

Since $\mathbf{u}_{\mathrm{HT}} = \mathbf{u}_{\mathrm{NI}} - \mathbf{V}_{\mathrm{HT}}$, we see from Equation (3.14) that $\mathbf{u}_{\mathrm{HT}} \times \mathbf{B} = 0$ and thus the plasma flow is parallel to the magnetic field in the HT frame both upstream and downstream from the shock. This is shown in Figure 3.3.

The velocity, V_{HT}, is the velocity with which the intersection point between a given magnetic field line and the shock plane moves as the field is swept into the shock and can become superluminal when θ_{Bn} approaches 90°. In this case, the HT frame is not physically realizable but one *can* transform to a frame in which the velocity of the intersection point is infinite. This, of course, means that, in this frame, $\theta_{\mathrm{Bn}} = 90°$ and the shock is strictly perpendicular.

In the majority of the discussions in this paper it should be understood that we are working in the Normal Incidence (NI) frame; whenever a different frame such as the deHoffman–Teller frame is used it will be explicitly so stated.

3.2. Diffusion-convection equation approach

Axford *et al.* (1977), Krymsky (1977), and Blandford and Ostriker (1978) applied the well-known diffusion-convection equation to show that a shock, propagating through a region in which energetic particles are diffusing, would produce a superthermal population of particles with a power-law momentum distribution. The derivation is quite straightforward in the one-dimensional case and involves only the simplest notions. If

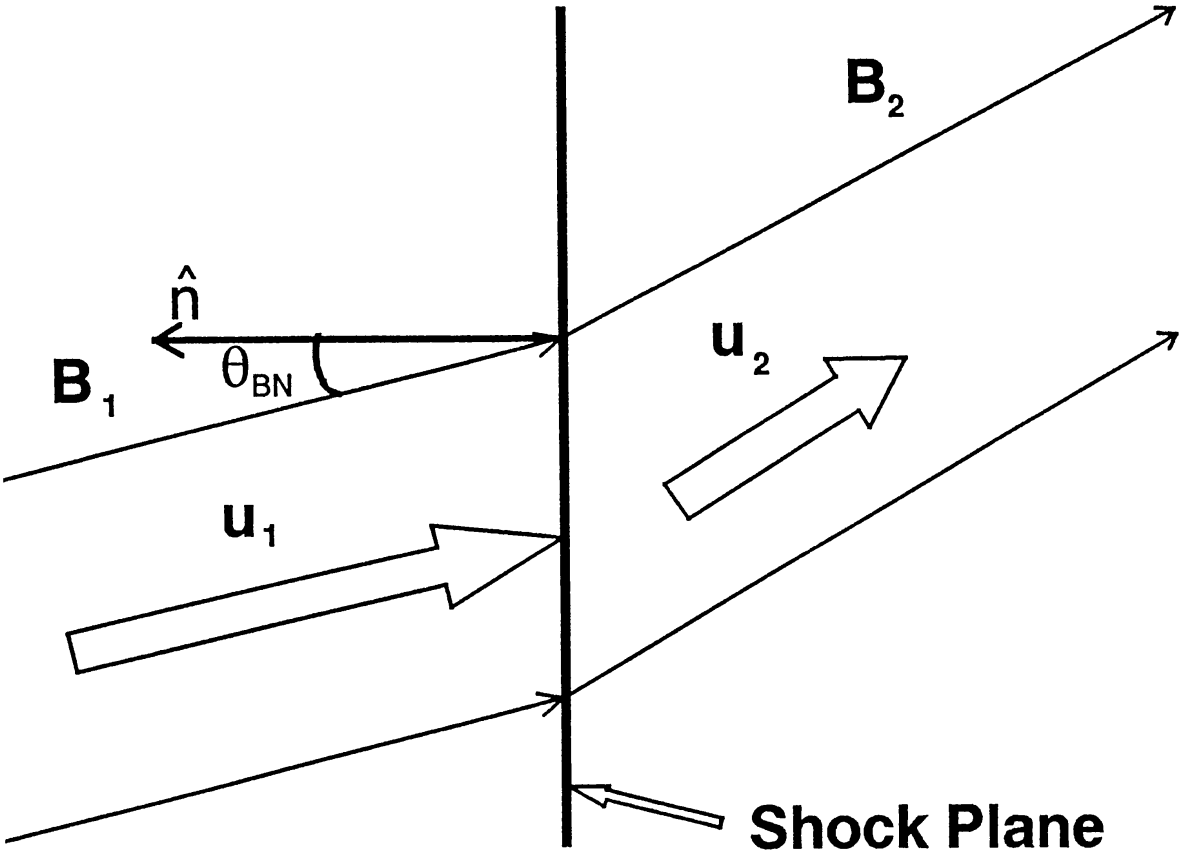

Fig. 3.3. The deHoffmann–Teller (HT) frame; plasma flows parallel to the magnetic field on both sides of the shock. There is, therefore, no $\mathbf{u} \times \mathbf{B}$ electric field in this frame.

we picture the shock as an infinite, plane discontinuity in a flowing plasma, the plasma flows in from $x = -\infty$ and out to $x = +\infty$ with a discontinuous transition in flow speed from a supersonic upstream speed, u_1, to a subsonic downstream speed, u_2, at $x = 0$. If we assume that the distribution function in space and scalar momentum of the accelerated particles, $f(x, p)$, is isotropic to first order (i.e., $f(x, p)$ is the same in all reference frames to first order in u/v, where u is the plasma flow velocity and v and p are the individual particle velocity and momentum measured in the local plasma frame), then the steady-state Boltzmann equation describing the transport of particles with $v \gg u$ in space and momentum can be written in the form of a diffusion-convection equation (see Jones, 1990a, and references therein):

$$\frac{\partial}{\partial x}\left[uf(x, p) - \kappa \frac{\partial f(x, p)}{\partial x}\right] = \frac{1}{3}\left(\frac{\partial u}{\partial x}\right)\frac{\partial}{\partial p}\left[pf(x, p)\right], \tag{3.16}$$

where $\kappa = \kappa_{\parallel} \cos^2 \theta_{\mathrm{Bn}} + \kappa_{\perp} \sin^2 \theta_{\mathrm{Bn}}$ is the diffusion coefficient in the direction normal to the shock, θ_{Bn} is the angle between the shock normal and the mean magnetic field, and $\kappa_{\parallel}$ and $\kappa_{\perp}$ are the diffusion coefficients parallel and perpendicular to the magnetic field, respectively. (We note that $f(x, p)\, \mathrm{d}p = F(x, \mathbf{p})\, \mathrm{d}^3\mathbf{p} = 4\pi p^2 F(x, \mathbf{p})\, \mathrm{d}p$ for isotropic distributions, where $\mathrm{d}^3\mathbf{p} = \mathrm{d}p_x\, \mathrm{d}p_y\, \mathrm{d}p_z$.) As long as scattering is strong enough to insure

that the assumptions of the diffusion-convection equation are valid, Equation (3.16) holds for all θ_{Bn} and contains shock-drift acceleration. Forman and Webb (1985) give a good discussion of the relation between κ and quasi-linear theory and other aspects of Equation (3.16).

Integrating Equation (3.16) from $x = -\infty$ to $x = +\infty$ and employing the boundary conditions $f(x = -\infty, p) = f_1(p)$, $f(x \geq 0, p) = f_2(p)$, and $\partial u/\partial x = (u_2 - u_1)\delta(x)$, we obtain*

$$u_2 f_2(p) - u_1 f_1(p) = \tfrac{1}{3}(u_2 - u_1) \frac{\partial}{\partial p} [p f_2(p)] . \tag{3.17}$$

Using the definition of the compression ratio $r = u_1/u_2 > 1$, we may express this differential equation in p for the downstream distribution function in the form

$$p \frac{\partial f_2(p)}{\partial p} + \left(\frac{r+2}{r-1}\right) f_2(p) = \frac{3r}{r-1} f_1(p) . \tag{3.18}$$

The solution to this equation is

$$f_2(p) = \left(\frac{3r}{r-1}\right) p^{-\sigma} \int_{p_0}^{p} dp' p'^{\sigma-1} f_1(p') + B p^{-\sigma} , \tag{3.19}$$

where $\sigma = (r+2)/(r-1)$ is the spectral index, B is an arbitrary constant of integration that multiplies the homogeneous term, the distribution $f_1(p)$ is the far upstream spectrum of ambient particles which convects into the shock and is accelerated, and p_0 is large enough so that the assumption $v \gg u$ holds. For completeness, we can write the resulting spectrum as a differential flux in particles/(cm^2 s ster E), i.e.,

$$\frac{dJ}{dE} = \frac{1}{4\pi} \frac{n_1 u_1}{m_0 c^2} \frac{3}{r-1} \frac{1}{\sqrt{\varepsilon_i(\varepsilon_i + 2)}} \left[\frac{\varepsilon(\varepsilon+2)}{\varepsilon_i(\varepsilon_i+2)}\right]^{-\sigma/2} , \tag{3.20}$$

where $f_1(p)$ is taken to be a δ-function distribution at kinetic energy E_i and number density n_1, $\varepsilon = E/(m_0 c^2)$, and m_0 is the rest mass. Equation (3.20) is properly normalized and fully relativistic. The limiting nonrelativistic and ultrarelativistic spectral indexes for the flux are $\sigma_{NR} = \sigma/2$ and $\sigma_{UR} = \sigma$, respectively. When measured versus energy, the power-law differential flux steepens above $E \sim m_0 c^2$, and the spectral index doubles.

No other source of particles is included in the above equations other than $f_1(p)$. In actual shocks with no particle creation (such as electron-positron creation), the homogeneous term should be zero and the downstream spectrum, $f_2(p)$, is produced solely from the ambient upstream spectrum, $f_1(p)$. Our analysis differs from that of Drury (1983) who has speculated that the homogeneous term might represent the injection into the acceleration process of particles from the thermal plasma making up the shock. We

* We continue our convention that the subscript 1 implies far upstream values and the subscript 2 implies far downstream values.

disagree with this suggestion for two reasons: first, the homogeneous term has no low-energy cutoff and hence cannot be normalized, and second, results from Monte-Carlo calculations (i.e., Ellison *et al.*, 1990a) strongly indicate that the injection of thermal particles should be treated *exactly* like the injection of any other seed particles. This is demonstrated in Figure 3.4 which shows spectra produced by a Monte-Carlo

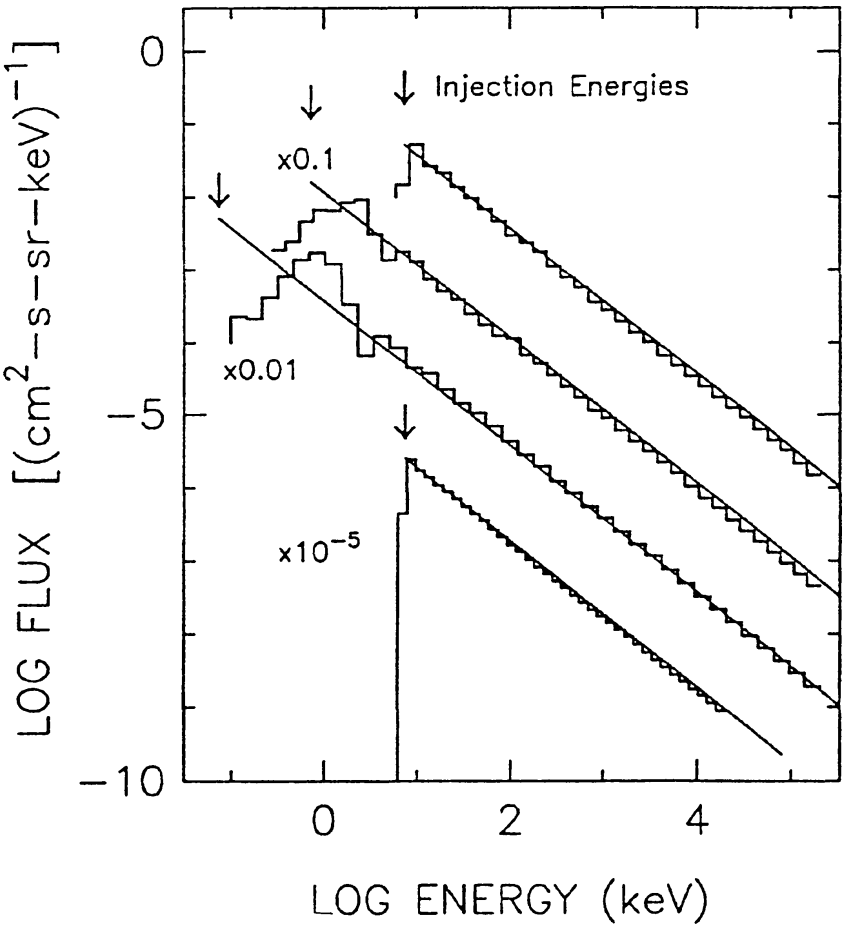

Fig. 3.4. Particle flux versus energy for nonrelativistic shock velocities. The upper six curves were calculated with $u_1 = 500$ km s^{-1}, $r = 4$, and $\alpha = 1$ (see Equation (6.3)). The lower two curves were calculated with $u_1 = 100$ km s^{-1}. The smooth curves are the test particle predictions (Equation (3.20)) while the histograms are the Monte-Carlo results. All spectra here and elsewhere are calculated in the reference frame of the shock, at a downstream position, and particle fluxes are normalized to 1 incoming particle/(cm^2 s). Injection energies are shown by arrows, and curves with numerical factors have been displaced by those factors for clarity. Figure from Ellison *et al.* (1990).

simulation described in detail in Section 6.5 below. The smooth curves are solutions of Equation (3.20) and they are shown to match, in shape and normalization, the Monte-Carlo results at energies high enough so that $v \gg u$ holds. In the Monte-Carlo model, injection comes solely from upstream thermal particles convected into the shock (i.e., $f_1(p)$) when some fraction of the shock-heated plasma scatters back across the shock and is accelerated. It is clear from the figure that there is no extra room for injection from the homogeneous term.

As far as Equation (3.19) is concerned, if we assume that $f_1(p)$ is a power law of the

form $f_1(p) \sim p^{-\sigma+\delta}$ for $p > p_0$ and zero for $p < p_0$, where δ may be any value, the solution is proportional to

$$p^{-\sigma}\left(\frac{p^{\delta} - p_0^{\delta}}{\delta}\right). \tag{3.21}$$

If $f_1(p)$ is steeper than $p^{-\sigma}$ (i.e., $\delta < 0$), the second term in the parentheses will dominate the first term and the shock will produce an accelerated spectrum proportional to $p^{-\sigma}$. If, on the other hand, $f_1(p)$ is flatter than $p^{-\sigma}$ (i.e., $\delta > 0$), the first term will dominate and the accelerated spectrum will retain the flatter slope of the injected spectrum with the injected particles shifted up in energy. Since most ambient distributions are expected to be thermal or steeper than $p^{-\sigma}$, strong shocks naturally produce power-law distributions with spectral index near 2 (see Section 2.2). The most remarkably property of Equation (3.19) is that the power-law index depends only on the compression ratio, all details of the scattering process and θ_{Bn} (contained in κ) drop out as long as the assumptions used to derive Equation (3.19) continue to hold. While it is clear that these assumptions must break down at some point, many objects seem to approach the ideal case over a wide dynamic range. The simplicity and lack of free parameters in Equation (3.19), coupled with the fact that shock acceleration has been observed taking place at the Earth's bow shock and interplanetary shocks, are the major reasons why shock acceleration has received such a great deal of attention.

3.3. Individual particle approach of Bell

Probably the most physically intuitive approach to the acceleration of charged particles by plasma shocks is the individual particle, or microscopic, method of Bell (1978a, b). In this description superthermal particles are assumed to scatter elastically in the local plasma frame and to have gyroradii much longer than the shock thickness. Consequently, if particles freely scatter from one side of the shock to the other and scatter against the converging plasma, they will gain a small amount of energy every time they cross the shock. It is easy to see that after many crossings a given particle can gain a considerable amount of energy and, hence, can be accelerated to high energy if it can 'stick around' the shock long enough and not share energy with the background plasma.

Although most authors compute the energy (or momentum) gain that a particle experiences upon crossing a shock in terms of the relativistic transformation of energy from one frame of reference to another, we will show that there is a simpler way of obtaining this value. To do so we simply consider the equation for the conservation of particles,

$$\frac{\partial}{\partial x}(j_x) + \frac{\partial}{\partial p}(j_p) = 0\,, \tag{3.22}$$

where j_x and j_p are the fluxes of particles along the x- and p-axes respectively. Since there is no diffusive component to the flux along the momentum axis, we may write $j_p = \dot{p}f(x, p)$. If we now compare Equation (3.22) with Equation (3.16) and recognize

that the right-hand side of Equation (3.16) is just the negative of the divergence of the flow of particles along the momentum axis, we may deduce that the rate of change of momentum of a particle in a region of converging or diverging plasma flow is given by

$$\dot{p} = -\frac{1}{3} p \left(\frac{\partial u}{\partial x}\right). \tag{3.23}$$

If we now follow a particle as it traverses the shock front from the upstream to the downstream region ($1 \rightarrow 2$), we may integrate Equation (3.23) in time as

$$\int_1^2 \dot{p}\, \mathrm{d}t = -\int_1^2 \frac{1}{3} p \left(\frac{\partial u}{\partial x}\right)\left(\frac{\mathrm{d}x}{v_x}\right) = \frac{1}{3}\left(\frac{p}{v\mu}\right)(u_1 - u_2), \tag{3.24}$$

where μ is the cosine of the angle the particle velocity makes with the shock normal as it traverses the shock front. We must now average Equation (3.24) over the distribution in μ of the particles crossing the shock front in a unit time. Since the flux of particles crossing the shock is proportional to μ, the properly normalized average yields

$$\langle \delta p \rangle = \frac{2}{3}\left(\frac{p}{v}\right)(u_1 - u_2). \tag{3.25}$$

For particles traversing the shock in the opposite direction, u_1 and u_2 are interchanged but the sign of $\mathrm{d}x$ is also reversed so Equations (3.24) and (3.25) remain unchanged. It should be noted that this is the same expression obtained by arguments involving frame transformations (e.g., Drury, 1983).

We now can see that if a particle with initial momentum p_0 has traversed the shock N times its average momentum will be

$$\langle p \rangle (N) = \prod_{i=1}^{N} [1 + \tfrac{2}{3}(u_1 - u_2)/v_i] p_0 . \tag{3.26}$$

In order to obtain a distribution of particles, however, we must include the probability that a particular particle will cross the shock N times. The probability that a particle that has traversed the shock from upstream to downstream will return to the shock can be calculated by means of a simple argument first given by Bell (1978a) and generalized to relativistic shocks by Peacock (1981). Figure 3.5 illustrates the basic elements of the argument. Consider all particles with speed v viewed in the downstream frame. As the shock moves in the negative x-direction with a speed u_2, particles with an x-component of velocity, $v_x < -u_2$, can overtake the shock and pass through from the downstream side to the upstream side. The flux of these particles through the shock is given by

$$\left| \int_{-v}^{-u_2} (u_2 + v_x)\, \mathrm{d}v_x \right| = \tfrac{1}{2}(u_2 - v)^2 . \tag{3.27}$$

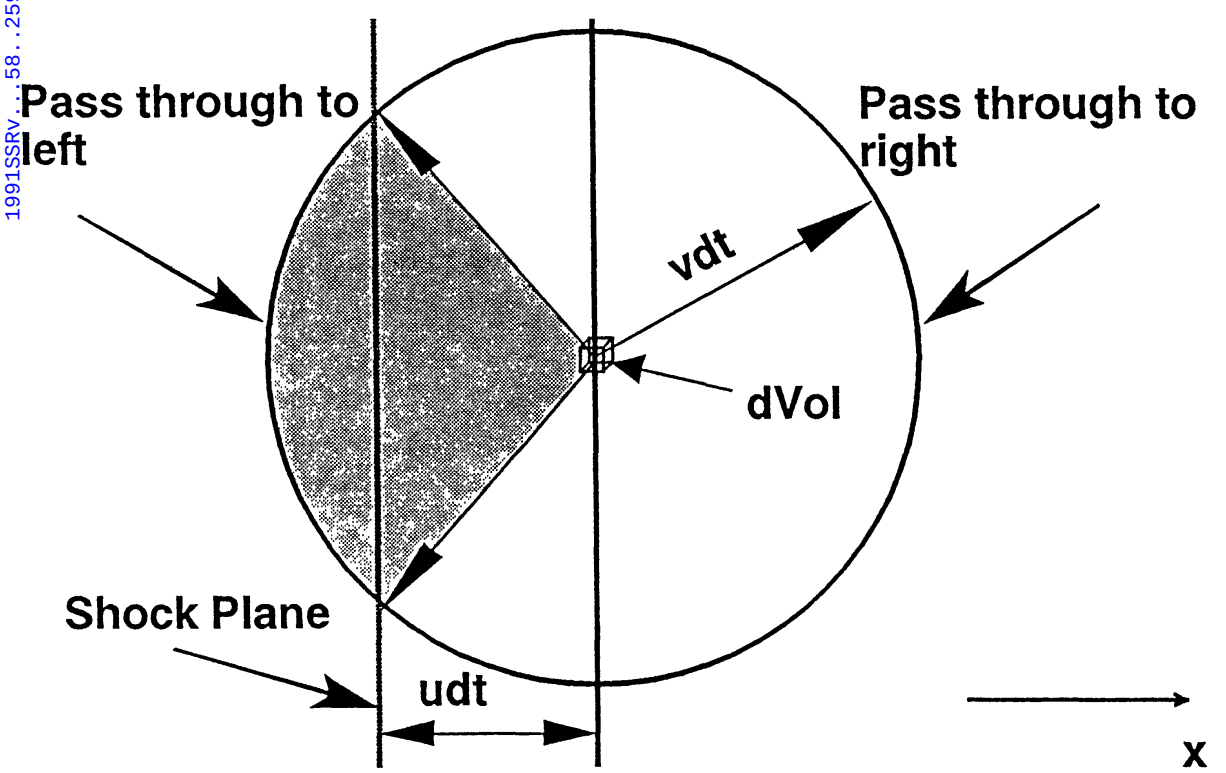

Fig. 3.5. Geometry showing the relative flux of particles crossing a moving shock in either direction.

By the same token, the flux of particles crossing from upstream to downstream is given by

$$\int_{-u_2}^{v} (u_2 + v_x)\, \mathrm{d}v_x = \tfrac{1}{2}(u_2 + v)^2 . \tag{3.28}$$

The probability of return is equal to the fraction of those particles passing through the shock from upstream to downstream that return to the shock and is, therefore, given by the ratio of the fluxes*

$$\mathscr{P}(\text{return}) = \frac{\tfrac{1}{2}(u_2 - v)^2}{\tfrac{1}{2}(u_2 + v)^2} = \left(\frac{1 - u_2/v}{1 + u_2/v}\right)^2 . \tag{3.29}$$

The probability that a particle that has traversed the shock from upstream to downstream will return to the shock *at least* $N/2$ times and thus cross the shock *at least* N times is given by

$$\mathscr{P}(N) = \prod_{i=1}^{N/2} \left(\frac{1 - u_2/v_i}{1 + u_2/v_i}\right)^2 = \left[\prod_{i=1}^{N/2} \left(\frac{1 - u_2/v_i}{1 + u_2/v_i}\right)\right]^2 \tag{3.30}$$

* This expression is valid for any value of $u_2 \leq v$ and has exactly the same form when $u_2 \to c$ (Peacock, 1981). However, the derivation *does* assume that the particle distribution is isotropic in the local plasma flow frame which is not valid directly behind the shock unless $u_2 \ll v$. It is nevertheless useful in numerical studies of thermal particles and relativistic shocks (where $u_2 \simeq v$) when one can assume that the particle distribution becomes isotropic in the flow frame a few mean free paths behind the shock (Ellison *et al.*, 1990a).

and taking the logarithm

$$\ln[\mathscr{P}(N)] = 2\sum_{i=1}^{N/2} \ln\left(\frac{1-u_2/v_i}{1+u_2/v_i}\right) = -4\sum_{i=1}^{N/2}\left[\frac{u_2}{v_i}+\frac{1}{3}\left(\frac{u_2}{v_i}\right)^3+\frac{1}{5}\left(\frac{u_2}{v_i}\right)^5+\cdots\right]. \tag{3.31}$$

Now the term v_i in Equations (3.26) and (3.31) are not exactly the same. In Equation (3.26), v_i is the particle velocity measured *in the shock frame* on each crossing of the shock. In Equation (3.31), v_i is he speed measured *in the downstream flow frame* of a particle that just crossed the shock. The increase in velocity that a particle undergoes in crossing the shock is of the order of $u_1 - u_2$ and the velocity difference as seen in the downstream frame as compared to the shock frame is of order u_2. If we assume that $u_2 < u_1 \ll v_i$ and neglect these differences, our results will be correct to order u/v. With this in mind we may write

$$\ln\left[\frac{\langle p\rangle(N)}{p_0}\right] = \frac{4}{3}(u_1 - u_2)\sum_{i=1}^{N/2}\frac{1}{v_i} \tag{3.32}$$

and

$$\ln[\mathscr{P}(N)] \approx -4u_2\sum_{i=1}^{N/2}\frac{1}{v_i}. \tag{3.33}$$

Combining these two equations gives

$$\ln[\mathscr{P}(p)] = -\frac{3u_2}{u_1 - u_2}\ln\left(\frac{p}{p_0}\right) \tag{3.34}$$

or

$$\mathscr{P}(p) = \left(\frac{p}{p_0}\right)^{-3u_2/(u_1-u_2)}. \tag{3.35}$$

Equation (3.35) represents the probability that a particle will cross and recross the shock enough times to achieve a momentum of p or higher. If the upstream number density is N_0 particles per unit volume, the resulting differential spectrum will be given by

$$\begin{aligned} f(p) &= -N_0\left(\frac{u_1}{u_2}\right)\left(\frac{\partial\mathscr{P}}{\partial p}\right) = \\ &= \left(\frac{N_0}{p_0}\right)\left(\frac{3u_1}{u_1-u_2}\right)\left(\frac{p}{p_0}\right)^{-(u_1+2u_2)/(u_1-u_2)} = \\ &= \left(\frac{N_0}{p_0}\right)\left(\frac{3r}{r-1}\right)\left(\frac{p}{p_0}\right)^{-\sigma}, \end{aligned} \tag{3.36}$$

where the extra factor of $r = u_1/u_2$ in the first equality accounts for the simple compression of the upstream density by the shock.

If we set $f_1(p')$ equal to $\delta(p' - p_0)$ in Equation (3.19) we obtain Equation (3.36), showing that the two approaches are equivalent.

3.4. Problems and Limitations

The equivalence of the diffusion-convection and individual particle approaches implies that they share the same limitations. First of all, use of the diffusion-convection equation in the macroscopic approach assumes that the particle distribution function is almost isotropic in all relevant frames of reference, namely the shock frame and the upstream and downstream flow frames, which in turn requires that u_1 and $u_2 \ll v$. Isotropy was explicitly required in the microscopic approach when the probability of return of a particle to the shock was computed and the requirement that the particle speed be much greater than the flow speeds was needed in order to neglect terms that were smaller than first order in u/v.

The next limitation is that the shock thickness must be the smallest scale in the problem. This manifests itself in the diffusion-convection approach by the description of the shock as a sharp discontinuity in the flow velocity. The real requirement is not that the energy producing term, $\mathrm{d}u/\mathrm{d}x$, be a δ-function, as was assumed in Equation (3.16), but rather that its entire contribution be contained in a region in which the distribution function does not vary. Likewise, in the microscopic approach the assumption was that the particle traversed the compression region at a constant speed v_i essentially unaffected by scattering. This requires that the scale of the shock be smaller than the mean free path λ of the particles.

If the shock is thick enough that the distribution function changes significantly across it, integrating Equation (3.16) from $x = -\infty$ to $x = +\infty$ yields an integro-differential equation whose solution is not easily approximated (see, however, Drury *et al.*, 1982, for such a solution under a particular set of assumptions; for a numerical solution in an arbitrary flow profile see Schneider and Kirk, 1987). In the microscopic approach the exponent of the integral spectrum, Equation (3.35), is just the ratio

$$\frac{\ln[\mathscr{P}(1)]}{\ln[1 + \delta p/p]} = -\frac{3u_2}{u_1 - u_2}\,, \tag{3.37}$$

where $\mathscr{P}(1)$ is the probability that a downstream particle will return to the shock *and traverse it*, and $\delta p/p$ is the incremantal gain in momentum that a particle undergoes in traversing the shock. If the shock has a finite thickness δx such that the particle does not traverse it without scattering we must replace v in Equation (3.25) with a quantity v_{eff} that is the 'effective' velocity with which the particle traverses the shock. Since this velocity is always slower than the particle speed it would appear that the spectral index would become smaller and, hence, the spectrum would become flatter (more energetic). However, we must now multiply the probability of return by the probability that the particle will traverse the no longer infinitesimally thin shock. This is given by the

'modulation' equation*

$$\mathscr{P}' = \exp(-\langle u \rangle \, \delta x/\kappa), \tag{3.38}$$

where $\langle u \rangle$ is the average flow speed through the shock transition.

From this we see that the integral spectrum exponent becomes

$$-\left(\frac{3v_{\text{eff}}}{u_1 - u_2}\right)\left(\frac{u_2}{v} + \frac{\langle u \rangle \, \delta x}{4\kappa}\right). \tag{3.39}$$

Taking $\langle u \rangle = (u_1 + u_2)/2$ and $\kappa = \lambda v/3$ and using the compression ratio $r = u_1/u_2$, this becomes

$$-\left(\frac{v_{\text{eff}}}{v}\right)\left(\frac{3}{r-1} + \frac{9}{8}\frac{\delta x}{\lambda}\frac{r+1}{r-1}\right). \tag{3.40}$$

Clearly if $\delta x \ll \lambda$, then $v_{\text{eff}} = v$ and the spectral index is unchanged. If, however, $\delta x > \lambda$ we have $v_{\text{eff}} \approx \kappa/\delta x$ and thus $v_{\text{eff}}/v = \lambda/(3\delta x)$ and the growth of the second term just compensates for the smallness of v_{eff}/v. Since this compensation is exact, one should not trust the numerical value of the index that it gives; once again the reader is referred to Drury *et al.* (1982) for a more correct investigation of this case. However, we can see that in the case when $\langle v \rangle \, \delta x/\kappa$ is large and $v_{\text{eff}} \approx \langle u \rangle$ (see Jones, 1990b, for a discussion of the various regimes of propagation speeds in the diffusion-convection equation), the spectral index becomes just

$$\sigma = 1 + \frac{3}{8}\frac{r+1}{r-1}\frac{\langle u \rangle \, \delta x}{\kappa}, \tag{3.41}$$

which is by supposition a large number. Actually when the shock thickness becomes large compared to the diffusion length scale $\kappa/\langle u \rangle$, the injected particles are just convected once through the shock and their energy is shifted upwards by adiabatic compression.

Analytic techniques have been developed to overcome the problems imposed by the approximation of a near-isotropic distribution function (see in particular Kirk and Schneider, 1987a; Kirk, 1988; Webb, 1987), but these techniques are quite complicated and the solutions are somewhat unwieldy. These techniques have been applied to relativistic shocks and thermal particles (e.g., Kirk and Schneider, 1989), where near-isotropic distributions can never be assumed, and oblique shocks (e.g., Kirk and Heavens, 1989, 1990) where relativistic flows (and, therefore, anisotropic distributions) can occur in the deHoffman–Teller frame regardless of the shock velocity.

One other assumption that is implicit in both the microscopic and macoscopic approaches is that there is no other scale in the problem other than he ones defined by

* This equation arises from the theory (Parker, 1958b) of the modulation of galactic cosmic rays by the solar wind. Modulation theory also applies the diffusion-convection equation and calculates the probability that a particle at the boundary of the heliosphere can propagate against the wind into the position of the Earth.

the physical processes. In other words, the only way a particle leaves the system is by being convected by the plasma flow to $x = +\infty$. If the mean free path, λ, and the shock thickness, δx, are taken to be infinitesimal, the only macroscopic scale defined by the physics is the diffusion length, $\kappa/\langle u \rangle$ and thus any length scales of the model in question must be long compared to this scale.

To summarize, for the simple macroscopic (diffusion-convection) or microscopic (individual particle) approaches to give valid results, the following length-scale hierarchy must hold

$$\delta x \ll \lambda \ll \kappa/\langle u \rangle \ll \text{scales of the model} . \tag{3.42}$$

This requirement has been known from the beginning (e.g., Blandford and Ostriker, 1978) but it needs to be kept in mind when we discuss the need for more effective techniques in studying shock acceleration.

We would also like to emphasize that the restriction to near-isotropic distributions and thus superthermal particles (i.e., $v \gg u$) made in the mathematical formulations of Fermi acceleration *in no way implies* that the process itself requires energetic seed particles with $v \gg u$ to work. On the contrary, there is considerable evidence from heliospheric shock observations (mentioned in Section 1.1) and plasma simulations (discussed in detail in Section 6) that shocks can directly accelerate ambient thermal particles.

4. Nonlinear Theories of Shock Acceleration

In the work that we have discussed so far, a shock propagating in a diffusive medium was taken as a given, pre-existing phenomenon and the accelerated particles were a by-product. It quickly became evident to early workers however that if a reasonable amount of energy was transferred to the accelerated particles ($\gtrsim 10\%$) they would become a dynamically important ingredient in the shock process itself (e.g., Axford *et al.*, 1977). Basically, four nonlinear processes are expected to occur if acceleration is efficient. First, if a significant flux of energetic particles backstream against the cold, unshocked material, instabilities will result and plasma waves or turbulence will be generated. The accelerated particles can influence, or even be mainly responsible, for the plasma turbulence required for acceleration to occur. Second, if accelerated particles constitute a dynamically important pressure, they will slow the unshocked plasma somewhat before it undergoes a sharp shock transition. The now smoothed shock is less efficient at accelerating particles and the acceleration process will be regulated by the accelerated particles. Third, if the diffusion coefficient increases with energy (as it almost surely will), high-energy particles will obtain large diffusion lengths and at some point will escape from finite size, steady-state shocks. These escaping particles will carry away energy and pressure and will allow the shock compression ratio to increase, an effect similar to what occurs in radiative shocks. The increased compression ratio increases the acceleration efficiency, the spectrum of the accelerated particles flattens, and the fraction of particles that escape increases. The fourth nonlinear effect occurs when a

significant fraction of the pressure of the shocked plasma is produced by relativistic particles. A relativistic gas has a lower ratio of specific heats than a nonrelativistic one and the R–H relations are modified accordingly. The more pressure in relativistic particles, the larger the compression ratio and the more efficient the acceleration. This, in turn, produces more relativistic particles, etc.

Several approaches for treating these processes have been developed using both analytic techniques and computer simulations. Elements of this work are discussed below.

4.1. Self-consistent treatment of the diffusion coefficient

4.1.1. *Bell's Self-Consistent Theory*

Most of the initial work that applied the diffusion-convection equation simply assumed that there was sufficient scattering to keep the accelerated particles isotropic in the flowing plasma. An exception to this was the work of Bell (1978a, b) in which he investigated the role that the accelerated particles would play in creating the plasma turbulence that would in turn scatter and hence accelerate them. In these papers Bell applied the original work of Wentzel (1968, 1974) who derived the growth rate of Alfvén waves due to the streaming of cosmic-ray particles through a cold plasma. Wentzel found that if the mean streaming velocity of the cosmic rays exceeded the local Alfvén velocity ($V_A \equiv B/(4\pi\rho)^{1/2}$ where B is the local magnetic field and ρ is the local plasma mass density) by a small amount the waves would be rapidly generated and he suggested that cosmic rays could not, therefore, stream through the galaxy with a flow speed much faster than this velocity. This work was later extended by Skilling (1975a, b, c) who derived a simplified set of coupled equations that treated the propagation of the cosmic rays and the growth, transport, and decay of the Alfvénic turbulence that limited the motion of the cosmic rays. It was these equations that were employed by Bell in his model of self-excited shock acceleration.

One starts, simply, with the one-dimensional diffusion equation for the particles that are accelerated by the shock that is positioned at $x = 0$:

$$u_1 \frac{\partial f}{\partial x} = \frac{\partial}{\partial x}\left(\kappa \frac{\partial f}{\partial x}\right). \tag{4.1}$$

Notice that unlike Equation (3.16) there is no energy change term in Equation (4.1). The acceleration process has already been described by the microscopic approach of the last section in which it was unnecessary to know about the generation or spatial distribution of the scattering, only that it existed. In this and following equations, energy and momentum are not dynamical variables but are merely parameters. One then notes that the diffusion coefficient, κ, is inversely proportional to the energy density of Alfvén waves per logarithmic bandwidth, $\mathcal{I}$, which are resonant with the particles of momentum p

$$\kappa \sim \mathcal{I}^{-1}. \tag{4.2}$$

The equation for the Alfvén wave energy density is

$$u_1 \frac{\partial \mathscr{I}}{\partial x} = \zeta \mathscr{I}, \tag{4.3}$$

where the damping of the waves has been neglected. Equation (4.3) simply asserts that the generation of Alfvén waves and the rate at which they are convected away are in local equilibrium.

The growth rate of the waves, ζ, is proportional to the local flux of the energetic particles which is in turn equal to $\kappa\, \partial f/\partial x$, so we have*

$$\zeta \sim \mathscr{I}^{-1} \frac{\partial f}{\partial x} \quad \text{giving} \quad \zeta \mathscr{I} \sim \frac{\partial f}{\partial x}, \tag{4.4}$$

yielding a nonlinear pair of coupled equations for f and $\mathscr{I}$

$$\frac{\partial f}{\partial x} = \frac{u_1}{\kappa} f = \alpha \mathscr{I} f, \qquad \frac{\partial \mathscr{I}}{\partial x} = \frac{\zeta}{u_1} \mathscr{I} = \beta \frac{\partial f}{\partial x}. \tag{4.5}$$

Since the gradients of f and $\mathscr{I}$ are proportional to each other and we shall impose the same boundary conditions on them, namely their vanishing far upstream at $x = -\infty$, we may set $\mathscr{I} = \beta f$ and obtain the single nonlinear equation for the particle distribution function, f;

$$\frac{\partial f}{\partial x} = \alpha \beta f^2, \tag{4.6}$$

re-arranging to give

$$\frac{\partial f}{f^2} = \alpha \beta \, \partial x, \tag{4.7}$$

which may be integrated directly from $x = 0$ to x to give

$$f(x) = \left(\frac{1}{f(0)} - \alpha \beta x \right)^{-1} = \frac{(\alpha\beta)^{-1}}{x_0 - x}. \tag{4.8}$$

where $x_0 = 1/[\alpha \beta f(0)]$.

Bell refers to x_0 as the scale length of the particle distribution in front of the shock and showed that for an $f(0)$ typical of the galactic cosmic-ray density,

$$x_0 = 5 \times 10^{14} n_e^{1/2} E^{1.5} \text{ m}, \tag{4.9}$$

* Bell (1978a, Equation (16)) has the wrong expression for ζ (see Skilling, 1975c, Equation (A8) for the correct expression), however, since he arrives at the correct solution one assumes that the error is only a typographical one.

where n_e is the electron density in the pre-shocked gas in cm^{-3} and E is the particle energy in GeV. It is evident from the energy dependence of Equation (4.9) that high-energy particles stream farther upstream of the shock than do low-energy ones.

However, one can write Equation (4.8) in a different form that displays the change in spectral shape that is observed as one looks at different upstream locations. Noting that, in Bell (1978), the diffusion coefficient κ and the wave growth rate ζ are momentum dependent, such that $\alpha\beta \sim p$, we may also write

$$f(x, p) = \frac{f(x = 0, p)}{1 + f(x = 0, p)/f(p')} , \tag{4.10}$$

where $f(p') \equiv (\alpha\beta x)^{-1} \sim (xp)^{-1}$. The quantity, $f(p')$, is an upper bound for $f(x, p)$ and is inversely proportional to the distance in front of the shock.

We see, therefore, that if $f(x = 0, p)$ is an inverse power law in energy or momentum the further one looks in front of the shock the more the low-energy particles are suppressed. The spectrum is not truncated but simply flattened to a p^{-1} spectrum so as not to rise above the value of $f(p')$ corresponding to that particular value of x. Figure 4.1 shows the particle spectrum as a function of p at the position of the shock and at two different positions upstream of the shock.

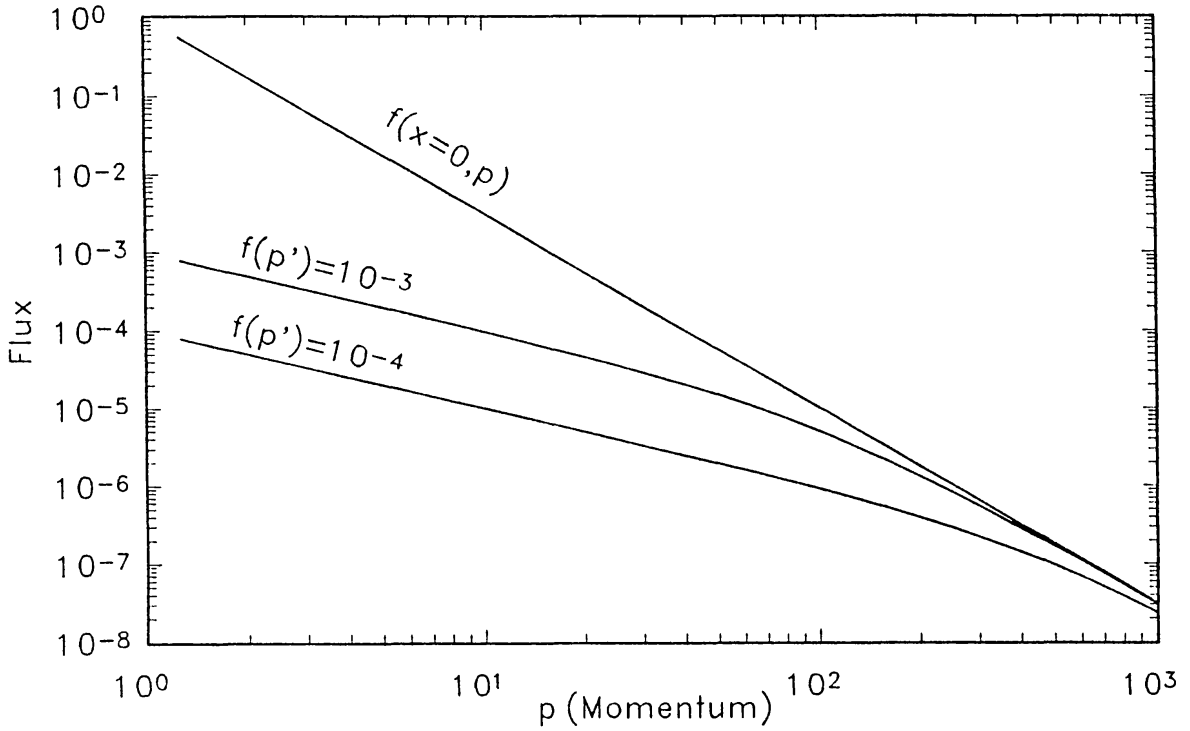

Fig. 4.1. The spectrum of particles produced by a shock with self-excited waves only. Spectra at the shock and at two positions upstream of the shock are shown. Adapted from Bell (1978b).

This result of Bell's was the first to show that, although the spectrum of accelerated particles downstream of the shock was a universal power law depending only on the compression ratio, upstream of the shock the spectrum depends on the point of observa-

tion and is harder (flatter) the farther upstream one looks. The fact that the spectrum merely flattens for low energies rather than exhibits an actual low-energy cutoff is due entirely to the assumption that *all* of the upstream scattering is due to the *self-induced* Alfvén waves. This is no longer true if one assumes that there are pre-existing waves that do not drop off proportionally to the particle density as one moves farther upstream from the shock.

4.1.2. *Lee's Theory of the Earth's Bow Shock and Interplanetary Shocks*

In a considerably more detailed theory, Lee (1982) modeled Fermi acceleration at the Earth's bow shock and at interplanetary traveling shocks (Lee, 1983). He applied the theory of linear wave growth to the particular types of waves believed to be appropriate for particle scattering in the solar wind paying particular attention to polarization states. He then used the quasi-linear theory of particle diffusion in these waves much as did Bell (1978a, b). Lee considered the 'seed' particles of the acceleration process to be produced by direct reflection of solar wind particles in regions of the Earth's bow shock where the shock geometry was quasi-perpendicular. These energized particles were then carried by the motion of the solar wind to regions where the shock geometry was quasi-parallel, allowing them to be accelerated by the Fermi mechanism. While Lee treats generation of Alfvén waves by the particles streaming upstream from the shock in considrably more detail then Bell did, he assumes that there is a pre-existing level of magnetic turbulence in the solar wind that continues to scatter the particles no matter how far they go upstream. Because of this, the particle densities drop off exponentially when one looks far enough upstream that the self-induced turbulence becomes unimportant compared to the pre-existing turbulence. Further, since the scale of the dropoff is longer for the more energetic particles, the spectrum upstream of the shock develops a low-energy cutoff rather than the flattening obtained by Bell. This characteristic of the upstream spectrum is borne out by observations of diffuse ions made upstream of the quasi-parallel Earth bow shock (e.g., Ipavich *et al.*, 1981, 1984). In addition Tan *et al.* (1989, 1990) have measured the diffusion coefficient just in front of six quasi-parallel interplanetary shocks and found excellent agreement with the predictions of Lee (1983). They did not find, however, the predicted spatial variation of the diffusion coefficient with distance in front of the shock. The reason for this does not seem to be understood.

In his bow shock theory, Lee (1982) included another factor that greatly modifies the spectrum at high energy, namely the finite probability that a particle can escape from the shock in some way other than being convected downstream. It is straightforward to see how this can affect the spectrum of accelerated particles since it changes the probability that a particle will return to the shock and be further accelerated. Equation (3.30) must be modified to become

$$\mathscr{P}(N) = \prod_{i=1}^{N/2} \left(\frac{1 - u_2/v_i}{1 + u_2/v_i} \right)^2 (1 - \varepsilon_i) , \tag{4.11}$$

where ε_i is the probability that the particle will *not* return to the shock but arrive at some other boundary of the system and be lost to the acceleration process. Proceeding just

as before but using Equation (4.11) instead of Equation (3.30) we obtain instead of Equation (3.35) for the integral spectrum

$$\mathscr{P}(p) = \left(\frac{p}{p_0}\right)^{-3u_2/(u_1-u_2)} \exp\left(\sum^{N/2} \varepsilon_i\right). \tag{4.12}$$

We may convert the sum over shock crossings to an integral over p by taking the differential of Equation (3.32) and noting that $\Delta n \equiv 1$ to obtain

$$\sum^{N/2} \varepsilon_i \Delta n \approx \int_{p_0}^{p} \frac{3v\varepsilon(p)}{2(u_1-u_2)} \frac{\mathrm{d}p}{p}, \tag{4.13}$$

where $\varepsilon(p)$ is now considered to be a function of p.

The next step is to obtain an estimate of the probability of non-return, ε. The most direct way is to solve the diffusion equation for particles injected one mean free path beyond the shock* and integrate the flux back through the shock from a time, t to ∞. This yields the probability that a particle will spent at least a time, t before recrossing the shock. After a straightforward, but rather tedious calculation that will not be repeated here one obtains

$$\mathscr{P}(t) = \mathrm{erf}\left[\left(\frac{\lambda^2}{vt}\right)^{1/2}\right] = \mathrm{erf}(n^{-1/2}) \approx \frac{2}{\pi^{1/2}} n^{-1/2} \quad \text{for} \quad n \gg 1, \tag{4.14}$$

where n is the number of times the particle scatters before recrossing the shock.

In Lee's theory of the Earth's bow shock, the alternate path out of the shock system was diffusion across the magnetic field of the solar wind to the outer edges where the particles freely escaped. Every time a particle scatters in a magnetic field its direction along the field is randomized but, in addition, its guiding center takes a gyroradius length random step across the field. If the width of the shock front is a, a particle would have to scatter n times to reach the edge of the shock where $n = \mathrm{a}^2/\mathrm{r}_\mathrm{g}^2$ and r_g is the particles gyroradius. From Equation (4.14) we have

$$\mathscr{P}(\text{escape}) \equiv \varepsilon \approx \frac{r_g}{a}. \tag{4.15}$$

Employing the expression for the gyroradius, $r_g = pc/(qB)$, we obtain for the integral in Equation (4.13)

$$\int_{p_0}^{p} \frac{3vpc}{2qBa(u_1-u_2)} \frac{\mathrm{d}p}{p} = \int_{E_0}^{E} \frac{3c}{2qBa(u_1-u_2)} \frac{1}{2} mv^2 \frac{\mathrm{d}E}{E} \approx \frac{3c}{2Ba(u_1-u_2)} \left(\frac{E}{q}\right), \tag{4.16}$$

* Particles passing through the shock will not have an isotropic distribution until they have scattered at least once, hence, they must travel a mean free path before they may be considered to be injected into a diffusion process.

where we have neglected the contribution of the lower limit. This gives for the integral spectrum

$$\mathscr{P}(p) = \left(\frac{p}{p_0}\right)^{-3u_2/(u_1-u_2)} \exp\left[\frac{3c}{2Ba(u_1-u_2)}\left(\frac{E}{q}\right)\right]; \tag{4.17}$$

an exponential cutoff in energy per charge.

This result was first obtained by Eichler (1981) who noted that in his derivation from the diffusion-convection equation the cutoff exponent was proportional to the product of the parallel and perpendicular diffusion coefficients, $\kappa_{\parallel}\kappa_{\perp}$. This product, as Eichler noted, is independent of the strength of the scattering process (i.e., the scattering frequency or the mean free path) and, hence, was a more reliably known quantity than were either of the two diffusion coefficients separately.

In the above derivation we have neglected the effect of convection in returning the particle to the shock; this is valid as long as the number of collisions required are not too large. Convection is important on scales of order $\lambda v/u$ therefore if $a/r_g \ll v/u$, diffusion is the dominant process and the preceding derivation is valid. If, however, the size of the shock front is large enough for this condition to be violated a different approach is required.

In this limt we see that the typical distance, Δy that a particle can diffuse parallel to the shock front before convection sweeps it back through the shock is much smaller than the scale of the shock front a. In this case $\Delta y^2 \approx \kappa_{\perp}\Delta t$ and $\Delta t \approx \kappa_{\parallel}/u_1^2$ so $\Delta y^2 \approx \kappa_{\perp}\kappa_{\parallel}/u_1^2 \approx r_g^2 v^2/u_1^2$, once again independent of the strength of the scattering. We may estimate the probability of escaping from the sides by the following argument: A particle will travel a distance, Δy parallel to the shock front in a time τ before convection sweeps it back across where $\Delta y^2 \approx \kappa_{\perp}\tau = \kappa_{\perp}\kappa_{\parallel}/u_1^2$. If it crosses the shock within a distance Δy from the edge, the previous arguments apply and it will escape with a probability r_g/a. The probability that it will cross this close to the edge is $\approx \Delta y/a$. Since $\kappa_{\perp}\kappa_{\parallel} \approx r_g^2 v^2$ we may multiply the two probabilities to obtain

$$\mathscr{P}(\text{escape}) \approx \frac{r_g^2 v}{a^2 u_1} \tag{4.18}$$

and since now $r_g/a < v/u_1$ we see that the probability for escape has been reduced by the effects of convection. We also see that the integral in the exponential function will now be proportional to E^2/q^2 rather than E/q as before.

As we shall see when we discuss the results of computer simulations of shock acceleration, similar results are obtained whenever free escape boundaries are introduced. The dependence on energy and the scattering process varies but the overall effect is to produce a steep, exponential like cutoff in the spectrum. It will also turn out that for the steady-state case some sort of loss other than downstream convection is necessary for the process to work at all if the shocks are sufficiently strong.

While Lee's model of diffuse ions at the Earth bow shock represented a breakthrough in the nonlinear treatment of wave-particle interactions, the fact that it is based on the

diffusion-convection equation and quasi-linear theory imposes two serious limitations. As we have emphasized above, the diffusion-convection equation requires that $v \gg u$ and precludes the treatment of thermal particle injection. Lee's model does not, therefore, describe particles with energies much below 20 keV/Q and he assumes that an independent seed population is convected into the quasi-parallel portion of the bow shock from the breakup of field-aligned beams originating at the quasi-perpendicular bow shock. While such seed particles may be important in certain bow shock configurations, recent observations made during times when the interplanetary magnetic field was nearly radial and when convection from the sides of the bow shock to the quasi-parallel regions did not occur, clearly show that Fermi acceleration can operate even without a separate, energetic and seed population. Lee's reliance on quasi-linear theory is also questionable in the light of recent simulation work (e.g., Zackary, 1987; Quest, 1988) which shows that large-angle scattering events are important in wave-particle interactions. This is discussed in more detail below.

4.2. Hydrodynamic effects of the accelerated particles: the 'two-fluid' approach

Particle acceleration at modified collisionless shocks, i.e., those shocks where acceleration is efficient enough for the accelerated particles to be dynamically important, has been described both analytically and with Monte-Carlo simulations. Blandford (1980) applied a perturbative approach in which the deceleration of the incoming gas was treated as a small parameter. While this steady-state approach is inadequate in most cases, it did show that when the diffusion coefficient was an increasing function of energy, the accelerated spectrum had positive curvature and the influence of the relativistic particles was to increase the compression ratio and the acceleration rate by decreasing the effective ratio of specific heats, γ_{eff}, of the gas. It is interesting to note that the main advantages of test particle shock acceleration (i.e., production of a power law with index near 2) are no longer strictly true when nonlinear effects are included.

In the so-called two-fluid model of particle acceleration (Drury and Völk, 1981), one takes a viewpoint that is the opposite extreme from the one used in the individual particle approach. Starting once again from the steady-state diffusion-convection Equation (3.16), an equation for the pressure produced by the energetic particles, P_c, is obtained by taking the suitable moment with respect to momentum, p, i.e.,

$$P_c = \frac{4\pi}{3} \int_0^\infty p^3 v f(p)\, \mathrm{d}p \tag{4.19}$$

yielding a 'hydrodynamic' equation for the pressure due to the energetic particles or cosmic rays

$$\frac{1}{\gamma_c - 1} \frac{\partial P_c}{\partial t} + \frac{\partial}{\partial x}\left(\frac{u P_c}{\gamma_c - 1}\right) + P_c \frac{\partial u}{\partial x} = \frac{\partial}{\partial x} \frac{\overline{\kappa}}{\gamma_c - 1} \frac{\partial P_c}{\partial x}\,, \tag{4.20}$$

where γ_c is the ratio of specific heats for the energetic particles ($\gamma_c = \frac{4}{3}$ if the particles are fully relativistic), and $\overline{\kappa}$ is the momentum averaged diffusion coefficient.

The accelerated particles can thus be treated as another fluid that interacts with the thermal plasma via its pressure. Equation (4.20) may be combined with the equations of mass, momentum, and energy flux conservation to form a set of equations that describe the composite or two-fluid system. They are:

$$\frac{\partial(\rho u)}{\partial x} = 0 \quad \text{mass flux}\,, \tag{4.21}$$

$$\frac{\partial}{\partial x}\,(\rho u^2 + P_g + P_c) = 0 \quad \text{momentum flux}\,, \tag{4.22}$$

$$\frac{\partial}{\partial x}\left(\frac{1}{2}\,\rho u^3 + \frac{\gamma_g}{\gamma_g - 1}\,uP_g + \frac{\gamma_c}{\gamma_c - 1}\,uP_c - \frac{\overline{\kappa}}{\gamma_c - 1}\,\frac{\partial P_c}{\partial x}\right) = 0 \quad \text{energy flux}\,; \tag{4.23}$$

where γ_g is the ratio of specific heats for the thermal gas ($\gamma_g = \frac{5}{3}$ for a monatomic non-relativistic gas), and P_g is the pressure of the thermal gas.

The difficulty with the set of conservation equations (Equations (4.21), (4.22), and (4.23)) is that it is not complete; there are three equations and four unknown quantities; ρ, u, P_g, and P_c. These equations do not supply enough information to integrate a set of starting values through the shock transition. In principle, one could employ Equation (4.20) as the fourth equation but a simpler solution is effected by employing two supplemental assumptions. The first is that the energetic particles do not transfer any heat to the gas, they only push it around. We may, therefore, add to the above equations one that describes the continuity of the entropy flux,

$$\frac{\partial(P_g u^{\gamma_g})}{\partial x} = 0\,. \tag{4.24}$$

This equation may not be used to deduce continuity of the entropy flux across a shock transition in the thermal plasma, however, because in the gas shock, dissipative processes will produce an increase in entropy and Equation (4.24) will not apply across the discontinuity. We must find some other consideration to reduce the number of independent variables. The additional assumption used in the two-fluid approach is that the presence of a gas shock has no 'local energetic' effect on the energetic particle population and thus their pressure and energy flux is continuous across the shock, i.e., $[P_c] = [\gamma_c u P_c - \overline{\kappa}\,\partial P_c/\partial x] = 0$. This condition completely decouples the energetic particles from the thermal plasma insofar as the jump across the thermal shock is concerned and thus the shock is a simple gas shock. (Equation (4.24) and the continuity of the energetic particles across the thermal gas shock can, in fact, be derived from the three conservation equations plus Equation (4.20), however, it is equally true that one may

take entropy conservation and continuity on an equal footing with the conservation equations and derive Equation (4.20) from them.)

An important implication of the above discussion is that the energetic particles can have no discontinuities because the diffusion term on the right-hand side of Equation (4.20) smooths out any tendency for such discontinuities to develop. The same would be true for the thermal gas if a dissipative term such as viscosity had been included for it, however, without such a term, dissipative transitions must be approximated by shock jumps.

Actually solving the above equations can be a rather complex procedure requiring several piecewise processes using different equations in different regions. For a more complete look at such solutions one should refer to the review article by Drury (1983) where it is pointed out that three basic types of solutions occur depending on the input parameters.

4.2.1. *'Weak Shock' Solution*

First, there are solutions for low Mach number shocks where an upstream pressure of energetic particles is amplified slightly by a shock in the thermal gas. The energetic particle pressure extends upstream of the shock for a few diffusion lengths, $\overline{\kappa}/u$, and the gradient of this pressure slows the incoming thermal gas somewhat before it undergoes the shock transition. The shock is weak enough, however, so that the increase in energetic particle pressure is not sufficient to completely smooth out the thermal shock. Since the relativistic particle pressure now plays a part in the overall shock dynamics, the compression ratio can no longer be determined by assuming that $\gamma = \frac{5}{3}$. Instead, the effective specific heat ratio, γ_{eff}, will have a contribution from relativistic particles and will approach $\frac{4}{3}$ as the shock strength increases. Perhaps most important of all, the compression ratio will no longer be limited to four but can increase to seven due to the smaller γ_{eff}.

4.2.2. *Cosmic-Ray Dominated Solution*

The second so-called 'cosmic-ray dominated' solution occurs for somewhat stronger shocks where the pressure provided by energetic (i.e., relativistic) particles is such that the entire transition is mediated by the diffusion of the energetic particles. In this solution, there is no shock at all in the thermal gas; the gas is heated only by adiabatic compression and its major role is in supplying the mass and flow kinetic energy to compress and heat the energetic particles. In this case, the four equations given above are valid throughout the entire transition and may be used to obtain the overall jump conditions. The compression ratio is given by the algebraic equation (after factoring out the trivial $r = 1$ solution)

$$\eta_c\left[1 - \left(\frac{1}{\gamma_c \mathscr{M}_{c1}^2}\right) r\right] - \frac{1}{2}(r+1) = (\eta_c - \eta_g)\left(\frac{1}{\gamma_g \mathscr{M}_{g1}^2}\right)\frac{r(r^{\gamma_g} - 1)}{r - 1}\,, \tag{4.25}$$

where $\eta_i \equiv \gamma_i/(\gamma_i - 1)$, the Mach numbers are $\mathscr{M}_{i1}^2 \equiv \rho_1 u^2/\gamma_i P_{i1}$, and $i = c$ or g (see also Baring and Kirk, 1991).

In the case that the thermal gas can be considered to be cold (i.e., its pressure plays no role in the dynamics), Equation (4.25) becomes even simpler, reducing to the expression for a single component gas shock

$$r = \frac{\mathcal{M}_{c1}^2(\gamma_c + 1)}{(\gamma_c - 1)\mathcal{M}_{c1}^2 + 2} \,. \tag{4.26}$$

For large values of $\mathcal{M}_{c1}^2$, r approaches 7 for $\gamma_c = \frac{4}{3}$, just as it would approach 4 in Equation (3.7) if $\gamma_g = \frac{5}{3}$. It should be noted that such shocks have been shown (Dorfi and Drury, 1985; Zank and McKenzie, 1985, 1987; Drury and Falle, 1986; Berezhko *et al.*, 1987) to be hydrodynamically unstable for certain situations.

The cosmic-ray dominated solution is basically a shock in the energetic particle gas with the thermal gas coming along for the ride apart from providing mass and thus flow momentum and energy. The transition would not look like a shock to the thermal gas since any compressional heating that it might undergo would be purely adiabatic. While such shocks are probably allowed by the laws of physics, it is hard to imagine what sort of process could initiate one. In the Galaxy, cosmic rays have scattering lengths on the order of 10^{13} cm, and the driver of a cosmic-ray dominated shock would have to be smooth on this scale and yet be energetic enough to accelerate the thermal gas to supersonic speeds by means of the cosmic rays diffusing through it, all without producing a shock in the gas itself. Such shocks probably do not exist in nature although they cannot be ruled out.

4.2.3. *Efficient Shocks*

The third type of two-fluid shock solution is even more unexpected; Drury and Völk (1981) noted that for Mach numbers (calculated using the combined pressures of the two fluids) greater than about 5, the downstream state did not always follow uniquely from the upstream state. For certain low values of the upstream value of P_{c1}, at least two values for the downstream P_{c2} were possible. One was the value obtained from the weak shock solution while the other was a considerably higher value of P_{c2}. In fact, Drury and Völk (1981) predict that for Mach numbers above about 6, large downstream cosmic-ray pressures can result even for a zero value of P_{c1}. The energetic particle pressure is created out of nothing! The solution with zero upstream P_{c1} is called the 'efficient' solution (Baring and Kirk, 1991) and it can occur even in the cosmic-ray dominated case where no thermal shock exists. The implication is that even with no thermal gas subshock to inject particles from the thermal gas and no upstream energetic seed particles, these shocks could still generate cosmic rays, creating them out of nothing. Baring and Kirk did not consider the cosmic-ray dominated case because of the possibility of instabilities (mentioned above), and restricted their treatment to profiles which included subshocks, though they made no self-consistent inclusion of particle injection at the discontinuity.

Since injection is not explicitly included in these models and since one can go continuously from efficient shocks with a gas subshock to ones with no subshock, there

is little reason to believe that models with a subshock are more physical than those without. By only allowing solutions that contain a subshock, Baring and Kirk draw the conclusion that only weak shocks can accelerate particles. This clearly contradicts a host of observational evidence.

Such unphysical solutions appear to us to arise out of the lack of conservation of energetic particle flux in the set of equations govenring the shocks. Since the two-fluid models involve only momentum, energy, and total mass flux, it is not clear how one could include this constraint in the analysis. However, conservation of cosmic-ray particle number must hold unless there is explicit injection, and such a constraint would prevent these 'something from nothing' solutions.

Another feature of the steady-state two-fluid models that contributes to the existence of such unphysical solutions is the lack of spectral information and with it the lack of a cutoff at high energy. In any real, finite-size shock of large Mach number, energetic particles are likely to escape from the shock and carry away an appreciable amount of energy flux before being convected far downstream. This will clearly happen if the diffusion coefficient increases with energy, as it is expected to do, because as the diffusion scale becomes larger it eventually exceeds the scale of the shock itself and, as discussed in Section 4.1, this will limit the acceleration process and produce a sharp cutoff in the spectrum of accelerated particles.

If energy escapes from the shock, this escaping flux must be included *explicitly* in the R–H relations and the compression ratio will not be as given in Equations (4.25) and (4.26) but instead will depend on the escaping energy flux. Much as in the case of radiative shocks, the compression ratio can become arbitrarily large. The problem of particle escape and, therefore, increased compression ratio is not necessarily eliminated simply by taking the limit as the cutoff energy $E_{\max} \to \infty$. For strong shocks, as $E_{\max}$ increases, the contribution to the downstream pressure from relativistic particles also increases and γ_{eff} approaches $\frac{4}{3}$. This can flatten the accelerated spectrum until the spectral index is less than 2 and the energy in accelerated particles no longer converges as $E_{\max} \to \infty$. Ellison and Eichler (1984) have shown that there exists some transition Mach number, $\mathcal{M}_t \sim 4$, which is quite insensitive to upstream conditions, below which the steady-state acceleration process will converge as $E_{\max} \to \infty$. For Mach numbers above $\mathcal{M}_t$, the relativistic particles play a sufficient role in the dynamics such that the compression ratio is greater than 4 over some finite length scale. Since the diffusion coefficient increases with energy there will be some energy, E_{crit}, such that cosmic-ray particles with $E > E_{\text{crit}}$ have a diffusion length long enough to feel a simple shock with a compression ratio greater than 4. The equilibrium spectrum above E_{crit} will, therefore, be flatter than E^{-2} and have a divergent energy density. This will occur no matter how large E_{crit} is and so the acceleration process must be truncated at some finite $E_{\max}$ if the process is ever to settle down to a steady-state solution. Since the steady-state, two-fluid models we have been discussing do not have energy cutoffs, particles can accelerate forever and realistic solutions only occur for shock with $\mathcal{M} < \mathcal{M}_t$.

In principle, this problem is avoided if κ is independent of energy. In this case, it has been shown (Drury *et al.*, 1982; see also Blandford and Eichler, 1987) that the competing

effects of shock smoothing due to the cosmic-ray pressure and the increase of the compression ratio due to the lowering of γ_{eff} just conspire to produce a spectral index that approaches 2 as $\mathcal{M} \to \infty$ without introducing a cutoff. However, κ must be strictly independent of energy. The definition of the pressure weighted diffusion coefficient that is used in two-fluid models with energy-dependent κ's,

$$\overline{\kappa}(x) = \frac{\int_0^\infty p^3 v \kappa(p) \frac{\partial f}{\partial x} \, dp}{\int_0^\infty p^3 v \frac{\partial f}{\partial x} \, dp} \tag{4.27}$$

requires that $\sigma > 2 + \varepsilon$ if $\kappa(p) \sim p^\varepsilon$. Thus a diffusion coefficient that increases with energy however slightly will cause the two-fluid models without a cutoff to become physically inconsistent above some critical Mach number.

Furthermore, it is not consistent to treat γ_{eff} as a parameter. Since γ_{eff} (thermal gas plus cosmic rays) will influence the compression ratio, and the compression ratio determines the spectrum, which then determines γ_{eff}, the properly weighted ratio of specific heats must be determined within the calculation (Achterberg84;Ellison and Eichler, 1984). Two-fluid calculations which do not include spectral information do not determine γ_{eff} self-consistently.

4.3. Extensions and Generalizations of Two-Fluid Method

4.3.1. Steady-State Calculations

The simple two-fluid model of Drury and Völk (1981) has been extended and generalized in several ways. In a steady-state calculation, Völk *et al.* (1984) (see also McKenzie and Völk, 1982) calculate interactions between the energetic particles and Alfvén waves with a finite Alfvén velocity. Cosmic-ray energy is assumed to produce the scattering responsible for particle diffusion and some cosmic-ray energy is transferred efficiently to the background gas since the magnetic waves are assumed to damp quickly. This transfer of energy heats the gas and increases the range of Mach numbers where 'weak-shock' solutions are allowed. However, the fundamental problems of the steady-state, two-fluid calculation remain: injection without conservation of cosmic-ray particle number, no energy escape in high-Mach number shocks, and no self-consistent determination of γ_{eff}. In addition, Völk *et al.* (1984) use an energy-independent diffusion coefficient.

Heavens (1983, 1984) extended the steady-state, two-fluid technique to include, in addition to wave generation and damping, a self-consistent calculation of γ_{eff} and an energy-dependent diffusion coefficient. When the diffusion coefficient is constant, the scale invariance of the hydrodynamic equations allows only a power-law cosmic-ray spectrum (see Schneider and Kirk, 1987). A diffusion coefficient which increases with energy will produce spectra which flatten as energy increases, as shown by Blandford

(1980), and will exacerbate the problems seen in Drury and Völk with cosmic-ray dominated shocks. The maximum Mach number where stable solutions exist decreases from about 12 (approximately what Völk *et al.* find) to about 6, most likely from the different weighting given γ_{eff} when the energy spectrum flattens with increasing energy. To allow analytic solutions, Heavens uses some approximation which relies on the assumption that if $\kappa \to \infty$ as $p \to \infty$, the high-energy spectral index will approach the test particle result, $\sigma = (r + 2)/(r - 1)$. The addition of wave generation and damping increases the range of stable solutions in the same way reported by Völk *et al.* (1984), but particle escape is not included in these calculations.

4.3.2. *Time-Dependent Calculations*

Substantial improvements on the two-fluid formalism are made when time-dependent calculations are performed and the problem of escape at high energies in steady-state shocks can be replaced by a cutoff resulting from a finite acceleration time. Falle and Giddings (1987) and Bell (1987) present similar numerical time-dependent calculations which allow a determination of the cosmic-ray particle spectrum (see Dorfi, 1984, 1985, for earlier studies in the hydrodynamic limit). Among other advantages, determination of the spectrum eliminates errors from demanding that particles are either fully non-relativistic (the thermal gas with $\gamma = \frac{5}{3}$) or fully relativistic (the cosmic-ray gas with $\gamma = \frac{4}{3}$), as done in analytic solutions. In reality of course, large contributions to the particle pressure can come from particles with energies near mc^2 and this may significantly change the analytic results. Each of these calculations include self-generated waves, a momentum-dependent κ ($\kappa \sim p^{\alpha}$ in each case), and the self-consistent determination of γ_{eff} from the particle distribution function. They differ in relatively minor ways; Bell is able to use a somewhat stronger momentum dependence than Falle and Giddings ($\frac{1}{3} < \alpha < \frac{1}{2}$ versus $\alpha = \frac{1}{4}$) and the details of injection differ. However, both techniques use a constant injection rate expressed as some fraction, ε, of either the upstream particle density (Bell) or the mass flux into the subshock (Falle and Giddings). While the injection rate can vary with time during the calculation due to changes in the density and flux, ε is a constant parameter in both cases. Both solutions also ignore the mass density of the cosmic rays in the conservation equations as was done in previous steady-state calculations.

One important difference between the calculations of Falle and Giddings and Bell lies in the treatment (or lack thereof) of particle escape. Bell has a maximum energy cutoff in this time-dependent solutions and particles are seen to freely leave the system in some models. He does not explain, however, whether or not the energy flux that escapes is included in the determination of the overall compressin ratio. Falle and Giddings, on the other hand, do not explicitly include a high-energy cutoff or particle escape in their calculations even when they run the solutions long enough to obtain quasi-steady-state results. Presumably, above some Mach number, and beyond some run time, significant particle escape would occur in both calculations. Bell shows one case (see Figure 4.2) with spectra extending to $p = 10^6 m_p c$ (i.e., $\sim 10^{15}$ eV) which show significant particle escape at the maximum energy after about 300 time units (one unit = L_1/u_1, where L is the scale length of $m_p c$ protons and u_1 is the shock velocity = $0.01c$).

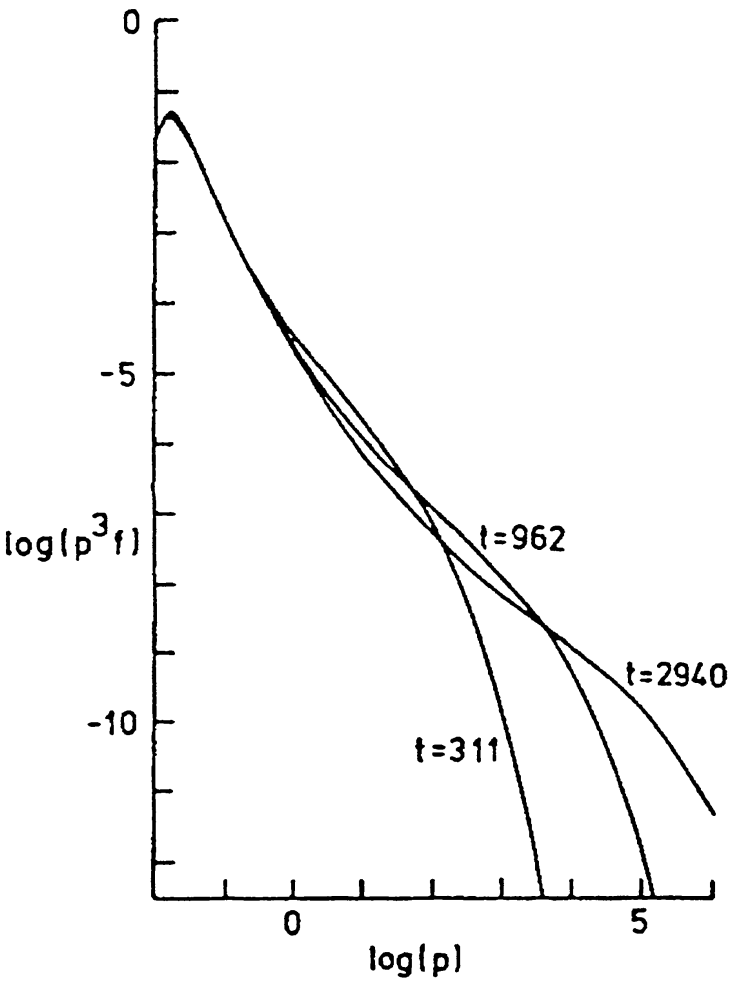

Fig. 4.2. Energetic particle spectra at various times over a large momentum range ($p_{max} = 10^6$; see Bell, 1987, for units and details of calculation). The upper end of the simulation box in momentum is at $p = 10^6$ and it is clear from the curve label $t = 2940$ that a significant fraction of the energy flux leaves the box at this cutoff. The concave nature of the spectra is evident and results from shock smoothing which produces more efficient acceleration for higher energy particles (assuming, as is done here, the κ increases with energy).

All of the two-fluid solutions we are aware of, steady-state and time-dependent, show the subshock vanishing for Mach numbers above some limit even in the limit when no upstream cosmic rays are injected. The Mach number limit may depend on wave generation and the details of the injection parameterization, but the fundamental inconsistency of not including cosmic-ray particle conservation remains. In addition, energy escape through an high-energy cutoff is not explicitly included in any of the models except those of Bell (1987). Since, in general, particles can escape for certain Mach numbers and for certain momentum dependencies of the diffusion coefficient even in the time-dependent calculations (e.g., Bell, 1987), this important nonlinear effect must be included in a general time-dependent solution.

For applications of the time-dependent two-fluid model to the production of cosmic-rays in supernova remnants, see Drury *et al.* (1989), Markiewicz *et al.* (1990), and Kang and Jones (1990, 1991).

4.4. Eichler's treatment of modified shocks

An alternative analytic treatment of modified shocks which avoids many of the problems intrinsic to the two-fluid technique and allows the calculation of the particle spectrum was developed by Eichler (1979, 1984, 1985) (see also Krymsky, 1981). This method is reviewed in Blandford and Eichler (1987) and we will not give a detailed description here. The essential features of Eichler's steady-state calculation are the following: first, it is clear from our discussion above that in all but low-Mach number cases, steady-state shocks must lose energy at some high-energy cutoff, $E_{\max}$, and this energy loss must be included in the R–H relations. In all real astrophysical shocks κ is expected to be an increasing function of energy, and particle escape becomes more important as the energy dependence of κ increases. Eichler is able to solve the diffusion-convection equation including energy escape by taking advantage of approximations resulting from the assumed rapid increase in κ with energy. If κ is a strong function of E, the diffusion length for high-energy particles will become extremely large and the shock will contain a large range of spatial and energy scales. These scales can, in effect, be separated by making the approximation that there is a characteristic distance upstream from the thermal subshock, $\bar{x}(E)$, out to which particles of energy E diffuse. The pressure in these particles is assumed to be constant downstream from $\bar{x}(E)$ and zero upstream from $\bar{x}(E)$. The more rapidly κ increases with E, the more accurate this approximation becomes, but it has been shown to be quite good (by comparison with Monte-Carlo simulations) for $k \sim p^{\alpha}$ with $\alpha \gtrsim 1$ (see Eichler, 1984; and Blandford and Eichler, 1987, for more complete discussions). This is a real advantage over the two-fluid models discussed above because even numerical solutions (e.g., Falle and Giddings, 1987; Bell, 1987) have difficulties when κ increases even slowly with energy.

Eichler's solutions are parameterized by the escaping energy flux, q, out $E_{\max}$, and by applying the condition that the accelerated particle solution develops a thermal peak at $E \simeq m_p u_2^2$, q can be constrained, within a factor of order unity, to some particular value and a unique solution can be found. In contrast to previous two-fluid models, it is predicted that the acceleration efficiency increases monotonically with Mach number, and cosmic-ray dominated shocks do not occur (note that pre-existing cosmic rays are not injected in Eichler's solution). As a consequence, there will always be some shock heating, an important consideration when interpreting observations of thermal X-rays in astrophysical objects.

Eichler's solutions have been compared directly to spacecraft observations of an interplanetary traveling shock. Ellison and Eichler (1984) show that the method produces a good fit to a proton spectrum from about 0.1 keV to above 1 MeV obtained during quasi-parallel shock conditions (Gosling81).

This technique has been further generalized to obtain a relativistic spectrum by treating the entire nonrelativistic shock structure as a subshock (Eichler, 1984). Energy is conserved in going from purely nonrelativistic to relativistic kinematics by matching the energy flux through the transition at $m_p c^2$ for both the nonrelativistic and relativistic portions of the calculation. In effect, the nonrelativistic solution has an $E_{\max} = m_p c^2$

which feeds power to the relativistic solution. The effective ratio of specific heats is found by taking a weighted average of $\gamma_g = \frac{5}{3}$ (nonrelativistic particles) and $\gamma_c = \frac{4}{3}$ (relativistic particles). This was the first calculation to self-consistently determine γ_{eff}, however, later calculations of Heavens (1984), Falle and Giddings (1987), and Bell (1987) do a better job in this regard in that γ_{eff} is determined from the distribution function.

The general properties of Eichler's solution were presented in Ellision and Eichler (1984). As mentioned above, they found a critical transition Mach number, $\mathcal{M}_t \sim 4$, in steady-state shocks, above which no solution exists unless energy flux escapes at some $E_{\max}$. The particle spectrum above $\sim m_p c^2$ is not a power law but flattens with increasing energy and, as a result, high Mach number shocks with a large dynamic range have their energy divided mainly betwee a thermal peak and a peak at the highest energies with the separation between these peaks becoming more pronounced as the energy dependence of κ increases. The spectrum and efficiency (i.e., the fraction of total energy flux which ends up in relativistic particles) for high Mach number shocks are nearly independent of the injection efficiency, i.e., the shock regulates the acceleration efficiency, via the effects of cosmic-ray backpressure on the subshock, to place approximately the same fraction of energy in the highest energy particles.

Wave generation and damping have also been included (Eichler, 1985; Ellison and Eichler, 1985) and applied to conditions expected for SNRs. A finite phase velocity, v_{ph}, for the waves producing particle scattering will decrease the acceleration efficiency considerably. However, it is shown that for the small v_{ph} expected in the interstellar medium ($v_{ph}/u_1 \gtrsim 0.05$), spectra that depend only weakly on the shock Mach number are produced and these appear to be close enough to E^{-2} to satisfy requirements on the source spectrum of cosmic rays as deduced from observations after energy-dependent leakage from the galaxy is included.

No time-dependent generalization of Eichler's method has yet been made, but Berezhko *et al.* (1990) have included acceleration of a pre-existing cosmic-ray background in a steady-state model.

5. Acceleration by Oblique and Quasi-Perpendicular Shocks

In our discussion up to now we have considered only parallel or nearly parallel shocks. In shocks of this kind the average magnetic field plays essentially no role since it is homogeneous, while fluctuations in the average field play a secondary role producing particle scattering. However, for oblique shocks, the magnetic field intensity and average direction change across the shock transition and the magnetic field becomes dynamically important. In most shocks, the magnetic field intensity increases across the shock and the increased magnetic field strength can reflect particles and produce an energy change. (In slow-mode shocks, the magnetic field decreases across the shock and is bent towards the shock normal.) To begin our discussion of oblique shocks, we describe some of the changes the magnetic field produces and why they come about.

5.1. THE COPLANARITY PLANE, POTENTIALS, AND OUT OF THE PLANE MAGNETIC FIELD COMPONENTS

In an infinite, plane-parallel shock, quantities change in only one direction (we have chosen the x-direction for our discussion) and the requirement that the magnetic field be divergence free requires that the field be unchanged through the shock transition. In an oblique shock, the magnetic field has a component perpendicular to the shock normal (we choose the z-direction without loss of generality) that will change across the shock although the divergence free requirement still requires that B_x remain unchanged. If we choose the field to lie in the $x - z$ plane upstream of the shock it may be shown (Kantrowitz and Petschek, 1966) that it must lie in the same plane downstream from the shock. Since there is no electric field in the upstream frame (the frame moving with the fluid), in the NI frame the upstream field is given by Equation (3.13), $\mathbf{E}_1 = -\mathbf{u}_1 \times \mathbf{B}_1/c$ and is in the y-direction. In a steady state, $\partial\mathbf{B}/\partial t = 0$ and thus $\mathbf{E}$ must be curl free.

Although there can be a charge separation layer in the transition region of the shock, overall charge neutrality requires that the integral of the charge density and, hence, the divergence of the electric field be zero. We therefore have $E_{1x} = E_{2x} = 0$ and the downstream electric field is also in the y-direction. This implies that $\mathbf{u}_1$, $\mathbf{B}_1$, $\mathbf{u}_2$, and $\mathbf{B}_2$ all lie completely in the $x - z$ plane which is therefore named (somewhat clumsily) the coplanarity plane.

Within the transition region the above arguments do not apply since there may be a component of the electric field in the x-direction and the magnetic field can make an excursion out of the coplanarity plane (see Goodrich and Scudder, 1984, 1986; Cairns, 1986). Although a detailed study of this layer requires computer simulations we can learn much about the structure of the collisionless shock transition layer by simply considering the balance of forces on the different components of the plasma. It is well known (Tidman and Krall, 1971; Ohsawa and Sakai, 1987) that a magnetosonic soliton requires a large electric field in the x-direction to deflect electrons in the y-direction. This produces the electric current which in turn produces the $\partial\mathbf{B}/\partial x$ for the pulse. In all except strictly parallel shocks, the average magnetic field changes across the transition layer so that the same considerations apply. Such changes must satisfy Maxwell's equations and in particular

$$\mathbf{j} = \frac{c}{4\pi} \nabla \times \mathbf{B}, \tag{5.1}$$

where $\mathbf{j}$ is the current density flowing in the plasma. The magnetic field exerts a ponderomotive force on the plasma given by

$$\mathbf{F} = \frac{1}{c} \mathbf{j} \times \mathbf{B}. \tag{5.2}$$

Combining the above two equations we obtain

$$\mathbf{F} = \frac{1}{4\pi} (\nabla \times \mathbf{B}) \times \mathbf{B} = \frac{\mathbf{B} \cdot \nabla \mathbf{B}}{4\pi} - \nabla \left(\frac{B^2}{8\pi} \right), \tag{5.3}$$

which may be written in component form as

$$F_x = -\frac{\partial}{\partial x}\left(\frac{B^2}{8\pi}\right), \qquad F_y = \frac{B_x}{4\pi}\frac{\partial B_y}{\partial x}, \qquad F_z = \frac{B_x}{4\pi}\frac{\partial B_z}{\partial x}. \tag{5.4}$$

The x-component of this ponderomotive force is balanced by the ram pressure of the plasma which is carried mainly by the ions but is applied to the electrons since they produce the majority of the current that interacts with the magnetic field. For the force to be transmitted to the ions there must be an electric field or a $\mathbf{u} \times \mathbf{B}$ force in the x-direction such that $ne[\mathbf{E} + (\mathbf{u} \times \mathbf{B})/c]_x = F_x$.

For a shock to exist, the upstream flow must be at least super-Alfvénic so that $u_1 > B/\sqrt{4\pi\rho}$ which implies that $\rho u_1^2/2 > B^2/8\pi$, i.e., the β of the plasma is not negligible. In this case we must consider the thermal pressures produced by the particles as well as the electromagnetic forces. Further we shall consider that the electrons are not the sole bearers of the current, rather we shall allow the ions to carry a fraction, ε, of the total current. We may thus write the forces on the electrons and ions, respectively, as:

$$\begin{aligned} F_{ex} &= -neE_x - (1-\varepsilon)\frac{\partial}{\partial x}\left(\frac{B^2}{8\pi}\right) - \frac{\partial}{\partial x}(P_e) + \frac{ne}{c}u_z B_y, \\ F_{ix} &= neE_x - \varepsilon\frac{\partial}{\partial x}\left(\frac{B^2}{8\pi}\right) - \frac{\partial}{\partial x}(P_i) - \frac{ne}{c}u_z B_y, \end{aligned} \tag{5.5}$$

where P_e and P_i are the electron and ion thermal pressures, respectively.

Since the x-component of acceleration must be the same for both species of particles, we require that $F_{ix}/m_i = F_{ex}/m_e$ and we may solve for the x-component of the electric field

$$E_x = \frac{u_z}{c}B_y - \left[\frac{(\delta-\varepsilon)}{ne}\frac{\partial}{\partial x}\left(\frac{B^2}{8\pi}\right) + \frac{\delta}{ne}\left(\frac{\partial P_e}{\partial x} - \frac{m_e}{m_i}\frac{\partial P_i}{\partial x}\right)\right], \tag{5.6}$$

where $\delta \equiv m_i/(m_i + m_e) \approx 1$. Applying the same argument for the z-component of acceleration we obtain the following expression:

$$\frac{\varepsilon B_x}{4\pi m_i}\frac{\partial B_z}{\partial x} + \frac{enu_x B_y}{m_i c} = \frac{(1-\varepsilon)B_x}{4\pi m_e}\frac{\partial B_z}{\partial x} - \frac{enu_x B_y}{m_e c}. \tag{5.7}$$

We may solve this expression for B_y to obtain:

$$B_y = (\delta - \varepsilon)\frac{cB_x}{4\pi neu_x}\frac{\partial B_z}{\partial x}. \tag{5.8}$$

An integrated (from upstream to downstream) form of this expression was obtained (with $\delta = 1$ and $\varepsilon = 0$) by Jones and Ellison (1987).

In the HT frame $u_z/u_x = B_z/B_x$ so that the first term on the right-hand side of Equation (5.6) may be written as

$$\frac{u_z B_y}{c} = \frac{u_x B_z B_y}{c B_x} = \frac{\delta - \varepsilon}{ne} \frac{\partial}{\partial x}\left(\frac{B_z^2}{8\pi}\right), \tag{5.9}$$

yielding the generalized Ohm's law

$$E_x = -\frac{\delta - \varepsilon}{ne} \frac{\partial}{\partial x}\left(\frac{B_y^2}{8\pi}\right) - \frac{\delta}{ne}\left(\frac{\partial P_e}{\partial x} - \frac{m_e}{m_i} \frac{\partial P_i}{\partial x}\right). \tag{5.10}$$

It is interesting to note that if we had a completely charge symmetric plasma such as an electron-positron plasma where $m_i = m_e$, $P_i = P_e$, and $\varepsilon = \frac{1}{2}$, the above equations show that we would have $E_x = B_y = 0$. The assumption that $\varepsilon = \frac{1}{2}$ for such a plasma, while quite plausible, is not, at present, proven. What can be shown rigorously is the following:

– The equations that govern plasma shocks, Maxwell's and Newton's (or Einstein's), are unchanged under the operations of parity inversion, rotation, and charge conjugation.

– An electron-positron plasma transforms into itself under charge conjugation.

Therefore, *any* solution of the above equations for an electron-positron plasma with a particular set of values for **B**, **E**, **u**, and spatial variations will lead to other, equally valid, solutions upon application of these symmetry operations. In particular a shock solution can be transformed in the following manner:

$$\begin{bmatrix} B_x & B_y & B_z \\ E_x & E_y & 0 \\ u_x & u_y & u_z \\ \partial_x & 0 & 0 \end{bmatrix} \xrightarrow{\text{parity}} \begin{bmatrix} B_x & B_y & B_z \\ -E_x & -E_y & 0 \\ -u_x & -u_y & -u_z \\ -\partial_x & 0 & 0 \end{bmatrix}$$

$$\begin{bmatrix} B_x & B_y & B_z \\ -E_x & -E_y & 0 \\ -u_x & -u_y & -u_z \\ -\partial_x & 0 & 0 \end{bmatrix} \xrightarrow{\text{rotate about } Y\text{-axis}} \begin{bmatrix} -B_x & B_y & B_z \\ E_x & -E_y & 0 \\ u_x & -u_y & u_z \\ \partial_x & 0 & 0 \end{bmatrix} \tag{5.11}$$

$$\begin{bmatrix} -B_x & B_y & -B_z \\ E_x & -E_y & 0 \\ u_x & -u_y & u_z \\ \partial_x & 0 & 0 \end{bmatrix} \xrightarrow{\text{charge conjugation}} \begin{bmatrix} B_x & -B_y & B_z \\ -E_x & E_y & 0 \\ u_x & -u_y & u_z \\ \partial_x & 0 & 0 \end{bmatrix}$$

Therefore, any shock solution for a charge symmetric plasma with particular values of B_y and E_x has an equally valid solution with these fields reversed. Since the equations

are nonlinear, the symmetric superposition of these solutions with zero value for these fields need not be a solution due to the possibility of spontaneous symmetry breaking. The study of such shocks is of considerable interest because the termination shock of a pulsar wind is expected to be of this type.

5.1.1. *Observations*

The integrated form of Equation (5.8) proposed by Jones and Ellison (1987) has been shown to be valid for subcritical shocks by several observations (Gosling *et al.*, 1988; Friedman *et al.*, 1990). In addition there is evidence (Burton *et al.*, 1988) that for slow shocks observed in the Earth's magnetotail, in which B_z decreases in traversing the shock from upstream to downstream, the sign of B_y is the opposite of that in fast shocks as would be predicted by Equation (5.8). The breakdown of the simpler prediction of Jones and Ellison for supercritical shocks is to be expected since it was assumed that all of the current responsible for the transition of the magnetic field across the shock was carried by the electrons ($\varepsilon = 0$). It is well known (e.g., see Kennel, 1988) that for supercritical shocks the conductivity of the electrons cannot furnish the dissipation required for the shock transition to occur and thus reflection of ions off of the shock plays an important role in the heating process. These ions carry a significant portion of the current of Equation (5.1); in other words $\varepsilon \neq 0$.

It would be a mistake to believe that Equation (5.8) represents a great step forward in the understanding of this phenomenon; the quantity ε is a free parameter and cannot at present be determined from first principles. We can, however, determine its sign. It can be shown (Jones and Ellison, 1987) that the current of Equation (5.1) when dotted into the $\mathbf{u} \times \mathbf{B}$ electric field gives

$$\mathbf{E} \cdot \mathbf{J} = -\nabla \cdot \left(\frac{c}{4\pi} \mathbf{E} \times \mathbf{B} \right) = -\nabla \mathbf{S}, \tag{5.12}$$

where $\mathbf{S}$ is the Poynting flux. Since in a fast shock the magnetic field increases from upstream to downstream, the Poynting flux also increases in traversing the shock. The current in the transition region, $\mathbf{j}$, must be in a direction such that the particles that produce it give up energy to the fields. The reflected ions, however, gain energy in the reflection process and thus contribute a negative amount ($\varepsilon < 0$) to the current. From Equation (5.8) we see that B_y must be *larger* than it would be if ε were zero and the ions did not contribute to the current. This is, in fact, what the observations (Gosling *et al.*, 1988; Friedman *et al.*, 1989, 1990) have shown.

5.2. Acceleration by Quasi-Perpendicular Shocks

As we have seen in Sections 3.2 and 3.3, the spectrum of energetic particles produced by diffusive shock acceleration does not depend on the diffusion coefficient, κ, to lowest order. The diffusion coefficient, together with the characteristic flow velocity, u, does, however, determine the overall length scale, κ/u, and the overall time scale, κ/u^2, of the acceleration process. It is not until other scales of the process, such as the shock thickness or curvature radius, the mean free path, or, as we shall see, the particle

gyroradius in the direction perpendicular to the magnetic field, become comparable to κ/u, or the lifetime of the shock becomes comparable to κ/u^2, do deviations from the pure power-law spectrum become evident. Lagage and Cesarsky (1983) have discussed how the fundamental time scale produced by the finite lifetime of a supernova shock limits the maximum cosmic-ray energy that such shocks can produce. They estimate that, based on the minimum value that the diffusion coefficient (and thus the acceleration time scale) can have, $\approx r_g v$, where r_g is the particle gyroradius, the maximum energy that a supernova shock can accelerate a particle to is $\approx 10^5$ GeV nucl^{-1}. Jokipii (1987) and Ostrowski (1988), on the other hand, have pointed out that the diffusion coefficient in directions perpendicular to the average magnetic field can be much smaller than this minimum value. In most theories of particle diffusion in magnetic fields, the following relation applies (Forman *et al.*, 1974)

$$\kappa_\perp = \frac{\kappa_\parallel}{1 + (\lambda_\parallel / r_g)^2} \,. \tag{5.13}$$

If we take $\kappa_\parallel = v\lambda_\parallel/3$ and assume $\lambda_\parallel \gg r_g$, we have $\kappa_\perp = v r_g (r_g/3\lambda_\parallel)$ which can be much smaller than the minimum value of κ chosen by Lagage and Cesarsky. If diffusion perpendicular to the magnetic field is important, as it will be in quasi-perpendicular shocks, this implies that the maximum particle energy that can be produced by a supernova shock may be increased substantially above the Lagage and Cesarsky estimate. Due to the important role that quasi-perpendicular shocks may play in producing the highest energy cosmic-ray particles, we must take a closer look at their properties and at the applicability of Equation (5.13).

5.2.1. *'Shock Drift' Versus Diffusive Acceleration*

Many authors (e.g., Armstrong and Decker, 1979; Pesses, 1979; Jokipii, 1982; Decker and Vlahos, 1986a) have pointed out that the principal process whereby a particle gains energy upon crossing a perpendicular or quasi-perpendicular shock is the so-called 'shock drift' process. This process, best viewed in the shock normal frame, is, as the name implies, the drift of the particles gyro-orbit in the steep magnetic gradient of the shock transition. This drift is in a direction that is perpendicular to both the magnetic field gradient (i.e., the shock normal) and the magnetic field and is given by

$$\mathbf{V}_d = \frac{pcv}{3e}\left[\nabla \times \left(\frac{\mathbf{B}}{B^2}\right)\right]. \tag{5.14}$$

The electric field that is induced by the motion of the plasma across the magnetic field, given by Equation (3.13), i.e., $\mathbf{E} = -\mathbf{u}_1 \times \mathbf{B}/c$, is in the same direction so that particles whose orbits intersect the shock, drift along the electric field. If the magnetic field strength increases as one traverses the shock from upstream to downstream, as it does in oblique, fast shocks, the drift is in a direction to cause the particle's energy to increase. There has been some misunderstanding about the nature of this process and some have believed that a term describing it needs to be added to the diffusion-convection

equation (3.16). However, Kóta (1979) and Jokipii (1979, 1982) have shown that the energy changes that a particle experiences when undergoing gradient and curvature drifts in a $\mathbf{u} \times \mathbf{B}$ electric field are included in the energy change term of the diffusion-convection equation. (For a detailed derivation of this result see Jones, 1990a; this point is also made in Forman and Webb, 1985.) Further, it has been shown (Jones, 1990a) that including an electric field *ab initio* in the derivation of the diffusion-convection equation simply produces the $\mathbf{E} \times \mathbf{B}$ drift motion of the plasma perpendicular to the magnetic field. We see, therefore, that *no* terms should be added to the basic diffusion-convection equation to take account of the shock drift mechanism in a perpendicular or oblique shock; this process is already included in the energy change (proportional to $\nabla \cdot \mathbf{u}$) term. This, of course, assumes that there is sufficient scattering so that the assumption (i.e., approximate isotropy of the particle distribution function) used in deriving the diffusion convection equation is valid.

Although the time scale for accelerating particles by perpendicular or quasi-perpendicular shocks can be much smaller than for parallel or quasi-parallel shocks, as pointed out by Jokipii (1987) and Ostrowski (1988), this does not mean that the acceleration time can be made arbitrarily short by reducing $\kappa_\perp$ without limit. Just as we have seen that when the diffusion length scale, κ/u, becomes comparable to the shock thickness, diffusive shock acceleration becomes ineffective, the same considerations apply to perpendicular shocks with the additional requirement that we must introduce the concept of the 'effective thickness' of the shock. In directions perpendicular to the magnetic field we must adopt a somewhat different picture of particle diffusion. Clearly for distances on the scale of the particle gyroradius or smaller, we may not use purely statistical reasoning to determine how many times a particle crosses the shock in a given time. If the guiding center (the center of the particles gyro-orbit) is within a gyroradius of the shock, the particle will cross the shock twice each gyroperiod or ω/π times per unit time, where ω is the gyrofrequency. This remains true regardless of how many times the guiding center may cross the shock because of scattering on a scale smaller than the gyroradius. This fact limits the rate of energy gain that a particle can experience in a quasi-perpendicular shock. As we saw in Equation (3.25), the momentum gain per shock crossing is given by $\langle \delta p \rangle = (2p/3v)(u_1 - u_2)$ and the rate with which the diffusing particles gain momentum is simply $\dot{p} = \langle \delta p \rangle \times \{\text{shock crossing rate}\}$. Since the particles that are being accelerated are within a diffusion length, $L \equiv \kappa/u$, of the shock their rate of crossing the shock is $\sim v/L$, therefore, the diffusion-convection (or individual particle) theory predicts a momentum gain rate,

$$\dot{p} \simeq \langle \delta p \rangle \, v/L = \frac{u_2(u_2 - u_1)p}{\kappa} \,, \tag{5.15}$$

where we have neglected factors of order unity. However, as we have just noted the crossing rate will never be faster than $\sim \omega$ so the momentum gain rate will, in fact, be limited to

$$\dot{p} \simeq \langle \delta p \rangle \, \omega = \frac{(u_1 - u_2)p}{r_g} \,, \tag{5.16}$$

so the effective diffusion length can never be smaller than the particles gyroradius and, hence, the theory is limited to the regime $L = \kappa_\perp / u > r_g$. In his original paper on this subject, Jokipii (1987) derived limits on the validity of the diffusion approximation from three different viewpoints, all different from the above argument. It is interesting to note that all three led to the above limit. What we (and Jokipii, 1987) have shown is that the diffusion approximation breaks down if the above limit is violated. In fact we can see more than that; we see that the gyro-motion of the particles imposes a strong coherence over distances of the order of the gyroradius and the notion of random walk or stochastic motion cannot be applied in directions perpendicular to the magnetic field on a scale smaller than this. We have seen that although the diffusion-convection equation does not apply to the thermal particles in the plasma making up the shock (they are highly anisotropic upstream of and just after the shock), nevertheless, Monte-Carlo simulations studies (Ellison *et al.*, 1990a, and Figure 3.4) show that if the theory (i.e., Equation (3.20)) is applied to them anyway it produces correct predictions in the high-energy portion of the spectrum. We would not expect to be so lucky in the case of perpendicular shocks. While before we could talk about the probability of a particle returning to and crossing the shock even in those situations where we could not calculate those probabilities, now we see that the notion of such probabilities has little meaning. When the guiding center of a particle is within a gyroradius of the shock its return is determined, its crossing rate is fixed by the gyro-motion and probability has little to do with the matter. A more fruitful way to consider a perpendicular shock would be to average all processes over a gyroperiod. Then one could consider the particle to be positioned at its guiding center and the shock transition would be broadened to a thickness of $2r_g$, its 'effective thickness'. From this point of view, the violation of the condition we have derived above is seen as simply a case of the diffusion scale becoming comparable to the scale of the shock transition and the analysis of Drury *et al.* (1982) would apply.

Another concern for rapid acceleration involves the stability of cosmic-ray mediated quasi-perpendicular shocks. Recent work with the two-fluid model by Zank *et al.* (1990) (following previous studies by McKenzie and Webb, 1984; Drury and Falle, 1986; Zank, 1989; and others) suggests that when cosmic-ray particles contribute significantly to the plasma pressure in quasi-perpendicular shocks, the shock precursor becomes unstable. Zank *et al.* (1990) find that a short wavelength drift instability exists which drives the diffusion coefficient to the 'Bohm' limit, i.e., $\kappa \to r_g c/3$. If this instability is, in fact, important, no gross reduction in acceleration time over the Lagage and Cesarsky limit can be expected for quasi-perpendicular shocks.

In addition to the above considerations, there is the well-known difficulty quasi-perpendicular shocks have in accelerating low-energy particles. In order to be diffusively accelerated, particles must interact with the shock a number of times and a downstream particle must be able to diffuse back to the shock. If we insert the expression, $\kappa_\perp = v r_g (r_g / 3\lambda_\parallel)$ into the limit on perpendicular shock acceleration, i.e., $L = \kappa_\perp / u > r_g$, we obtain the requirement

$$\left(\frac{v}{u}\right)_2 > \frac{3\lambda_\parallel}{r_g} , \tag{5.17}$$

where $(v/u)_2$ is the downstream ratio of random to bulk flow speed. Since $\lambda_{\|}$ is always considerably larger than r_g (if it is of comparable size to r_g it means that the magnetic field has become totally disordered and any distinction between parallel and perpendicular shocks becomes meaningless) we see that the downstream particle speed must be very much larger than the flow speed. This is, of course, never true for the thermal ions of the plasma; downstream of the shock the thermal energy is at most 9 times the flow energy so that $v_2/u_2 \leq 3$, not enough to satisfy the condition shown above. It is even unlikely for recently ionized 'pickup' ions that are believed to be the source of the anomalous component of cosmic rays since their upstream 'thermal' speed is just equal to the upstream flow speed, not enough to significantly change this picture. For this reason proponents of the theory that this component is accelerated by the solar wind termination shock (Pesses *et al.*, 1981) have suggested that the most likely place for this process to take place is over the solar poles where the termination shock is most likely to be a parallel one.

6. Computer Simulations

We have shown above that analytic techniques have been quite effective in studying particle acceleration at shocks. However, analyses based on the diffusion-convection equation assume that particle distribution functions are isotropic to first order, and since this condition is never satisfied for thermal particles at shocks, the shock structure itself, together with thermal particle injection, cannot be studied with this equation. This analytic difficulty has led to intensive computer modeling of collisionless shock structure.

Computer simulations of collisionless shocks show that an important relationship exists between shock structure, dissipation, and particle acceleration. Such a relationship was suggested by early analytic work for quasi-parallel shocks (i.e., Parker, 1961), but current simulation results suggest that superthermal particles provide an important part of the dissipation in both quasi-perpendicular and quasi-parallel shocks of all Mach numbers, and may in fact be essential for dissipation in high Mach number shocks. In addition, simulations have been prominent in studying the injection of ambient particles into the acceleration process, the overall efficiency of particle acceleration, the shape of the accelerated spectrum when nonlinear effects are included, the relative efficiency for accelerating different ion species at both quasi-perpendicular and quasi-parallel shocks, and the θ_{Bn} dependence of the shock drift acceleration process. Several reviews have been written recently on various aspects of these simulations and we refer the reader to Goodrich (1985) for a review on large-scale plasma simulations of quasi-perpendicular shocks, Leroy (1984), Burgess (1987b), and Quest (1988) for reviews on quasi-parallel plasma simulations, and Decker (1988) for a review on simulations of shock drift acceleration in oblique shocks. A description of a Monte-Carlo simulation of parallel shock structure coupled with first-order Fermi acceleration is given in Ellison *et al.* (1990a, and references therein). Except for the papers by Decker and Ellison *et al.*, the above reviews have concentrated on the physics of the shock structure and dissipa-

tion rather than particle acceleration. Decker does test-particle simulations of particle acceleration with an assumed shock structure, while the Monte-Carlo simulations neglect the microphysics of wave-particle interactions and concentrate on nonlinear backreactions of accelerated particles on the average shock structure. Here we focus on the particle acceleration aspect of shocks as seen through the medium of computer simulations, but emphasize that the microphysics of the shock structure and particle acceleration must be addressed together.

Simulations are of such importance because the complexity of wave-particle interactions prohibit analytic shock structure calculations in all but a very few idealized cases and it is unlikely that collisionless plasmas will be realistically described analytically. In addition, since the parameter regime of astrophysical plasmas is so far removed from collision dominated laboratory plasmas, it is unlikely that laboratory experiments will ever contribute significantly to our understanding of collisionless shocks. Because of these limitations, numerical simulations and spacecraft observations have been particularly useful. We will only briefly refer to the vast amount of observational data obtained in the age of spacecraft and refer the reader to reviews of the observations which can be found in the American Geophysical Union Monographs 34 and 35 (i.e., *Collisionless Shocks in the Heliosphere: A Tutorial Review*, R. G. Stone and B. T. Tsurutani (eds.), and *Collisonelss Shocks in the Heliosphere: Reviews of Current Research*, B. T. Tsurutani and R. G. Stone (eds.), AGU, Washington, 1985) as well as in *Journal of Geophysical Research*, Volumes 86 (1981) and 90 (1985). A recent update can be found in Onsager and Thomsen (1991).

Simulations of collisionless shocks are divided into two major types: (a) Large-scale plasma simulations where particle trajectories are calculated from the magnetic and electric fields present, and (b) smaller-scale Monte-Carlo simulations where particle trajectories are determined from a prescribed scattering law. The large-scale simulations are further divided into those which self-consistently determine the magnetic and electric fields from the particles (see the review by Burgess, 1987a) and those which move test particles in predetermined fields (see the review by Decker, 1988). Below we briefly describe the contributions and limitations of the various simulations and attempt to give the status and direction of current work in particle acceleration.

6.1. Large-scale plasma simulations

The most detailed information we have of collisionless shock structure and dissipation processes come from the large-scale, self-consistent plasma simulations. These simulations can be either hydrodynamic, full particle, or hybrid. Hydrodynamic simulations treat the plasma as a fluid and do not follow individual particle trajectories. They solve a set of fluid equations combined with Maxwell's equations and some prescription for the plasma pressure*. The relative efficiency of the fluid approximation makes these simulations ideal for studying long-term behavior. However, they are of limited use in

* These differ from the two-fluid hydrodynamic calculations discussed above in the way the diffusion is treated. The hydrodynamic simulations calculate the diffusion from Maxwell's equations at each time-step, whereas the two-fluid calculations assume a diffusion coefficient.

studying thermal shock structure because fundamental shock processes occur on scales less than fluid length scales. Also, because they are hydrodynamic descriptions, they give no information on heat flux (i.e., the transport of energy via particle motion along field lines) or nonthermal particle distributions. Both of these are important if particle acceleration is to be modeled. In principle, however, hydrodynamic simulations could provide a measure of the pressure in an accelerated population as is done in the two-fluid models.

Full particle simulations, on the other hand, follow both electron and proton trajectories and can cover all relevant length scales. If sufficient computer time is available (and if simulators received funding long enough to analyze the results) the precise behavior of the shock can, in principle, be simulated. In practice this is never possible and full particle codes can only run on the order of one or two gyroperiods, not long enough to see particle acceleration or even the start of the injection process in quasi-parallel shocks. One compromise which can be made is to use an artificially high electron to proton mass ratio (see Papapdopoulos *et al.*, 1971; and Forslund, 1985) which narrows the range of length scales, but severe restrictions will still exist in the total number of particles used and the size of the simulation box.

Hybrid simulations, where one component (electrons in most cases) is treated as a massless fluid and the other (ions) is treated as individual particles, offer a productive compromise. These simulations retain ion length scales, which are believed to be the most important for shock structure, but are fast enough to run many ion gyroperiods since electron time scales do not need to be treated explicitly and a large time-step can be used. Most current plasma shock simulations used in astrophysics are of the hybrid type and these employ the concept of 'macroparticles' or, equivalently, the 'particle in a cell' (PIC) method. The simulation box is divided up into some number of cells and the field moments are calculated at the center of each cell. When moments of the fields are calculated, individual simulation particles are treated as having a macrosopic size of at least one cell length. Since a particle has a finite size, its contribution to the moments is spread out over more than one cell and the resultant fields are smoother than would have been calculated using point particles. Since particles have a finite size and deposit information onto and take information from the grid, they do not undergo large angle collisions from a close approach but experience only small angle collisions as they pass one another (e.g., Forslund, 1985). The net advantage of the PIC technique is that the numerical noise is distributed more smoothly between the cells and fewer particles can be used. Disadvantages of the hybrid method include the fact that charge neutrality or quasi-neutrality is forced on the system. This approximation makes use of the fact that electron (n_e) and ion (n_i) charge densities are nearly equal, and if one is not concerned with electron scales above some scale length (the Debye length, say) n_e is set equal to n_i for scales larger than this. For smaller scale lengths, a nonlinear Poisson equation can be used to give a relation between the electrostatic potential and the electron charge density (see Winske, 1985). Since the Debye length can be several orders of magnitude smaller than the ion gyroradius, electrostatic potentials in the shock layer on the ion gyroradius scale are not modeled and the massless electron fluid carries no

heat flux. Electron effects such as whistler damping are introduced with a phenomenological resistivity. Perhaps the most important limitation from an astrophysical point of view is the fact that electron acceleration cannot be addressed. In most astrophysical sources outside the heliosphere, such as radio emission from SNRs, we see the result of energetic *electrons*. Gamma rays from relativistic ions have not yet been detected from SNRs so we have little or no information on accelerated ion populations in these sources*.

The actual algorithms used to move the particles and calculate the fields will not concern us here and the reader is referred to the above reviews and references therein for details.

One important technical aspect we will discuss is the different ways in which the shock can be initialized in the simulation. The most direct method (and the one most often used in astrophysical investigations) is to reflect particles off a *rigid boundary*. Particles with a given temperature are injected at one side of the simulation box and flow with a given supersonic bulk velocity until they bounce off the opposite side of the box. The reflected particles form a counter streaming beam which interacts with the cold incoming plasma and magnetic waves and turbulence are generated. Eventually, the magnetic field disturbances steepen and form a shock. The shock moves away from the rigid boundary and a clear separation between shock and boundary should occur after a sufficient time. The great advantage of this method is that it is easy to initiate without presuming any shock properties and without introducing extraneous effects from the initialization process. In this way it approximates how a real shock might develop in response to a piston or a barrier (such as the solar wind impinging on the Earth's magnetic field). The disadvantages include the fact that the simulation must be run long enough so directly reflected particles stop influencing the shock and the pre-shocked plasma (see Cargill, 1990). Another disadvantage is that new particles are continually injected into the box and the number of particles that must be followed increases with time. This increases the computing time, as well as the computer memory needed as the code runs. Also, since the shock advances across the simulation box with time, the pre-shocked plasma decreases in extent as the shock matures if the box size is keep constant.

A technique which allows the shock to remain more or less stationary in the simulation box and uses a constant number of simulation particles is the so-called *injection method*. Here, the initial conditions at either end of the simulation boundary are calculated from the Rankine–Hugoniot conservation relations for the shock to be simulated. The transition from upstream state to downstream state is initially approximated near the center of the box with some smooth function (e.g., hyperbolic tangent, see Mandt and Kan, 1990) such that mass flux is conserved and the simulation is begun. Particles are then injected at both the upstream and downstream boundaries with the appropriate boundary conditions and it is hoped that the transition will quickly relax to a shock. In effect,

* In fact, there is some evidence from an apparent excess of gamma rays from several SNRs that energetic protons are produced in these sources (e.g., Bhat *et al.*, 1986).

particles are injected at the upstream boundary and removed at the downstream boundary, although some fraction of the downstream particles can propagate upstream toward the shock due to their large thermal speed. The advantage of a stationary shock and a constant number of simulation particles is balanced by the disadvantage that the shock must conform to the prescribed boundary conditions, which include the distribution function of particles at the downstream boundary. However, from an acceleration viewpoint, these simulations are extremely important because they offer a check on the ability of quasi-parallel shocks to 'leak' ions. As already mentioned, a critical aspect of particle acceleration concerns reflected (or leaked) ions which backstream into the incoming cold ions. Initializing the shock by bouncing particles off a wall will always bias the early stages of the simulation with backstreaming ions. The injection method does not start with this bias so reflected particles must be produced solely by the shock turbulence. This is, in fact, what is seen and the shock dissipation results from waves produced by backstreaming ions in essentially the same way as in other methods. If the proper shock physics is included, of course, all initiation techniques should relax to the same state after a sufficient time.

A third technique for initializing the shock is via a *magnetic piston.* Here a stationary, uniform plasma is suddenly subjected to an electric field applied to one boundary of the box. The electric field forces the particles to move and magnetic flux is created which pushes the plasma along. The moving plasma sets up a shock which moves away from the piston. This technique has disadvantages in that the piston and shock do not separate as clearly as in the reflecting boundary case and the magnetic piston can heat the plasma and produce waves which can disturb the shock structure. Magnetic pistons are not often used in astrophysical simulations.

6.2. Perpendcular and quasi-perpendicular plasma simulations

Plasma simulations have been particularly successful in elucidating the structure of quasi-perpendicular shocks. This is so primarily because the laminar nature of these shocks occurs on length scales comparable to a single ion gyroradius and they can be simulated relatively easily. Simulations carried out by Leroy *et al.* (1982) and Leroy and Winske (1983) show qualitatively similar behavior to the Earth's bow shock and, in particular, show upstream particles being reflected in the steep magnetic field ramp. Significantly, the simulations show that the reflected particles are important for determining the shock structure and the dissipation of the upstream bulk kinetic energy. In high Mach number, supercritical shocks, in fact, ion reflection (and consequently acceleration) was found to be the *dominant form of dissipation.* In these high Mach number shocks, no other dissipation process is effective enough in converting the bulk kinetic energy into random particle motions. The shock must, instead, develop a large enough magnetic field overshoot to reflect some ions. These reflected ions, after gyrating in the shock ramp, enter the downstream region having converted some bulk kinetic energy of the incoming plasma into random particle energy.

Important aspects of the physics of quasi-perpendicular shocks can be deduced from observations of field-aligned beams (FABs) observed upstream of the quasi-perpendicu-

lar Earth bow shock (e.g., Paschmann *et al.*, 1981). The foreshock region contains electrons and ions streaming away from the shock (the FABs) as well as wave activity and the cold solar wind (i.e., $T_{SW} \sim 10^5$–10^6 K) streaming toward the shock. Since it is clear that in most cases the FABs result from some type of reflection process of the solar wind off the shock, these beams carry information on how thermal particles interact with quasi-perpendicular shocks. Most FABs tend to come from shocks with $30° < \theta_{Bn} < 60°$ and they typically have a number density approximately 1% that of the solar wind. The proton spectra, which tend to be very steep, peak near 3–5 keV and sometimes contain particles with energies greater than 30 keV (see Scholer *et al.*, 1980). As θ_{Bn} gets closer to 90° the probability that a particle will be reflected decreases, offsetting the increased energy gain in the highly oblique shock.

Quasi-perpendicular plasma simulations have been particularly successful in describing FABs and the nature of the reflection process. A recent observation by Ipavich *et al.* (1988) of the He^{2+} to H^+ density ratio in FABs (i.e., $(n_\alpha/n_p)_{FAB}$) shows that this ratio is *very much smaller* than the simultaneously observed ratio in the solar wind. Ipavich *et al.* report that the integrated $(n_\alpha/n_p)_{FAB}$ for 23 events is $(n_\alpha/n_p)_{FAB} \simeq 5 \times 10^{-4}$. This is approximately 10^{-2} that of the solar wind density ratio measured during the same period and shows that He^{2+} is not reflected from the quasi-perpendicular bow shock with anything like the efficiency of protons. The observations also show that the backstreaming He^{2+} and H^+ ions have approximately the same peak speed and that there is an inverse correlation between $(n_\alpha/n_p)_{FAB}$ and θ_{Bn}. The energy and angular distributions of the FABs are close to what is expected from direct reflection from the shock when it is assumed that the particle kinetic energy is conserved in the deHoffmann–Teller frame (Soneerup, 1969; Paschmann *et al.*, 1980; Burgess, 1987a), but clearly conflict with what is predicted if the FABs are particles leaked from the magnetosphere (e.g., Sibeck *et al.*, 1987). These results are particularly important for Fermi acceleration injection models, such as Lee's, which rely on convection from quasi-perpendicular portions of the bow shock to quasi-parallel portions where diffuse ions are observed. Since the He^{2+}/H^+ ratio in *diffuse ions* is essentially the same as that in the solar wind (Ipavich *et al.*, 1981, 1984), FABs cannot be the seed particles for the diffuse ions. This is consistent with recent two-dimensional bow shock simulations (Thomas and Winske, 1990). When Lee (1982) proposed his model for diffuse ions, $(n_\alpha/n_p)_{FAB}$ had not been measured and the disruption of FABs and the subsequent convection of these particles along the shock front seemed a natural way to provide seed particles for the diffuse ions. These recent observations, however, further support the assertion that quasi-parallel shocks can draw seed ions directly from the solar wind and requires an extension of Lee's model to treat the injection and acceleration of thermal ions directly from the ambient plasma. The power of plasma simulations can be gauged from the fact that the properties of the reflected protons were predicted by Burgess (1987a) who carried out an extensive 1-D simulation study of FAB protons (using the hybrid code described in detail by Winske and Leroy, 1984). The simulation predicted that (a) the energy is not quite conserved on reflection, (b) the beam density is anti-correlated with θ_{Bn}, and (c) that there would be a thermal anisotropy, all of which agree

with the observations reported by Ipavich *et al.* (1988). Burgess's simulation showed that, unlike specular reflection, the reflected particles encounter the shock more than once while remaining in the shock vicinity and undergo a 'trapping' process followed by an energy gain followed by detrapping.

After the Ipavich *et al.* (1988) observations, Burgess (1989a) expanded his simulations to include alpha particles self-consistently in a $\theta_{Bn} = 45°$ supercritical shock. His results are consistent with the Ipavich *et al.* observations and confirm that the low He^{2+} densities in FABs are compatible with the mechanism of direct reflection. Furthermore, the simulation indicates that the composition of FABs depends mainly on the relative temperatures of the upstream ion species, with reflected particles coming primarily from the tail of the thermal distribution so that a large $(T_\alpha/T_p)_{SW}$ will produce a large $(n_\alpha/n_p)_{FAB}$. The simulation also shows that the plasma β will influence $(n_\alpha/n_p)_{FAB}$. Both of these predictions can be tested with the next generation of spacecraft. Significantly, Burgess's results do not rule out the possibility that turbulence plays an important role in returning downstream ions to the foreshock region as suggested by Winske and Quest (1988).

6.2.1. *High Mach Number Simulations of Electron Heating in SNRs*

Cargill and Papadopoulos (1988) (see also Papadopoulos, 1988) use a hybrid plasma simulation of a high Mach number ($\mathcal{M}_A = 50$) quasi-perpendicular shock to investigate the possibility that electrons can be strongly heated by the Buneman and ion-acoustic instabilities. The reflected ion beam is susceptible to the Buneman instability against the ambient electrons when

$$2u_1 > v_e \quad \text{or} \quad \mathcal{M}_A > 20\sqrt{\beta_e}\,, \tag{6.1}$$

where β_e is the electron plasma β and v_e is the electron thermal speed. The above condition is easily satisfied for a SNR shock with $\mathcal{M}_A \gtrsim 100$. The Buneman instability is very rapid and may heat electrons to a point where T_e is high enough for the ion-acoustic instability to set in, further heating the electrons. The simulations suggest that electrons in SNRs are able to gain a great deal of energy (a factor of 10^3 for $\mathcal{M}_A = 50$) by this two-step mechanism which may be enough to explain the observed X-ray emission. What's more, there seems to be no fundamental reason (P. Cargill, private communication) why this heating process could not occur at quasi-parallel shocks as well, and this may offer a way of generating a seed population of energetic electrons which can then be further accelerated to relativistic energies by the first-order Fermi mechanism.

6.2.2. *Higher Dimensional Effects in Perpendicular Shock Simulations*

One-dimensional codes only vary parameters in the shock normal direction and cannot study wave-particle dynamics in cross-field directions. This could limit the number of wave modes influencing the shock physics and higher-dimensional simulations have been run to test the validity of the one-dimensional results. Of course, two- and

three-dimensional codes take much longer to run and cannot yet cover the dynamic ranges of the one-dimensional codes.

As mentioned above, one-dimensional perpendicular shock simulations demonstrate the importance of ion reflection in providing the shock dissipation. However,a one-dimensional simulation cannot relax the large ion temperature anisotropy generated at the shock front by the reflected ions. Two-dimensional simulations (Thomas and Brecht, 1986; Winske and Quest, 1988) showed that the addition of the second dimension allowed a self-consistent relaxation of the large ion temperature anisotropy. The wave modes generated by this process lead to a rippled shock front with large density fluctuations and magnetic field components that are about equal magnitude in all components. This effect is in reasonable agreement with observations of the high Mach number ($\mathcal{M}_A \simeq 22$) Uranian bow shock (Bagenal *et al.*, 1987) except that the observed fluctuations were considerably smaller than predicted by the two-dimensional simulation. When a third dimension is added (Thomas, 1989), phase coherence is not required in any direction and the amplitudes of the magnetic field components and density fluctuations are reduced. The three-dimensional results are in considerably better agreement with the high Mach number Uranian observations. The most important conclusion so far obtained from these multi-dimensional simulations is that they show no qualitative difference in the shock physics or role of the reflected ions from previous one-dimensional results.

6.3. Parallel and oblique plasma simulations

On the basis of theoretical studies and plasma simulation results, several instabilities are currently believed responsible for the formation of quasi-parallel shocks. The first is the firehose instability proposed by Parker (1961). Parker suggested that particles could reflect off the shock front (or leak from the downstream region) and stream upstream. This hot beam would then interact with the cold incoming beam and generate a fluid-like *nonresonant* ion beam instability. This so-called firehose instability occurs when the difference between the plasma pressure parallel to the magnetic field, $P_{\|}$, and the pressure perpendicular to the field, $P_{\perp}$, is greater than the magnetic field pressure (see Blandford and Eichler, 1987, for a more complete discussion), i.e.,

$$P_{\|} - P_{\perp} > \frac{B^2}{4\pi} \,. \tag{6.2}$$

When this condition is satisfied, the magnetic field will kink in much the same way that a high pressure firehose kinks. Once the waves are produced in the upstream flow, they convect back into the shock and are compressed and amplified. The amplified turbulence then scatters the incoming ions and provides dissipation. Parker (1961) also predicted that the ions which originate at the shock transition and stream out ahead of the shock would form an extended shock precursor. The traditional idea, formed from knowledge of *collisinal* shocks, of an abrupt transition between shocked and unshocked material with no communication from the downstream back to the upstream region was abandoned. In addition, the backstreaming ions would of necessity be more energetic

than the bulk of the thermal downstream ions. If these ions could scatter elastically off the upstream wave field and return to the shock they would gain additional energy and be clearly superthermal. The connection between shock dissipation and particle acceleration was made.

After Parker introduced his model, several other workers explored this and related analytic parallel shock models (e.g., Kennel and Petschek, 1968; Galeev and Sagdeev, 1970). Kennel and Sagdeev (1967) suggested a similar nonresonant instability driven by a temperature anisotropy rather than pressure (i.e., $T_{\parallel}/T_{\perp} > 1$). This thermal compression model was only applicable to low Mach number shocks however. Additional work was done to determine whether or not the upstream waves would group-stand in the shock frame or be convected back into the shock (e.g., Lee, 1982). For a fuller discussion of early theoretical ideas on parallel shocks see Quest (1985) and the Introduction in Quest (1988).

Early numerical work on parallel shocks was performed by Auer and Völk (1973) who integrated the nonlinear fluid equations in a low Mach number shock. They found stationary shock-like solutions many ion gyroradii thick which were marginally unstable to the firehose instability. Kan and Swift (1983), using a one-dimensional hybrid code, showed that when $\mathcal{M}_A \gtrsim 3$ the nonresonant firehose instability occurs and magnetic turbulence is generated in the downstream region. One advantage of the firehose, beam-driven models over other suggested models is that (at least in principle) they are applicable to a wide range of shock parameters and Mach numbers.

A significant advance in our understanding of parallel shocks and their role in accelerating ions occurred when Quest (1988) performed an extensive study of parallel shock ($\theta_{Bn} = 0°$) formation using a one-dimensional hybrid (macro-particle ions combined with massless fluid electrons) plasma simulation. The simulation was initiated by allowing a beam of ions to reflect off a rigid boundary, thus creating forward and backward moving interpenetrating particle beams. He found that, for a wide range of Mach numbers, a shock formed with dissipation provided by magnetic turbulence created from parallel (to the magnetic field) propagating, interpenetrating ion beams becoming firehose unstable. Essentially what Parker had predicted was seen to occur at least during shock formation and when the shock responded to changes in the upstream conditions. The nonresonant firehose instability is violent and rapid and is important for initially forming the shock and reacting to changes in the upstream boundary conditions. However, Quest (1988) suggested that the steady-state shock maintained itself below the threshold for excitation of the nonresonant instability and that a *resonant* cyclotron mode was responsible for shock dissipation. This electromagnetic ion/ion right-hand resonant instability is currently under study.

When conditions are fairly steady, the resonant cyclotron instability dominates the parallel shock structure. Golden *et al.* (1973) had shown earlier from linear theory that resonant modes could group-stand in the flow and grow to large amplitude. The upstream waves in Quest's simulations do not group stand in the shock frame, however. Instead, Quest showed that they convect through the shock and the downstream turbulence resulted from the compression and amplification of these upstream waves.

A third mechanism for producing waves at the quasi-parallel shock involves the production of whistler waves which phase-stand in the shock frame. It has been shown (e.g., Kan and Swift, 1983; Mandt and Kan, 1985, 1990; Omidi and Winske, 1988, 1990) that ions reflected off the shock can excite these short wavelength whistler modes. Simulations by Lyu and Kan (1990) show that whistlers can scatter ions at the shock and provide dissipation. They also claim that the backstreaming ions 'leak' from the downstream region rather than reflect from the shock ramp. The above simulations show a mixture of waves with some upstream waves (the whistlers) phase standing in the shock frame while others convect through the shock. Waves that are downstream continue to convect downstream. Mandt and Kan (1990) do several simulations at different Mach numbers and find that the average upstream wavelength decreases with increasing M_A. This results because the phase velocity of the waves increases with decreasing wavelength and the slower waves cannot phase stand in the flow at higher Mach numbers. Apart from the upstream phase-standing whistlers, the wave modes seen by Mandt and Kan (1990) are similar to those seen by Quest (1988). However, Quest did not see the short wavelength whistlers and Mandt and Kan suggest this is because Quest used a spatial grid about a factor of two coarser than theirs.

Parallel geometry simulations take much longer to run then do perpendicular simulations. The parallel geometry allows ions to freely stream far upstream of the shock and the foreshock region can extend over hundred's of ion inertial lengths (i.e., 100's of c/ω_{pi}; ω_{pi} is the ion plasma frequency based on the upstream density), much larger than in quasi-perpendicular shocks which can be well formed in 1 or 2 c/ω_{pi}. As a result, the simulation box and run time must also be much longer. Quest's simulation represented something of a breakthrough because he was able to run a hybrid code longer than previous quasi-parallel simulations such as Leroy and Winske (1983), Kan and Swift (1983), and Mandt and Kan (1985). Since it appears that the foreshock region is responsible for an essential part of the shock physics (production of waves which steepen to form the shock), previous simulations with smaller simulation boxes gave misleading results.

6.3.1. *Higher Dimensional Effects in Parallel Shock Simulations*

A major question left unanswered by Quest (1988) was whether or not his results for a one-dimensional, strictly parallel shock ($\theta_{Bn} = 0°$) would carry over to quasi-parallel geometry. This is no easy problem because quasi-parallel shocks are intrinsically multi-dimensional and we still lack the computing power to run two- or three-dimensional shocks for extended times. Recent work has been done on multi-dimensional quasi-parallel shocks and preliminary results suggest that, as with perpendicular shocks, no major difference in the shock physics occurs when a second dimension is added (e.g., Thomas *et al.*, 1990; Winske *et al.*, 1990). We discuss these results in more detail below.

It is fortunate that one-dimensional oblique shock simulations give a good approximation of the true shock because they are currently our only way to examine long time behavior. The single dimension eliminates spatial variations anywhere except along the shock normal. This means that there is an artificially restricted wave number space

available for the growth of instabilities and wave decay processes. Backstreaming ions are most unstable to electromagnetic beam instabilities that propagate along the mean magnetic field direction. In one-dimensional codes when $\theta_{Bn} \neq 0°$, variations are still only allowed in the shock normal direction, and unstable modes are restricted to a component of wave propagation parallel to $\hat{\mathbf{n}}$. Two-dimensional simulations show, however, that upstream waves have little tendency to align along $\mathbf{B}$ or $\hat{\mathbf{n}}$. While long-wavelength resonant ion beam modes have linear growth rates that maximize along the magnetic field direction, growth is not reduced very much at modest angles ($\theta_{Bn} \lesssim 30°$). Another reason nearly parallel ($\theta_{Bn} \lesssim 20°$ say) shocks should not differ much from strictly parallel shocks is that the amplitude of the magnetic turbulence is so large that the difference between a mean magnetic field direction of $\theta_{Bn} = 0$ or $30°$ would go unnoticed by the shock (Mandt and Kan, 1990).

6.3.2. *Shock Initialization*

Another area of concern is the effects of shock initialization on shock development and particularly on the role played by backstreaming ions. The simulations of Mandt and Kan (1990) (and earlier work by Kan and Swift, 1983; and Mandt and Kan, 1985, 1988), use the injection method to initialize the shock. Even without a reflecting wall, particles are seen to leak out of the downstream region across the shock and stream into the upstream region. The scale length of the density jump is around $10–20c/\omega_{pi}$ for super-critical Mach numbers. This is consistent with the results of Scudder *et al.* (1984) who determined the density jumps in the quasi-parallel Earth bow shock and an interplanetary shock. Mandt and Kan also find that the magnetic ramp length is of a similar scale and consistent with the interplanetary shock studied by Kennel *et al.* (1984). As the Mach number increases, the upstream waves obtain wavelengths comparable to the streaming gyroradius of the upstream plasma and the waves and plasma begin to interact strongly, presumably via the cyclotron instability. The result is a large increase in entropy. The principal temperature increase occurs, however, at the main shock ramp. While these results differ in detail from those of Quest (1988), the main elements are similar: reflected or leaked particles are critical for shock formation because they produce upstream waves which, when compressed in the shock ramp, scatter and thermalize the incoming ions. Even when no wall is present, the shock can reflect or leak ions into the upstream region and begin the first stage of Fermi acceleration.

6.3.3. *Cyclic Behavior*

An interesting phenomenon seen in quasi-parallel shock simulations is the so-called cyclic behavior of shock reformation. This was first reported by Burgess (1989b) but has since been seen in most quasi-parallel simulations (e.g., Winske *et al.*, 1990). (This effect was not noticed in earlier quasi-parallel simulations because they did not run long enough to cover the period of reformation.) Burgess showed that in a high Mach number shock with $\theta_{Bn} = 30°$, the shock alternates between times when the transition is sharp and times when it is extended (see Figure 6.1). The cycling (which should not be expected to be periodic) is due to the intermittent intensity of the backstreaming reflected

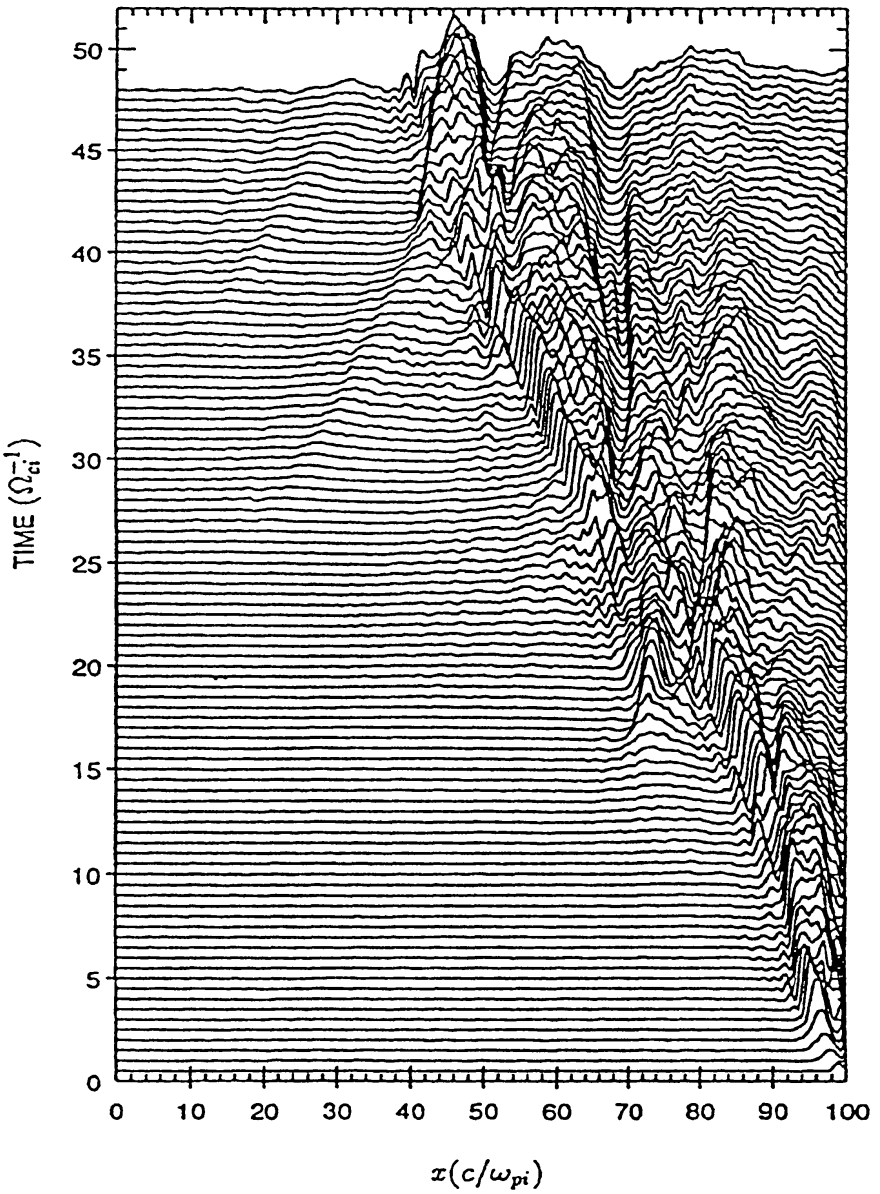

Fig. 6.1. Stacked profiles of magnetic field magnitude showing evolution of simulation. Each trace is separated by 25 time-steps. Figure from Burgess (1989b).

(or leaked) ion flux. As we have seen before, the backstreaming ions produce waves which convect into the shock and are amplified. Once the amplified waves steepen sufficiently, they can then scatter ions back into the upstream region. Burgess suggests that as the upstream waves are convected into the shock they create perturbations which disturb the immediate upstream conditions to which the shock has attempted to adjust. When a wave pulse hits the shock, the shock and wave pulse merge and form an extended region, smoothing the transition from upstream to downstream. This extended region is less efficient in scattering ions and few backstreaming ions are produced. However, the extended region will only persist for a short time until the sharp shock can reform and start scattering particles again. These backstreaming particles then produce a new wave pulse which disrupts the shock, etc. Burgess expects that the

quasi-periodic nature of reformation is most likely the result of the finite size simulation box-and-run time which do not allow a mature foreshock region to develop. If the simulation could be run longer and backstreaming ions kept regardless of how far upstream they went, a more or less continuous supply of wave pulses might be convected into the shock. The unsteady behavior would become less periodic and more stochastic with a frequency typical of the frequency of the long wavelength upstream waves.

Recent results by Scholer (1990) (see also Scholer and Terasawa, 1990) using a one-dimensional hybrid simulation of a $\theta_{Bn} = 20°$ shock also show that the shock directly accelerates thermal particles. In this simulation, some thermal particles originating in a certain part of phase space stay near the shock for an extended period of time and gain appreciable energy. Scholer suggests that, while magnetoacoustic waves in the upstream region scatter particles back to the shock, this scattering is not responsible for the initial particle acceleration. Instead, more coherent processes resembling shock-drift acceleration at the shock are claimed to produce a 'seed' population which then undergoes first-order Fermi acceleration. It will be interesting to see how this scenario holds up when longer simulations are run with more mature upstream wave fields. We suggest that the longer simulations are run, the more upstream waves will be produced by backstreaming particles (provided the smulation box is large enough to hold them), and the less likely it is that coherent processes will be important.

Thomas *et al.* (1990) have run one- and two-dimensional simulations to further explore the shock reformation process and to check how multi-dimensional simulations compare with one-dimensional simulations. They have used a transverse dimension of $50c/\omega_{pi}$ combined with a longitudinal dimension of $150c/\omega_{pi}$. Periodic boundary conditions are applied to the transverse boundaries of the box. This simulation box is larger than that used by Thomas and Brecht (1987) in their two-dimensional simulation. Thomas *et al.* (1990) see the reformation occurring and confirm that the process is not a consequence of restricting the problem to one dimension. Furthermore, they show that the reformation cycle is not in phase along the shock front; there is a lack of coherence along the front even though the shock remains fairly laminar. Several different models of electron heating (i.e., isothermal, adiabatic, resistive) are used but this makes little difference to the cyclic properties of the shock. In addition, they consider cases where backstreaming ions are removed from the simulation at varying distances upstream from the shock to see how the shock reformation process depends on these ions. When reflected ions are removed from the system the intensity of long wavelength upstream waves decreases but is not eliminated. The number of reflected particles, on the other hand, actually increases! The presence of upstream waves convecting into the shock gives rise to large amplitude waves that propagate downstream. The more waves convecting across the shock the more turbulence in the downstream region. The increased wave activity contributes significantly to the dissipation and to the balance of energy and momentum fluxes (i.e., the R–H relations). If these waves are not present downstream, as happens when backstreaming ions are removed, the shock must find another way to satisfy the R–H relations. It does this by reflecting more particles. The shock must always conspire to balance momentum and energy fluxes.

Thomas *et al.* also show that the magnetic field is quite turbulent in all components, and that all components fluctuate with comparable magnitudes. This contributes to the observation that the reformation process does not seem to depend strongly on the local value of θ_{Bn}. Greenstadt (1985) and Fuselier *et al.* (1986) have argued that most ion reflection would occur, as in quasi-perpendicular shocks, when the local value of θ_{Bn} approached 90°. Thomas *et al.* find little correlation between number of reflected particles and the local value of θ_{Bn} and values of $\theta_{Bn} \simeq 90°$ appear to have little effect on the number or dynamics of the reflected ions.

One-dimensional runs of very large scale ($\sim 1500c/\omega_{pi}$) and run times ($\sim 500\Omega_i^{-1}$, where Ω_i is the ion gyrofrequency) were carried out to test if the unsteady shock would persist long after the startup. The behavior lasted throughout the run and does not seem to be a transient associated with how the shock was originally formed. Thomas *et al.* do not report on the fraction of ions accelerated or the highest energies obtained in these long runs.

All in all, quasi-parallel shock simulations are in good qualitative agreement with recent observations made at the quasi-parallel Earth bow shock and interplanetary (IPSs). In particular, the Earth's foreshock region occasionally shows coherent, cold beams that appear to be nearly specularly reflected by the shock as well as hot ions that appear to have been leaked from the downstream. In addition, relatively cold ions are sometimes observed in the shock layer or even somewhat downstream from the shock (Gosling *et al.*, 1989; Onsager *et al.*, 1990). These cold high-density ions often alternate with hotter lower density regions. There is also an energetic diffuse ion component which is virtually always seen upstream from the quasi-parallel bow shock and occasionally observed to be continuous across the shock (Gosling *et al.*, 1978; Ipavich *et al.*, 1984; Ellison *et al.*, 1990b). While current plasma simulations have not been run long enough to produce ions as energetic as the diffuse ions, the start of the acceleration process seems to be occurring and the other observations just mentioned are quite well modeled. The intermittent nature of the shock reformation process produces alternate beams of hot and cold ions.

Mandt *et al.* (1986) have compared the magnetic field structure in three quasi-parallel IPSs with their simulations and found relatively good agreement. Besides the Mach number, they found the shock structure to be most sensitive to the plasma β (β is the ratio of plasma pressure to magnetic pressure). The IPSs studied were low Mach number ($1.4 < \mathcal{M}_A < 2.9$) laminar shock in contract to the generally much higher Mach number turbulent bow shock.

6.3.4. *The Initiation of First-Order Fermi Particle Acceleration*

Clearly, quasi-parallel shocks are complicated structures and several instabilities may be active at some stage and at some level. However, despite the complexity, the instabilities all have one common feature; they are electromagnetic beam instabilities generated by the interaction of backstreaming ions with the incoming plasma. Except for whistlers, the upstream waves then convert back into the shock front where they are strongly compressed and amplified. The compressed waves interact strongly with

incoming ions, scattering and slowing them, and provide the entropy production for the shock. The process continues when some small fraction of fresh thermal ions are back-scattered by the large amplitude waves and return upstream to create new waves which convect into the shock, sustaining the shock. This process, first reported by Quest (1988), has been confirmed by all subsequent parallel and quasi-parallel simulations. Of primary importance for particle acceleration is the observation (also reported first by Quest) that, at high Mach numbers at least, some of the backstreaming ions scatter in the upstream region, reverse direction, and return to the shock. An energetization results because, in effect, they are scattered from an approaching wall. Quest sees that some ions are further accelerated from successive reflections between the converging upstream and downstream waves and energies as high as ~ 10 times the ram energy are reported (i.e., $E_i \simeq 10E_R$, where $E_R = m_p u_1^2/2$; see Figure 6.2). This is just the start of the

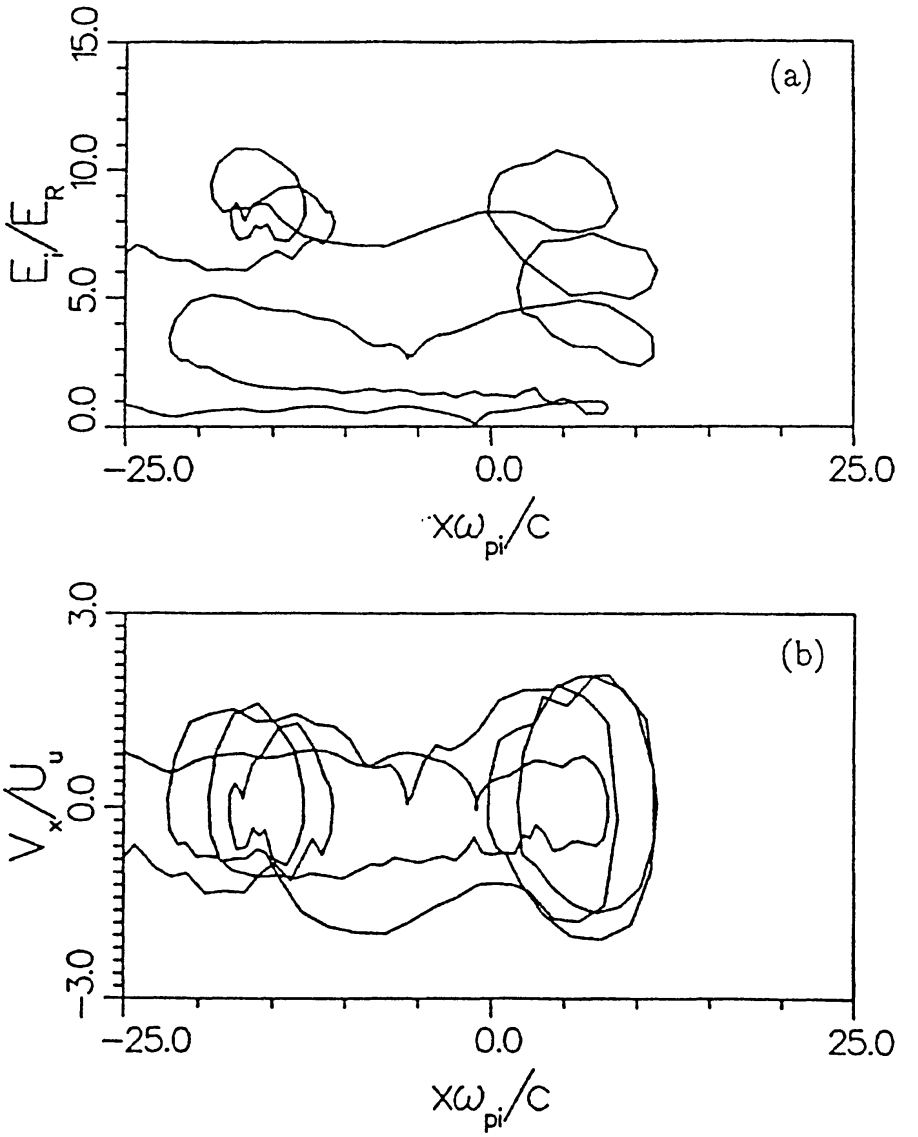

Fig. 6.2. (a) Plot of the total kinetic energy, E_i, of a single particle, normalized to the shock ram energy, $E_R = m_p u_1^2/2$, plotted against position. (b) The x-component of velocity normalized to the shock speed plotted against position for the same particle as in (a). The particle followed is strongly energized by its interaction with the shock-generated electromagnetic waves. Figure from Quest (1988).

first-order Fermi process which was postulated analytically for superthermal particles but is now seen to apply to thermal particles as well. The finite size of the simulation box (particles which reach the upstream end of the box are simply removed from the simulation) limits the acceleration. There is every reason to believe, however, that a larger box with a larger foreshock region would continue to accelerate ions until the ion diffusion length takes them out of the box. These simulations support the contention that parallel shocks can accelerate particles directly from the ambient thermal plasma. Furthermore, the simulations provide confirmation of the suggestion by Eichler (1979) and Ellison *et al.* (1981) that first-order Fermi acceleration and parallel shock dissipation are two limits of the same process as long as the scattering is controlled by nearly stochastic, large amplitude turbulence. The simulations confirm that not only is particle acceleration a result of high Mach number parallel shock dissipation, but is actually an intrinsic part of parallel shock formation. The waves which steepen to form the shock and produce entropy are generated by reflected or leaked (i.e., accelerated) ions and no other dissipation mechanism seems adequate for high Mach number parallel shocks.

Questions that remain for plasma simulations in one or more dimensions include: a more complete determination of how changes in input parameters (such as shock Mach number, β, etc.) influence the resultant shock structure, what particular instabilities are involved at specific stages of the shock formation process, what fraction of the incoming ions are reflected off the shock ramp versus the fraction leaked back upstream by scattering off large amplitude waves downstream from the shock, and how these various questions relate to each other. In addition to these specific questions concerning quasi-parallel shock microphysics, future work will address the feedback of accelerated particles of the shock structure when Fermi acceleration is allowed to produce significant energy densities in a superthermal population. In all current quasi-parallel plasma simulations, backstreaming ions which reach the upstream end of the simulation box are simply discarded. In fact, some fraction of these ions would scatter back to the shock and receive additional energy. The fraction returning would increase as the foreshock wave-field developed with time. The finite simulation box, which is imposed because of computing limitations, truncates the Fermi acceleration process and limits the feedback effects of energetic particles on the shock structure.

Finally, it must be emphasized that none of the simulations discussed here contained electrons explicitly and the role of electrons is still poorly understood. We do not have a clear idea how they participate in the microphysics of the shock and whether or not thermal electrons are Fermi accelerated with efficiencies at all comparable to those of ions. The prevalence of energetic electron populations in astrophysics make these questions of the upmost importance.

6.4. Test particle simulations of oblique shock acceleration

Decker (1988) has performed simulations of superthermal test particles interacting with oblique shocks having a range of θ_{Bn}. As discussed in Section 5.2, an electric field, $\mathbf{E} = -\mathbf{u}_1 \times \mathbf{B}_1/c$, exists in the shock frame and, in the limit of scatter-free propagation (i.e., where particles move with helical trajectories in uniform magnetic fields with no

waves or turbulence), upstream particles will gyrate along the shock front as they convect through the shock and gain energy from this electric field. Depending on pitch angle and gyrophase, some upstream particles can drift along the shock front for long distances and receive large energy gains. Also depending on pitch-angle and θ_{Bn}, some particles will gyrate in such a way that they will be returned back upstream, i.e., be reflected. The reflection occurs via magnetic mirroring since the magnetic moment is conserved. If the shock thickness is assumed to be much smaller than the particle gyroradius and the particle velocity is much greater than the flow velocity, the particle can make many gyrations while drifting through the shock. The drift along the front comes about because the gyroradius is smaller in the larger downstream magnetic field than in the upstream field. This shock drift acceleration (SDA) occurs because the electric field accelerates the particle when it is undergong a large orbit on the upstream side of the shock and decelerates it during the smaller orbit on the downstream side of the shock. The positive work on the large circle exceeds the negative work on the small circle and a net acceleration occurs (see Toptyghin, 1980; and Figure 6.3). Decker and

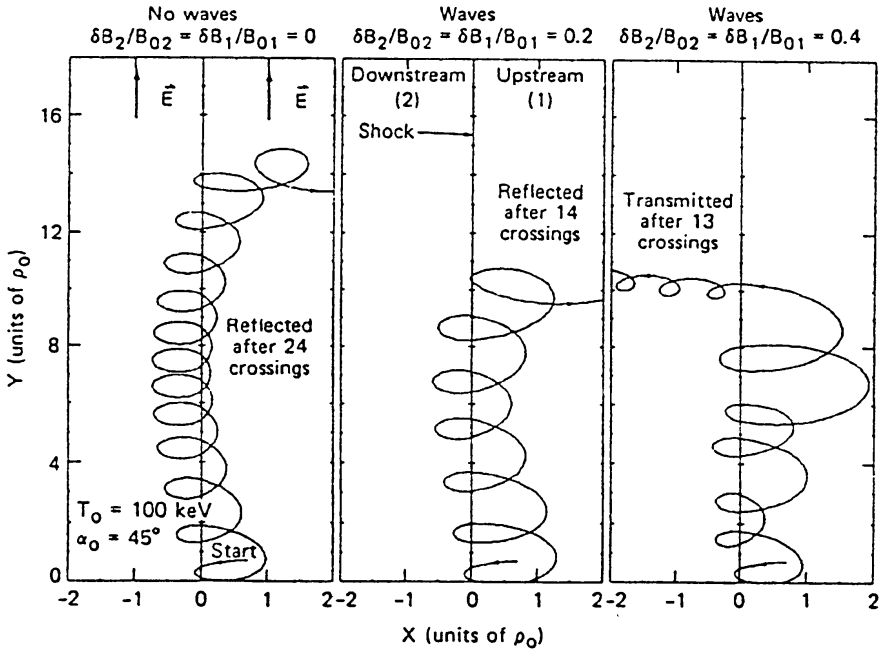

Fig. 6.3. Projection onto $(x - y)$ plane in shock frame of three proton orbits. Parameters $\delta B_1/B_{01}$ and $\delta B_2/B_{02}$ are relative r.m.s. amplitudes of magnetic fluctuations upstream and downstream, respectively (from Decker and Vlahos, 1985).

Vlahos (1985) and Decker (1988) have made careful studies of this process using a simulation which follows superthermal test particles by numerically integrating along exact phase-space trajectories. They have looked at both scatter-free conditions and turbulent conditions where transverse magnetic fluctuations have been superimposed on the mean field.

The basic features of SDA are the following: (a) For $\theta_{Bn} \lesssim 90°$ large energy gains are theoretically possible in a single encounter with the shock. This results because the shock layer electric field is large and certain pitch angles can result in particles gyrating

for long distances along the shock front. (b) As $\theta_{Bn} \to 90°$, the fraction of particles with a given velocity which have pitch angles which allow a large energy gain decreases rapidly. (c) In the scatter-free case, there is a lower limit on the velocity of an upstream particle below which the particle will not be reflected. Particles with velocites below this limit are convected through the shock with little more than adiabatic compression. This kinematic limit is $v \gtrsim u_1 \sec\theta_{Bn}$ and becomes superluminal as $\theta_{Bn} \to 90°$. (d) Since a particle must gyrate along the shock front for long distances to get a large energy boost, any finite shock curvature will limit the possible energy gain.

Other properties of oblique shocks and SDA include the fact that, unless considerable scattering occurs from a turbulent magnetic field, particles which are transmitted through the shock do not re-encounter the shock. Particles in a scatter-free, or near-scatter-free environment will, therefore, only receive a single energy gain, a situation which cannot produce the extremely high energies often seen in astrophysics. The addition of magnetic turbulence and the resultant scatterings, changes the character of SDA. Decker (1988) has investigated this and he shows that as the strength of the scattering (i.e., $\delta B/B$) increases: (a) fewer ions are reflected, (b) power-law tails develop as some ions are accelerated to several times the maximum energy of the scatter-free case; adding small amounts of scattering perturbs the orbits of some particles and causes some to stay in the shock plane longer, incrasing the possibility of some particles gaining a great deal of energy in nearly perpendicular shocks, but at the same time reduces the fraction of particles which gain this energy, and (c) the approximate invariance of the magnetic moment which is seen in nearly scatter-free simulations is violated (Decker and Vlahos, 1986b; see Burgess, 1987b, for a similar result from simulation work).

For low levels of turbulence, Decker shows that particle acceleration is a combination of first-order Fermi and SDA. However, as $\delta B/B$ increases, the process begins to look more and more like diffusive shock acceleration. This should not be surprising in light of our discussion in Section 5.1 where it was pointed out that if enough scattering is present to keep the energetic particles approximately isotropic, the 'shock drift' mechanism is contained in diffusive shock acceleration.

Chiueh (1988, 1989) obtains similar results and shows that when $\delta B/B$ is increased even further ($\delta B/B \gtrsim 0.4$), ions slightly above thermal energies may be scattered in the downstream region and returned to the shock for acceleration. Chiueh suggests that this might be an effective injection mechanism for diffusive shock acceleration in nearly perpendicular shocks.

Burgess (1986, 1987) has studied SDA with the aid of a plane, hybrid simulation (see Section 6.2). This work is analogous to that of Decker and Chiueh except that the quasi-perpendicular shock is now formed self-consistently with the plasma simulation. Once the shock is formed, test-particle ions are injected and followed. Burgess finds that *thermal* ions can be reflected and energized for $\theta_{Bn} \lesssim 60°$ (depending on $\mathcal{M}_A$) producing FABs with energies up to ~ 20 keV. As θ_{Bn} increases, however, SDA requires higher and higher initial energies to begin to operate. Also, as θ_{Bn} increases, the drift distance along the shock front and the interaction time also increase and the drift distance can

become $\gtrsim 10R_E$ for $\theta_{Bn} \gtrsim 80°$. This clearly limits the validity of the plane shock model in these parameter regimes.

Similar work combining plasma simulations with test-particle injection was done by Krauss-Varban *et al.* (1989), only now superthermal *electrons* were injected into the shock. These results are necessarily more speculative because the hybrid simulation does not contain scale lengths relevant for low-energy electrons. However, these results indicate that the assumption of magnetic moment conservation is justified up to fairly high final energies of the reflected electrons ($\gtrsim 10$ keV).

While theoretical work (i.e., Jokipii, 1987; Ostrowski, 1988, see Section 5.2) suggests that quasi-perpendicular shocks can accelerate particles more rapidly than quasi-parallel ones and Decker (1988) concludes that 'all other parameters being fixed, the acceleration rate increases dramatically with increasing θ_{Bn}', we do not believe that the simulation results of Decker actually confirm this, at least not in the strong scattering limit. Much of the support for the contention that oblique shocks are good accelerators comes from simulation results such as those shown in Figure 6.4 which were run for a fixed number of gyroperiods. A dot in Figure 6.4 indicates where a particle was in energy space at the end of the simulation. As indicated by the density of dots in the figure, particles in the oblique shocks have gained more energy in less time than in the quasi-parallel shocks. However, most particles in the oblique shocks have stopped being accelerated *before the simulation ends*, i.e., before 500 gyroperiods, while in the low θ_{Bn} cases, a much larger fraction of particles are still gaining energy and would continue to gain energy if the simulation continued to run. It is by no means clear that the advantage claimed for quasi-perpendicular shocks would persist if the simulation was run longer and it seems that at some point, acceleration in the quasi-parallel shocks could well overtake acceleration in the quasi-perpendicular ones. Furthermore, as just mentioned, Decker shows that the difference between quasi-perpendicular and quasi-parallel shocks decreases as the turbulence increases (see Section 5.2) and the prediction of Jokipii will depend on the level of turbulence as well as other effects such as whether or not the backreaction of accelerated ions on the shock structure disrupts the particle drift along the shock front, and whether or not the shock is curved.

Apart from questions concerning acceleration [illegible] more fundamental question concerns acceleration efficiency. Clearly, the concept of efficiency must be related to that fraction of the incoming flow energy that is transferred to the superthermal particles by the shock. It is not enough to have some particles gain energy very rapdly to have efficient acceleration. A complete spectrum must be produced and the fraction of total particles which are accelerated must be known. This cannot be done with a test particle model which does not include thermal particles.

Before a definitive answer can be found to the important question of whether quasi-parallel or quasi-perpendicular shocks are more efficient, it is necessary to include nonlinear effects from the accelerated particles on the shock structure and injection from the thermal background. Nonlinear effects include magnetic overshoots and shock smoothing. Any model which relies heavily on the magnetic field jump for the acceleration must include the magnetic overshoot to be realistic, and shock smoothing

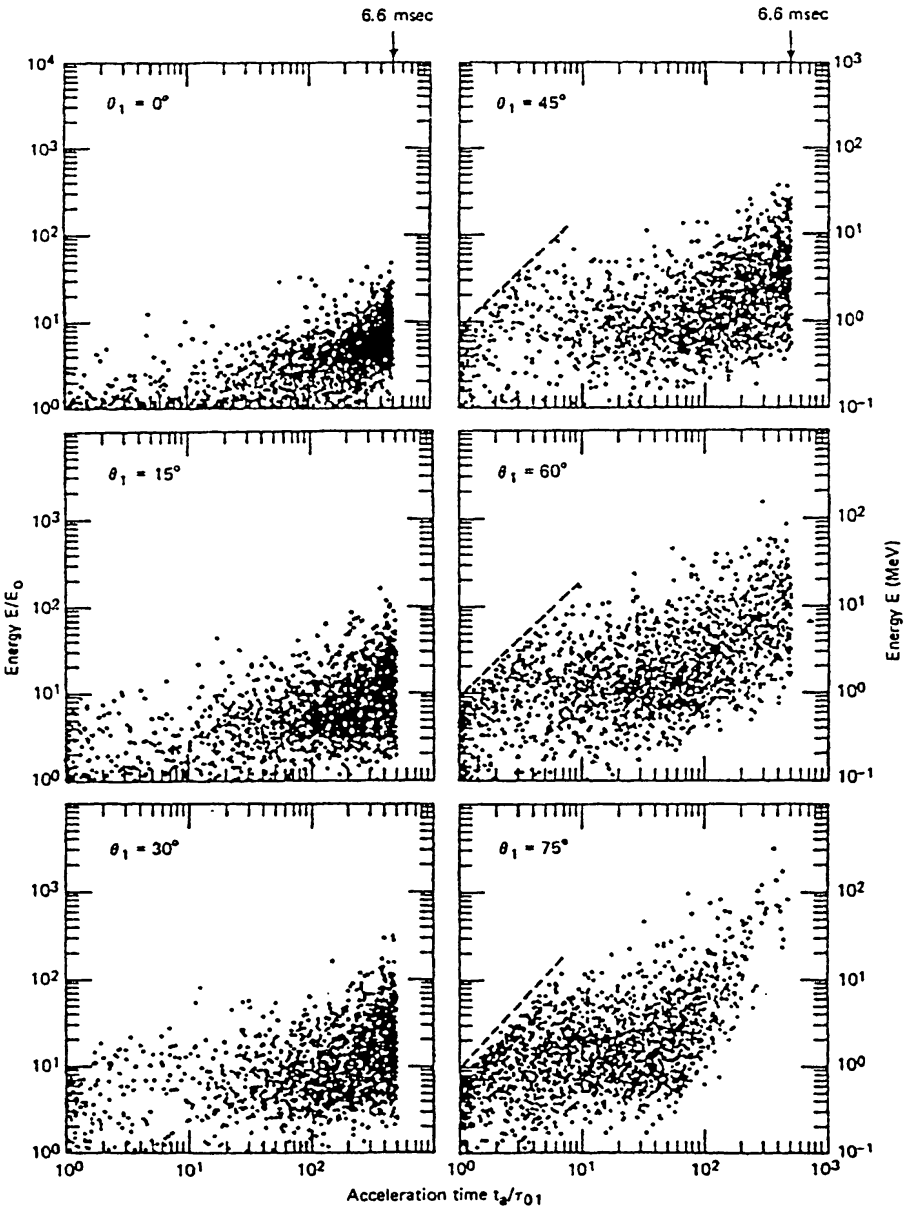

Fig. 6.4. Energy E/E_0 (E_0 is the superthermal injection energy) versus acceleration time for ~2100 protons injected as an isotropic distribution immediately upstream from shocks with θ_{Bn} = 0, 15, 30, 45, 60, and 75°. Each particle remained in the system for 500 gyroperiods. The acceleration time is the time of the particle's last shock crossing. Figure from Decker and Vlahos (1986a) (see also Decker, 1988).

may be critical in oblique shocks where test particle results show that particle reflection is a very sensitive function of particle energy and shock thickness.

6.5. Monte-Carlo nonlinear shock simulations

Over the past ten years, we have devleoped Monte-Carlo simulation techniques to model parallel shock structure coupled with Fermi acceleration. These simulations are based on the assumption that the same scattering processes responsible for producing energetic particles can also be applied to thermal particles producing the gas subshock. This idea, orginally from Eichler (1979), allows a self-consistent treatment of shock

structure and particle acceleration, with no artificially imposed distinction between thermal and superthermal particles. We assume that all particles scatter elastically and isotropically off some background magnetic turbulence with a mean free path, λ, that is some function of momentum. The theoretical justification for assuming that all particles could be treated in this uniform fashion came from Parker's (1961) firehose shock model discussed above. Since thermal particles, as well as high-energy particles (i.e., the reflected ions) generate the turbulence responsible for creating the shock, Eichler postulated that the large amplitude turbulence would produce near-elastic scattering for all energy particles and would allow a relatively simple description of the thermal shock. The important prediction stemming form this assumption was that *the creation of a high-energy particle population was an inherent part of the shock process itself* (Ellison *et al.*, 1981). When this was first suggested, there was little hard evidence in its favor. However, spacecraft observations of diffuse ions at the quasi-parallel Earth bow shock (e.g., Ellison and Möbius, 1987; Ellison *et al.*, 1990b) and large-scale plasma simulations of quasi-parallel shocks discussed above in Section 6.3, have shown that quasi-parallel shocks can directly accelerate thermal ions; the turbulence produced by energetic particles is an essential part of the thermal shock dissipation and there seems to be no physical reason to treat thermal and superthermal populations differently.

We have emphasized several times that analytic descriptions of shocks are hampered by the approximation needed to formulate the diffusion-convection equation, i.e., $v \gg u$. If the standard diffusion-convection equation is used, the gas shock cannot be described. If more fundamental equations, such as the Boltzmann equation, are employed which do not make this assumption, the equations cannot be solved in closed form. This mathematical difficulty, which forces a division between thermal and superthermal particles, has led, we suggest, to a belief among many workers that there is, in fact, a physical separation between thermal and superthermal particles in collisionless shocks. In particular, it is often assumed that an energetic seed population must be present for the Fermi process to work when, in fact, quasi-parallel shocks are observed to accelerated thermal ions quite efficiently.

Our Monte-Carlo simulation bridges the two opposite regimes covered by transport equations and plasma simulations. We describe the gas shock in some simplified way, while at the same time, by not treating the scattering in detail, we are able to follow the evolution of individual ions long enough to model acceleration to high energies. Once a scattering description has been assumed, important nonlinear effects such as particle loss and the large-scale slowing and heating of the upstream plasma by the backpressure of the accelerated ions can be modeled self-consistently. Predictions of the Monte-Carlo simulation which cannot yet be made by either transport equations or plasma simulations include (a) the complete particle distribution function and the accompanying *absolute* ion injection and acceleration efficiencies, (b) the complete distribution functions for all ion species at all distances from the shock, (c) the relative scale lengths of the shock precursor and thermal subshock, and (d) the gyrophase averaged anisotropies at all particle energies for all ion species.

6.5.1. *Details of the Monte-Carlo Simulation*

The scattering mean free path, λ, is taken to be

$$\lambda \sim \frac{R^{\alpha}}{\rho} , \tag{6.3}$$

where $R = pc/(Ze)$ is the particle rigidity, ρ is the plasma density, e is the electron charge, and Z is the charge state number. As just mentioned, the scattering is not determined self-consistently from the particle distribution function and the background magnetic field, but the rigidity dependence of the mean free path can be varied to model pitch-angle scattering off hydromagnetic turbulence with various power spectra. In all cases, an exponential distribution of path lengths is used. Particles are allowed to scatter in three dimensions but we have thus far treated only plane, parallel shocks, so fluid quantites vary only in x. The background magnetic field, which is assumed to produce the particle scattering via unspecified wave-particle interactions, lies along x and does not contribute to the jump conditions and we assume the scattering centers are at rest in the local fluid frame.

The code has been generalized to include relativistic particle energies and relativistic flow velocities (Ellison *et al.*, 1990a). These generalizations are quite straightforward and consist of a relativistic transformation of particle momentum each time a particle scatters between positions where the flow velocity changes, so that its scattering can be elastic in the local fluid frame. In general, for smoothed shock profiles, this transformation is required on every scattering. In addition, since the scattering mean free path is always calculated in the local plasma frame, the distance traveled in the shock frame must be determined with the proper relativistic transformation. Particles are followed in momentum space, so no relativistic corrections to the spectrum are necessary until the final energy spectra are calculated.

It is assumed that shock-heated downstream ions can freely scatter back across the subshock into the upstream region without being thermalized (i.e., the viscous subshock is assumed to be transparent to all energy ions). Such 'thermal leakage' of downstream ions provides our injection mechanism for Fermi acceleration, since a few ions will manage to scatter across the subshock many times and receive repeated energy gains. The fraction of thermal ions that become superthermal is determined solely by the statistics of the scattering process, i.e., by the balance between diffusion upstream and convection downstream in the downstream flow. Thus the model treats thermal particle injection and acceleration as an inherent part of the shock dissipation mechanism and unifies parallel shock structure with first-order Fermi acceleration. This unification is, of necessity, strongly nonlinear in high Mach number shocks such as the Earth's bow shock, because the accelerated ions can obtain large fractions ($\gtrsim 10\%$) of the incoming solar wind energy flux (see Möbius *et al.*, 1987; Ellison *et al.*, 1990b) and they modify the shock structure. The slowing and heating of the upstream flow, mandated by the presence of accelerated ions ahead of the shock, strongly influences thermal ion injection: the more the unshocked gas is slowed, the smoother the shock and the fewer injected ions. Only when particle injection and acceleration are coupled through the

pressure of the accelerated particles on the unshocked plasma can quantitative predictions for the absolute injection and acceleration efficiencies and complete ion distribution functions over all energy ranges be made.

The model also includes the escape of energetic particles at an upsteam free escape boundary (FEB). The FEB phenomenologically models a finite shock size and/or the lack of sufficient scattering far upstream to turn particles around; ions which cross the FEB are assumed to decouple from the shock system. The loss of energy flux at the FEB is strongly nonlinear, acting in the same fashion as escape at $E_{\max}$ discussed in Section 4.2. The compression ratio, which depends on the FEB and particle escape, is determined including escape.

The Monte-Carlo simulation can model large-angle scattering or pitch-angle diffusion, but in either case the scattering is assumed to be elastic and isotropic in the local plasma frame. If large angle scattering is assumed, a particle is scattered after moving a mean free path chosen from an exponential distribution. Pitch-angle diffusion is modeled by allowing the tip of the particle's momentum vector to undergo a random walk on the surface of a sphere within a small range of polar angles. After a small increment of time, $\delta t \ll t_c$, where t_c is the collision time, a particle's momentum vector, **p**, undergoes a small change in direction, $\delta\theta$. If the particle originally had a pitch angle, θ (where θ is measured relative to the x-direction in the local plasma frame), it will now have a new pitch angle, θ', given by the spherical trigonometric formula

$$\mu' = \mu \cos\delta\theta + \sqrt{1-\mu^2}\,\sin\delta\theta\cos\phi\,, \tag{6.4}$$

where $\mu' = \cos\theta'$, $\mu = \cos\theta$, and ϕ is the azimuth angle measured with respect to the original momentum direction. All angles are measured in the local plasma frame. If we identify the mean free path, λ, with the mean distance a particle travels in a given direction, it can be shown (Ellison *et al.*, 1990a) that

$$\frac{\langle \delta\theta^2 \rangle}{\delta t} = \frac{2v}{\lambda} = \frac{2}{t_c}\,, \tag{6.5}$$

giving the desired relation between the small-angle scattering coefficient and the more phenomenological mean free path. This relation assures that the distance between deflections of order 90° is λ in both the large-angle scattering and pitch-angle diffusion cases.

Particles are injected far upstream from the shock with a thermal distribution and allowed to scatter and convect through the shock. Injection far upstream simulates how ambient particles actually approach the shock and is essential if thermal effects are to be investigated and the absolute acceleration efficiency calculated. When a particle scatters, the momentum is calculated in the new local plasma frame. In addition to particle loss at a FEB or $E_{\max}$, ions which cross a particular downstream point on the x-axis are either removed or returned to the system according to the probability of return given by Equation (3.29)*.

* See Ellison *et al.* (1990a) for techniques which have been developed to calculate acceleration times when the downstream scattering is truncated by the probability of return calculation.

In order to achieve a large dynamic range, it is essential to split particles as they gain momentum. Some fraction of particles which have obtained momentum p_i will achieve the higher momentum p_{i+1}. At p_{i+1}, the number of particles is increased with the corresponding statistical weight of each particle decreased. As acceleration continues, some fraction of these particles will achieve the still higher momentum p_{i+2} and are split again with the weight further decreased, etc. The p_i values, or splitting momentums, are chosen so that the number of particles stays constant within a factor of 2 throughout the simulation. In this fashion, uniform statistics are obtained and the equivalent of 10^{13-15} particles can be simulated with a minimum of computing time.

The shock structure, or flow velocity profile, is found by iteration until the mass, momentum, and energy fluxes are conserved across the shock. Figure 6.5 shows an example of this procedure applied to diffuse ions at the Earth's bow shock. The initial velocity profile labeled '1' is chosen arbitrarily and produces the momentum flux profile

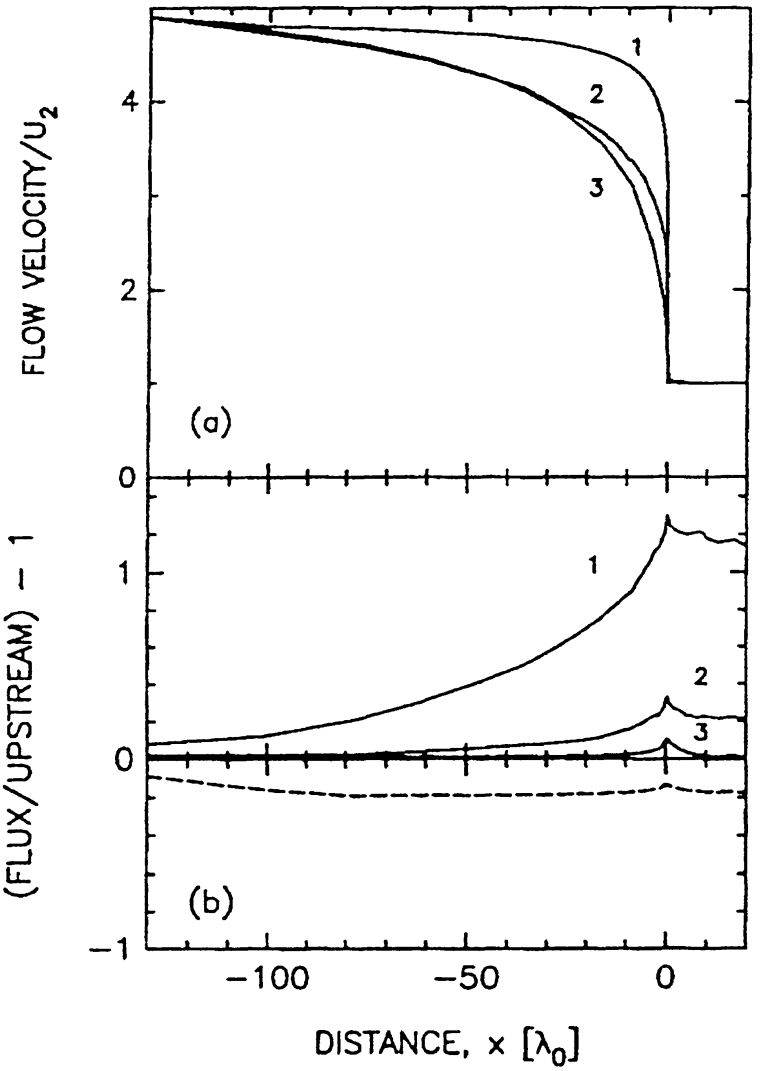

Fig. 6.5. (a) Flow velocity versus distance as obtained from the Monte-Carlo simulation. (b) Solid lines are the momentum flux and the dashed line is the energy at distances upstream and downstream from the abrupt subshock positioned at $x = 0$. Numbers indicate successive iterations. Fluxes are normalized so that the x-axis represents the far upstream value. Figure from Ellison *et al.* (1990b).

also labeled 1. It is clear that this relatively sharp profile does not conserve momentum flux across the shock. The code uses this result to predict the next shock profile and the process is iterated until a constant momentum flux is obtained. Both the shape of the profile and the overall compression ratio must be iterated simultaneously. For a given compression ratio, r, the code iterates the shock profile until the momentum and energy fluxes are as close to constant across the shock as possible. However, the conservation of these fluxes will depend on the value of r and if the 'correct' r is not used, the fluxes will not be constant across the shock even after the shape of the shock profile has been changed. The compression ratio is then varied and the shock profile iterated again until the fluxes are as constant as possible. This is continued until an r and a shock profile are found which conserve momentum and energy fluxes, to some predetermined level of accuracy. We find that a unique r and profile exist which allows simultaneous conservation of momentum and energy fluxes from far upstream through the shock to the downstream region. Figure 6.5 shows the rapid convergence of the momentum flux iterations (solid lines) plus the final energy flux (dashed line). The momentum flux is extremely flat across the shock except for the small rise at $x \simeq 0$. This rise is produced by gradients in the flow velocity (included for computational reasons) which occur over less than one mean free path. In any case, the momentum flux is held well within $\pm 10\%$ of the far upstream value across the abrupt subshock transition. The energy flux in Figure 6.5 falls below the upstream value due to particles escaping at an upstream FEB. When the escaping flux is added to the flux shown in the figure, energy flux is conserved across the shock*.

Once the shock profile is determined for protons, heavier ions are treated as test particles and scattered off the proton profile.

The compression ratio can also be determined directly from the R–H relations if the escaping energy flux is known (Ellison, 1985), i.e.,

$$\frac{1}{r} = \frac{1}{8}\left\{5 + \frac{3}{\mathcal{M}_1^2} - \left[9\left(1 - \frac{1}{\mathcal{M}_1^2}\right)^2 + 16\left(1 + \frac{3}{\mathcal{M}_1^2}\right) q_{\mathrm{esc}}\right]^{1/2}\right\}, \tag{6.6}$$

where $\gamma = \frac{5}{3}$ (this result is for nonrelativistic flows only). For the bow shock example used here, the r and q_{esc} determined by the simulation are within a few percent of that predicted by Equation (6.6).

One important aspect of the smooth profile in Figure 6.5 is the presence of a 'subshock' with a length-scale on the order of the upstream thermal particle convection length. This subshock heats the incoming cold gas and produces a hot downstream particle population which provides seed particles for further acceleration. We find, in contrast to analytic two-fluid results, that a subshock exists regardless of the acceleration efficiency as long as only thermal ions are injected and accelerated by the shock.

* For the illustration shown in Figure 6.5, the sharp profile (labeled 1) has the correct final $r = 4.9$. In an actual calculation, the correct r would not be known for the initial sharp shock run.

6.5.2. *Bow Shock Modeling and Other Applications*

Results of the simulation have been compared to spacecraft observations of diffuse ions made at the quasi-parallel Earth bow shock. This work has been described in detail in a series of papers (i.e., Ellison, 1981a, 1985; Ellison and Möbius, 1987; Ellison *et al.*, 1990b, and references therein) and will not be repeated here. However, certain points should be made. Most importantly, we believe it has been shown conclusively that the quasi-parallel bow shock can directly inject and accelerate ambient solar wind protons and alpha particles with similar efficiencies. No separate energetic seed population is required for acceleration to occur, although, of course, such a population would be accelerated along with the thermal ions if it were present. The Monte-Carlo simulation does a good job of fitting the spectral observations. In Figure 6.6 we show a comparison

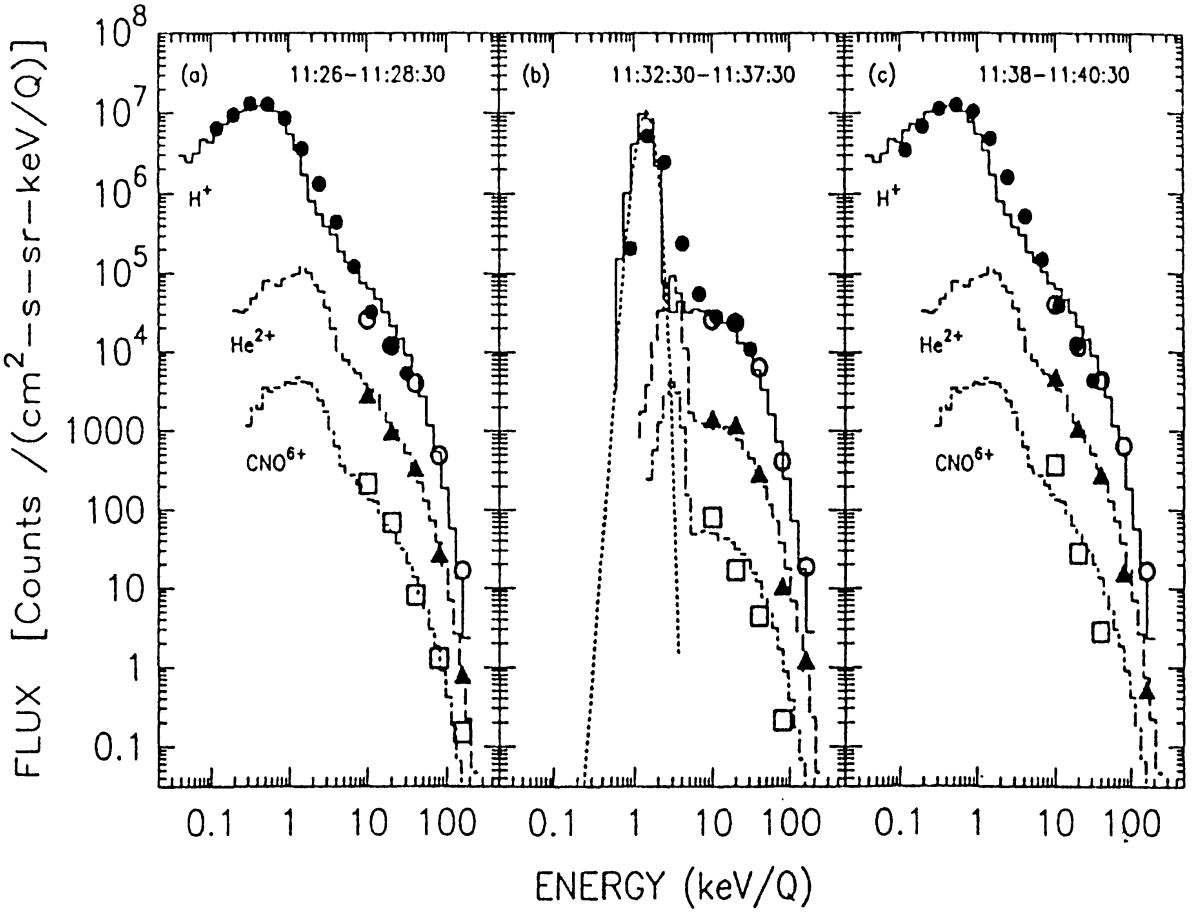

Fig. 6.6. Monte-Carlo simulation fits to downstream, upstream, downstream sequence of spectra observed by the AMPTE/IRM spacecraft. Filled and open circles are protons, triangles are He^{2+}, and squares are CNO^{6+}. The simulation uses $\alpha = 1$ (see Equation (6.3)) and all parameters are the same in each of the three panels except for the observation position and the normalization. The normalization is determined from the observations and panels (a) and (c) show downstream spectra, while panel (b) shows upstream spectra. This figure is from Ellison *et al.* (1990b) and that paper should be referred to for a complete description.

between the model and observations made at the nose of the Earth's bow shock during a time when the interplanetary magnetic field was nearly radial (i.e., along the solar wind direction). These observations provide an excellent test of injection and acceleration

during quasi-parallel shock conditions and are matched extremely well by the theory. The spectra are not power laws because they are dominated above ~ 30 keV/Z by particle loss. When the particle mean free path becomes comparable to the size of the acceleration region, particles will 'leak' from the shock system and the spectrum will steepen approximately exponentially. This can be expected at relatively low energies at the small Earth bow shock and has been explained by the presence of either a lateral boundary (e.g., Eichler, 1981; Lee, 1982), where resonant cross-field diffusion allows particles to escape out of the flux tube into the foreshock region, or by an upstream boundary (e.g., Forman, 1981; Lee *et al.*, 1981; Ellison, 1985; Ellison and Möbius, 1987), as modeled with a FEB. At the Earth's bow shock, the FEB determines the overall efficiency of converting the bulk solar wind flow energy into accelerated particles if steady-state conditions obtain. The larger the distance to the FEB in mean free paths, the greater the energy obtained in the highest energy ions and the larger the overall efficiency of the shock acceleration. Observations (i.e., Ipavich *et al.*, 1981, 1984) show that the quasi-parallel bow shock injects and accelerates both protons and heavy ions (i.e., He^{2+}, CNO^{6+}) with similar efficiencies. In fact, there is evidence suggesting that heavier ions are preferentially accelerated. Such preferential acceleration of high A/Z ions was predicted to occur if ions scattered with $\lambda \sim R$ in a shock smoothed by the backpressure of the accelerated ions (Ellison *et al.*, 1981). The simulation predicts enhancements of heavy ions relative to protons by a factor of 2–3 at the bow shock, a value consistent with the Ipavich *et al.* observations. In addition, the efficiency of Fermi acceleration is observed to be high. A model-independent lower limit can be found from the bow shock observations reported in Ellision *et al.* (1990b) showing that at least 15% of the solar wind energy flux goes into energetic particles.

Besides the bow shock, composition changes produced during acceleration are important when considering solar flare particles and galactic cosmic rays. The expected enhancement of high A/Z ions may be one factor in producing the observed over-abundance of heavy ions relative to protons and helium in cosmic rays (Cesarsky *et al.*, 1981; Ellison, 1981b).

The quality of the bow shock observations are sufficient to allow constraints to be placed on assumptions used in the simulation. As an example, if the scattering mean free path has the form given in Equation (6.3), α must be in the range $\frac{1}{2} < \alpha < \frac{3}{2}$ to obtain satisfactory fits. We also find that λ is on the order of 2–10 gyroradii. A tighter constraint is not possible with a single spacecraft observation.

The versatility of our model can be judged from the fact that the code can be applied directly to Fermi acceleration in relativistic shocks. Since the diffusion approximation never applies in a system with relativistic flow speeds, analytic treatments of relativistic shocks are extremely difficult and the approximate solutions which result are unwieldy (see Kirk, 1988, for a review of relativistic shock acceleration work). Once the relativistic transformations are included, however, the Monte-Carlo simulation treats relativistic and nonrelativistic shocks identically and, in fact, we see no qualitative difference in our results when shock speeds become relativistic. Test particle results (e.g., Kirk and Schneider, 1987b) do show that relativistic shocks tend to produce flatter spectra (see

Figure 6.7) than nonrelativistic ones and this implies that the nonlinear effects we have discussed will be even more important. But the nature of the shock structure and particle spectra are essentially the same and do not depend on relativistic kinematics. In

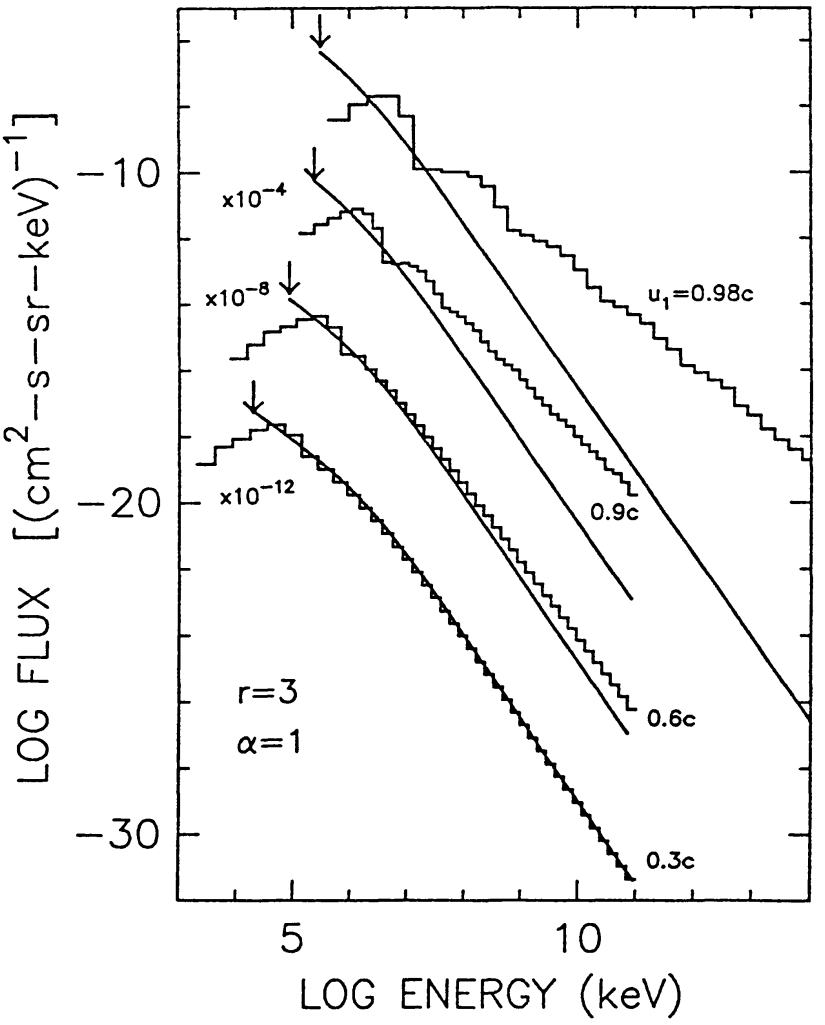

Fig. 6.7. Accelerated particle spectra for various shock velocities all with $r = 3$ and $\alpha = 1$. The right-hand numbers show the shock velocities, while the left-hand numbers show the factor curves have been displaced for clarity. The smooth curves are the predictions of the nonrelativistic shock equation (3.20). The arrows show the energies at which particles are injected with a delta-function distribution. Figure from Ellison *et al.* (1990a).

Figure 6.8 we show steady-state spectra determined for a shock with $u_1 = 0.9c$ and an upstream temperature $T_1 = 1 \times 10^8$ K. This is fast enough so that relativistic effects are noticeable, however, the important characteristics of the spectra shown in Figure 6.8 show up in nonrelativistic shocks as well. The dot-dashed, dashed, and solid curves have $E_{max} = 10^7$, 10^8, 10^9 keV, respectively, and in each case the shock profile and compression ratio were determined iteratively as describe above. As E_{max} increases, several effects occur: (1) the overall shock compressin ratio increases from $r \simeq 3.7$ to 4.4; (2) γ_{eff} decreases from 1.49 to 1.43; (3) the fraction of incoming energy flux which escapes at E_{max} increases from 0.10 to 0.14; (4) the thermal peak shifts to lower energy;

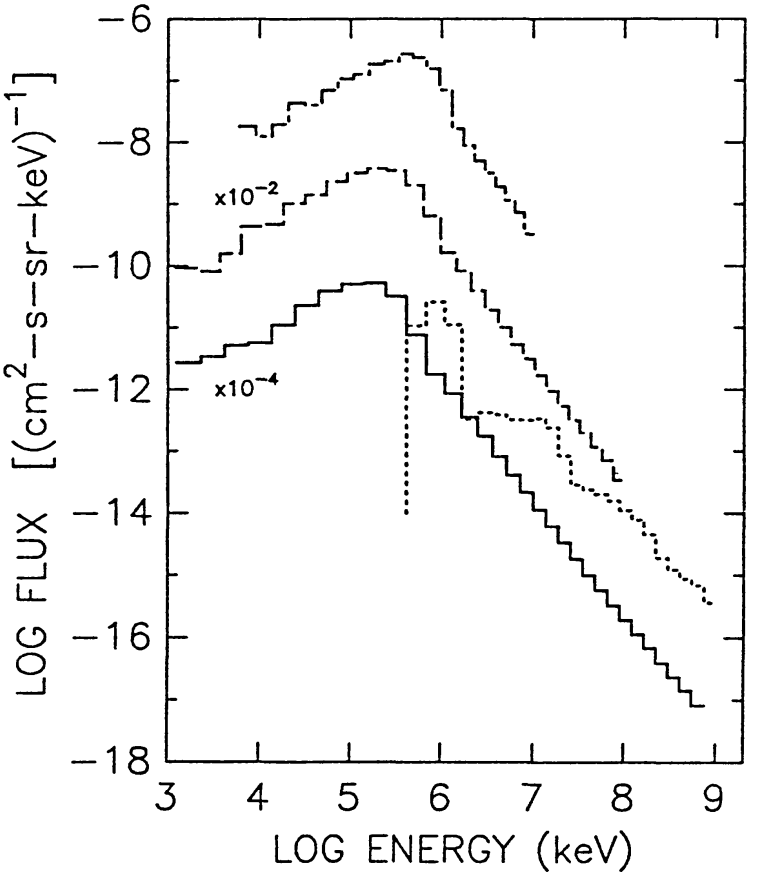

Fig. 6.8. Spectra from the Monte-Carlo simulation for shocks with a speed $u_1 = 0.9c$ and an upstream temperature $T_1 = 1 \times 10^8$ K. The dot-dashed, dashed, and solid curves show fully nonlinear results for $E_{max} = 10^7$, 10^8, and 10^9 keV, respectively. The dotted curve is the result obtained for $E_{max} = 10^9$ keV when the shock remains a discontinuity. The left-hand numbers indicate the factors curves have been displaced for clarity.

and (5) the concave spectral shape, a result of the shock being smoothed by the back pressure of the accelerated particles, while still slight, becomes more noticeable.

These effects are all related and the increase in r comes about both because the spectra with larger E_{max} have a greater fraction of the particle pressure in relativistic particles and because a greater fraction of energy flux is lost at the high-energy cutoff. All of these effects occur in nonrelativistic shocks and have been described in Ellison and Eichler (1984).

The dotted curve in Figure 6.8 shows the spectrum produced in a discontinuous shock with no smoothing (i.e., a test particle result). The test particle spectrum shows humps which result from individual shock crossings. The lowest energy hump is produced by particles having crossed the shock once, the next higher energy hump is produced by particles having made three crossing of the shock, etc. When the shock is allowed to smooth (solid curve), these humps disappear, the spectrum becomes steeper, and the energy is distributed between the thermal peak and the highest energy particles. It is clear that the test particle result does not even approximate the self-consistent calculation and shows how important nonlinear effects are.

7. Conclusions

The primary notion that has illuminated our discussion of the plasma physics of shock acceleration has been the intimate connection between the acceleration of charged particles by the shock and the plasma physics of the shock formation itself. First of all is the evidence, both theoretical and observational, that charged particle acceleration is a very common feature of plasma shocks. Second, it has become evident during recent years that the acceleration of a few of the ambient particles to superthermal energies is the method of choice, at least in supercritical shocks, for dissipating the incoming flow energy and producing the irreversible transition from the upstream state to the downstream state that is the defining characteristic of a shock. In other words, the acceleration of charged particles by a collisionless plasma shock is *not just a byproduct* of the shock but rather an essential part of the shock formation process itself.

That this should be so is not too surprising when one contemplates the fundamental difference between a collision*al* gas shock and a collision*less* plasma shock. In the former the incoming free energy is transformed from one degree of freedom, the fluid flow, *directly* into $\sim 10^{23}$ degrees of freedom via particle-particle collisions. This process is rapid enough for the particles to distribute the energy evenly (i.e., thermally) among themselves and hence a thermal particle distribution results. In a collisionless plasma this process is not possible; rather the incoming free energy is transformed via collective plasma processes into a small number (i.e., $\ll 10^{23}$) of modes whose effective temperature is immense. The particles in turn try to come into equilibrium with these collective modes but are convected out of the process before equilibrium can be achieved. This situation, as has been known since Fermi (1949) first proposed his acceleration mechanism, leads to power-law particle spectra.

Unlike a collisional gas shock there *is* communication from the downstream side of a shock to the upstream side. The diffusion scale of even slightly energized particles (those that have crossed the shock only one time) is long enough for a significant fraction of them to 'leak' back upstream and be carried through the shock again*. The primary implication of this fact is that *shock acceleration does not need 'seed' ions*. The evidence for this comes from studies of the Earth's bow shock and from Monte-Carlo simulations, as has been described in Section 6.5. The belief that energetic seed ions were required for shock acceleration to work arose from years of working with theories that employed the diffusion-convection equation or the individual particle approach. The real need for such particles was the need for a particle population whose distribution function would remain approximately isotropic in *either* the upstream or downstream flow frame so that the diffusion approximation or the probability of return argument could be employed. This was, of course, a requirement of the theoretical approximation not of the physics.

* A distinction in detail can be made between upstream particles which convect into a quasi-parallel shock and 'reflect' off the large amplitude turbulence in the shock layer and return upstream, and particles which spend some time downstream before 'leaking' back upstream. However, we believe that plasma simulations show that these processes occur together and for all purposes relevant to acceleration, are indistinguishable.

In some sense this finding might have been predicted from the fact that particle acceleration and shocks are so often found together in astrophysics (see Section 1.1). Shocks are observed (or expected) on scales from the size of comets to the bow shocks around galaxies moving through the intergalactic medium, and wherever shocks appear, energetic particles are also observed or inferred. While one must obviously be cautious about the logic of this argument, it does imply that shocks are 'self-sufficient' accelerators that do not require independent sources of seed particles.

The second primary notion of this paper is that the first-order Fermi process that is the 'engine' of shock acceleration is quite efficient, i.e., $\gtrsim 10\%$ of the incoming energy flux can routinely be converted into energetic particles. Because of this efficiency, the effects of the accelerated particles on the shock itself are too important to be ignored and *nonlinear models are necessary*. These nonlinear effects include the smoothing of the shock due to the diffusion of accelerated particle pressure upstream, the increasing of the overall compression of the shock because of the change of the equation of state of the gas as more particles escape or become relativistic, and the production of magnetic turbulence by the accelerated particles.

Two-fluid hydrodynamic models were quite useful in first showing some of the consequences of these feedback effects. However, there is some question as to how real some of the 'efficient' solutions of these nonlinear equations are. It is clear that shocks with no upstream energetic 'seed' particles must regulate themselves by the injection process whereby they transfer some of their thermal particle population to the relativistic particle population. The two-fluid models do not attempt to model this process. Furthermore, we have seen that if the particle diffusion coefficient increases with energy, as we know it must, then in high Mach number shocks the energetic particle spectrum *must* have an upper energy cutoff either from particle escape in finite shocks or from limited acceleration in time-dependent shocks. Even models, such as two-fluid ones, which do not calculate a spectrum explicitly, are subject to this physical requirement and it would appear that models that do not deal with the particle spectrum directly suffer from a handicap. They are probably not going to tell us much more about the details of shock structure and particle acceleration unless some way can be found to include the energy variation of the diffusion coefficient and cutoffs in the particle spectra in a meaningful way. Numerical solutions of two-fluid models have made progress in this direction, but have yet to include injection self-consistently. It should come as no surprise that we believe that computer simulations and Monte-Carlo methods, in particular, have much to offer in this direction.

One of the most embarrassing aspects of shock acceleration theory concerns our lack of knowledge of how (or whether) electrons are accelerated at quasi-parallel shocks. The primary difficulty is the lack of known mechanisms for scattering and compressing low-energy electrons near the shock until they obtain energies where their rigidity is comparable to that of the ions. Simulation of electron energization is difficult, as was discussed in Section 6.1, because of the widely differing time scales involved in treating ions and electrons simultaneously. Even the phenomenological approach of Monte-Carlo simulations has difficulties because so little is understood about the diffusive

behavior of electrons in random magnetic fields. Furthermore, the cross shock potential discussed in Section 5.1 will probably play a much more important role in electron acceleration than it does in ion acceleration.

An understanding of how electrons are accelerated is essential if we are to fully interpret observations since it is (presumably) the radiation from energetic electrons that is most often observed from astrophysical sources. Much effort needs to be directed towards improving our understanding of how thermal electrons interact with quasi-parallel shocks and future space missions could play a vital role in this. We need improved sensitivity for detecting low-energy electrons to determine whether or not quasi-parallel shocks in the heliosphere do accelerate electrons directly from the ambient plasma. Such observations (or even lower limits) will directly influence modeling of SNRs and other sources, as well as guide theoretical efforts.

Another area that requires study is how charge symmetric plasma shocks would differ from their normal plasma counterparts. As we saw in Section 5.1, an electron-positron plasma would probably not exhibit a cross shock potential or out of the coplanarity plane component of the magnetic field. Since all of the dissipation would be of the 'electron conductivity' type, the distinction between sub- and supercritical shocks might not exist and reflection from the shock of some of the particles to start the acceleration process might be inhibited. Such shocks are of considerable interest because the termination shock of a pulsar wind should be of this type (see Arons *et al.*, 1990, for preliminary simulation work on perpendicular electron-positron shocks).

Our Monte-Carlo studies of nonlinear shock acceleration have thus far been concerned wholly with parallel shocks. Such studies must be extended to oblique shocks if questions concerning the relative importance of acceleration in quasi-parallel versus quasi-perpendicular shocks are to be resolved. In addition to the additional dimensions involved, these extensions will be difficult because processes such as resonant scattering, shock drift energization, and shock front reflection must be modeled without becoming bogged down with the high-speed time scale on which these processes take place. The rewards will be worth the effort, however, because an understanding of the tradeoffs between acceleration rate versus the fraction of ambient particles accelerated as the angle between the shock normal and the magnetic field varies, is essential if we are to achieve a global picture of particle acceleration in supernova remnants and interplanetary shocks. This is a must if we are to resolve the constant yet elusive connection between supernovae and the cosmic rays that pervade our and other galaxies.

Much has been learned about the plasma physics of shocks and shock acceleration; a reasonably clear picture is emerging showing that the two phenomena are most likely two sides of the same coin. Yet it is clear that we must know much more before we can say that we 'know all we need to know' about this ubiquitous and important astrophysical process.

Acknowledgements

The authors wish to thank M. Baring, P. Cargill, R. Decker, D. Eichler, C. McKee, and S. Reynolds for helpful comments and A. Ford for his help in gathering reference material. Partial support for this work came from NASA grants NAG 5–1042, NAG 5–1131, and NAGW 2001 and NSF grant AST-88–17567.

References

Achterberg, A., Blandford, R. D., and Periwal, V.: 1984, *Astron. Astrophys.* **132**, 97.
Armstrong, T. P. and Decker, R. B.: 1979, *Particle Acceleration Mechanisms in Astrophysics*, AIP Conf. Proc. No. 56, p. 101.
Armstrong, T. P., Pesses, M. E., and Decker, R. B.: 1985, in B. T. Tsurutani and R. G. Stone (eds.), *Collisionless Shocks in the Heliosphere: Reviews of Current Research*, AGU Monograph Vol. 35, AGU, Washington, D.C., p. 271.
Arons, J., Gallant, Y. A., Hoshino, M., Langdon, A. B., Max, C. E.: 1990, in 'The Magnetospheric Structure and Emission Mechanisms of Radio Pulsars', *IAU Colloq.* **128** (in press).
Auer, R. D. and Völk, H. J.: 1973, *Astrohys. Space Sci.* **22**, 243.
Axford, W. I.: 1981, *Proc. 17th Int. Cosmic Ray Conf., Paris* **12**, 155.
Axford, W. I., Lear, E., and Skadron, G.: 1977, *Proc. 15th Int. Cosmic Ray Conf., Plovdiv* **11**, 132.
Bagenal, F., Belcher, J. W., Sittler, E. C., and Lepping, R. P.: 1987, *J. Geophys. Res.* **92**, 8603.
Baring, M. G. and Kirk, J. G.: 1991, *Astron. Astrophys.* **241**, 329.
Begelman, M. C., Blandford, R. D., and Rees, M. J.: 1984, *Rev. Mod. Phys.* **56**, 255.
Bell, A. R.: 1978a, *Monthly Notices Roy. Astron. Soc.* **182**, 147.
Bell, A. R.: 1978b, *Monthly Notices Roy. Astron. Soc.* **182**, 443.
Bell, A. R.: 1987, *Monthly Notices Roy. Astron. Soc.* **225**, 615.
Berezhko, E. G. and Krymsky, G. F.: 1988, *Soviet Phys. Usp.* **31**, 27.
Berezhko, E. G., Krymsky, G. F., and Turpanov, A. A.: 1990, *Proc. 21th Int. Cosmic Ray Conf., Adelaide* **4**, 101.
Berezhko, E. G., Yelshin, V. K., Krymsky, G. F., and Turpanov, A. A.: 1987, *Proc. 20th Int. Cosmic Ray Conf., Moscow* **2**, 175.
Bhat, C. L., Issa, M. R., Mayer, C. J., Wolfendale, A. W., and Zan, M.: 1986, *J. Phys. G: Nucl. Phys.* **12**, 1067.
Biermann, P. L. and Strittmatter, P. A.: 1987, *Astrophys. J.* **322**, 643.
Blandford, R. D.: 1980, *Astrophys. J.* **238**, 410.
Blandford, R. D. and Eichler, D.: 1987, *Phys. Reports* **154**, 1.
Blandford, R. D. and McKee, C. F.: 1977, *Monthly Notices Roy. Astron. Soc.* **180**, 343.
Blandford, R. D. and Ostriker, J. P.: 1978, *Astrophys. J.* **221**, L29.
Boyd, T. J. M. and Sanderson, J. J.: 1969, *Plasma Dynamics*, Barnes and Noble, New York.
Burgess, D.: 1986, *Adv. Space Res.* **6**, 63.
Burgess, D.: 1987a, *Proc. Int. Conf. on Collisionless Shocks,* Omikk-Techoinform, Balatonfüred, Hungary, p. 89.
Burgess, D.: 1987b, *J. Geophys. Res.* **92**, 1119.
Burgess, D.: 1989a, *Geophys. Res. Letters* **16**, 163.
Burgess, D.: 1989b, *Geophys. Res. Letters* **16**, 345.
Burton, M. E., Smith, E. J., Bame, S. J., and Gosling, J. T.: 1988, *EOS* **69**, 465.
Cairns, R. A.: 1986, *J. Geophys. Res.* **91**, 7134.
Cane, H. V. and Reames, D. V.: 1988, *Astrophys. J.* **325**, 895.
Cane, H. V., Reames, D. V., and von Rosenvinge, T. T.: 1988, *J. Geophys. Res.* **93**, 9555.
Cane, H. V., von Rosenvinge, T. T., and McGuire, R. E.: 1990, *J. Geophys. Res.* **95**, 6575.
Cargill, P. J.: 1990, *Adv. Space Res.* (in press).
Cargill, P. J. and Papadopoulos, K.: 1988, *Astrophys. J.* **329**, L29.
Cassiday, G. L., Cooper, R., Dawson, B. R., Elbert, J. W., Fick, B. E., Green, K. D., Ko, S., Liebing, D. F., Loh, E. C., Salamon, M. H., Smith, J. D., Sokolsky, P., Sommers, P., and Thomas, S. B.: 1989, *Phys. Rev. Letters* **62**, 383.

Cesarsky, C. J., Rothenflug, R., and Cassé, M.: 1981, *Proc. 17th Int. Cosmic Ray Conf., Paris* **2**, 269.
Chanmugam, G. and Brecher, K.: 1985, *Nature* **313**, 767.
Chupp, E. L.: 1990, *Science* **250**, 229.
Clark, D. H. and Caswell, F. L.: 1976, *Monthly Notices Roy. Astron. Soc.* **174**, 267.
Colgate, S. A. and Johnson, M. H.: 1960, *Phys. Rev. Letters* **5**, 235.
Darwin, C.: 1949, *Nature* **164**, 1112.
Decker, R. B.: 1988, *Space Sci. Rev.* **48**, 195.
Decker, R. B. and Vlahos, L.: 1985, *J. Geophys. Res.* **90**, 47.
Decker, R. B. and Vlahos, L.: 1986a, *Astrophys. J.* **306**, 710.
Decker, R. B. and Vlahos, L.: 1986b, *J. Geophys. Res.* **91**, 13 349.
deHoffmann, F. and Teller, E.: 1950, *Phys. Rev.* **80**, 692.
Dorfi, E. A.: 1984, *Adv. Space Res.* **4**, 205.
Dorfi, E. A.: 1985, *Proc. 19th Int. Cosmic Ray Conf., La Jolla* **3**, 115.
Dorfi, E. A. and Drury, L. O'C.: 1985, *Proc. 19th Int. Cosmic Ray Conf., La Jolla* **3**, 121.
Drury, L. O'C.: 1983, *Report Prog. Phys.* **46**, 973.
Drury, L. O'C. and Falle, S. A. E. G.: 1986, *Monthly Notices Roy. Astron. Soc.* **223**, 353.
Drury, L. O'C. and Völk, H. J.: 1981, *Astrophys. J.* **248**, 344.
Drury, L. O'C., Axford, W. I., and Summers, D.: 1982, *Monthly Notices Roy. Astron. Soc.* **198**, 833.
Drury, L. O'C., Markiewicz, W. J., and Völk, H. J.: 1989, *Astron. Astrophys.* **225**, 179.
Edmiston, J. P., Kennel, C. F., and Eichler, D.: 1982, *Geophys. Res. Letters* **9**, 531.
Eichler, D.: 1979, *Astrophys. J.* **229**, 419.
Eichler, D.: 1981, *Astrophys. J.* **244**, 711.
Eichler, D.: 1984, *Astrophys. J.* **277**, 429.
Eichler, D.: 1985, *Astrophys. J.* **294**, 40.
Eichler, D. and Vestrand, W. T.: 1985, *Nature* **318**, 345.
Ellison, D. C.: 1981a, *Geophys. Res. Letters* **8**, 991.
Ellison, D. C.: 1981b, Ph.D. Thesis, The Catholic University of America.
Ellison, D. C.: 1985, *J. Geophys. Res.* **90**, 29.
Ellison, D. C. and Eichler, D.: 1984, *Astrophys. J.* **286**, 691.
Ellison, D. C. and Eichler, D.: 1985, *Phys. Rev. Letters* **55**, 2735.
Ellison, D. C. and Möbius, E.: 1987, *Astrophys. J.* **318**, 474.
Ellison, D. C. and Ramaty, R.: 1985, *Astrophys. J.* **298**, 400.
Ellison, D. C., Jones, F. C., and Eichler, D.: 1981, *J. Geophys.* **50**, 110.
Ellison, D. C., Jones, F. C., and Reynolds, S. P.: 1990a, *Astrophys. J.* **360**, 702.
Ellison, D. C., Möbius, E., and Paschmann, G.: 1990b, *Astrophys. J.* **352**, 376.
Falle, S. A. E. G. and Giddings, J. R.: 1987, *Monthly Notices Roy. Astron. Soc.* **225**, 399.
Fermi, E.: 1949, *Phys. Rev. Letters* **75**, 1169.
Fermi, E.: 1954, *Astrophys. J.* **119**, 1.
Ferraro, V. C. A. and Plumpton, C.: 1966, *An Introduction to Magneto-Fluid Mechanics*, Clarendon Press, Oxford, p. 96.
Fisk, L. A.: 1971, *J. Geophys. Res.* **76**, 1662.
Fisk, L. A. and Lee, M. A.: 1980, *Astrophys. J.* **237**, 620.
Forman, M. A.: 1981, *Proc. 17th Int. Cosmic Ray Conf., Paris* **3**, 467.
Forman, M. A. and Webb, G. M.: 1985, in R. G. Stone and B. T. Tsurutani (eds.), *Collisionless Shocks in the Heliosphere: A Tutorial Review,* AGU Monograph, Vol. 34, AGU, Washington, D.C., p. 91.
Forman, M. A., Jokipii, J. R., and Owens, A. J.: 1974, *Astrophys. J.* **192**, 535.
Forman, M. A., Ramaty, R., and Zweibel, E. G.: 1986, *Physics of the Sun,* Vol. II, D. Reidel Publ. Co., Dordrecht, Holland.
Forslund, D. W.: 1985, *Space Sci. Rev.* **42**, 3.
Friedman, M. A., Russell, C. T., and Gosling, J. T.: 1989, *EOS* **70**, 423.
Friedman, M. A., Russell, C. T., Gosling, J. T., and Thomsen, M. F.: 1990, *J. Geophys. Res.* **95**, 2441.
Fuselier, S. A., Gosling, J. T., and Thomsen, M. F.: 1986, *J. Geophys. Res.* **91**, 4163.
Fuselier, S. A., Klumpar, D. M., and Shelley, E. G.: 1991, *J. Geophys. Res.* **96** 47.
Gaisser, T. K., Harding, A. K., and Stanev, T.: 1987, *Nature* **329**, 314.
Galeev, A. A. and Sagdeev, R. Z.: 1970, *Soviet Phys. JETP* **30**, 571 (English translation).

Golden, K. I., Linson, L. M., and Mani, S. A.: 1973, *Phys. Fluids* **16**, 2319.
Gombosi, T. I., Lorencz, K., and Jokipii, J. R.: 1989, *J. Geophys. Res.* **94**, 15011.
Goodrich, C. C.: 1945, in B. T. Tsurutani and R. G. Stone (eds.), *Collisionless Shocks in the Heliosphere: Reviews of Current Research,* AGU Monograph, Vol. 35, AGU, Washington, D.C., p. 153.
Goodrich, C. C. and Scudder, J. D.: 1984, *J. Geophys. Res.* **89**, 6654.
Goodrich, C. C. and Scudder, J. D.: 1986, *J. Geophys. Res.* **91**, 7135.
Gosling, J. T., Asbridge, J. R., Bame, S. J., Paschmann, G., and Sckopke, N.: 1978, *Geophys. Res. Letters* **5**, 957.
Gosling, J. T., Asbridge, J. R., Bame, S. J., Feldman, W. C., Zwickl, R. D., Paschmann, G., Sckopke, N., and Hynds, R. J.: 1981, *J. Geophys. Res.* **86**, 547.
Gosling, J. T., Thomsen, M. F., and Winske, D.: 1988, *J. Geophys. Res.* **93**, 2735.
Gosling, J. T., Thomsen, M. F., Bame, S. J., and Russell, C. T.: 1989, *J. Geophys. Res.* **94**, 10027.
Green, D. A.: 1984, *Monthly Notices Roy. Astron. Soc.* **209**, 44.
Greenstadt, E. W.: 1985, in B. T. Tsurutani and R. G. Stone (eds.), *Collisionless Shocks in the Heliosphere: Reviews of Current Research,* AGU Monograph, Vol. 35, AGU, Washington, D.C., p. 169.
Harding, A. K. and Gaisser, T. K.: 1990, *Astrophys. J.* **358**, 561.
Heavens, A. F.: 1983, *Monthly Notices Roy. Astron. Soc.* **204**, 699.
Heavens, A. F.: 1984, *Monthly Notices Roy. Astron. Soc.* **210**, 813.
Heavens, A. F. and Drury, L. O'C.: 1988, *Monthly Notices Roy. Astron. Soc.* **235**, 997.
Hillas, A. M.: 1984a, *Nature* **312**, 50.
Hillas, A. M.: 1984b, *Ann. Rev. Astron. Astrophys.* **22**, 425.
Hillas, A. M. and Johnson, P. A.: 1990, *Proc. 21th Int. Cosmic Ray Conf., Adelaide* **4**, 19.
Hoyle, F.: 1960, *Monthly Notices Roy. Astron. Soc.* **120**, 338.
Hua, X.-M., Ramaty, R., and Lingenfelter, R. E.: 1989, *Astrophys. J.* **341**, 516.
Hynds, R. J., Cowley, S. W. H., Richardson, I. G., Sanderson, T. R., Tranquille, C., Wenzel, K.-P., and Daly, P. W.: 1986, *Adv. Space Res.* **5**, 17.
Ipavich, F. M., Galvin, A. B., Gloeckler, G., Scholer, M., and Hovestadt, D.: 1981, *J. Geophys. Res.* **86**, 4337.
Ipavich, F. M., Gloeckler, G., Hamilton, D. C., Kistler, L. M., and Gosling, J. T.: 1988, *Geophys. Res. Letters* **15**, 1153.
Ipavich, F. M., Gosling, J. T., and Scholer, M.: 1984, *J. Geophys. Res.* **89**, 1501.
Jokipii, J. R.: 1979, *Proc. 16th Int. Cosmic Ray Conf., Kyoto* **14**, 175.
Jokipii, J. R.: 1982, *Astrophys. J.* **255**, 716.
Jokipii, J. R.: 1987, *Astrophys. J.* **313**, 842.
Jokipii, J. R. and Kóta, J.: 1990, *Proc. 21th Int. Cosmic Ray Conf., Adelaide* **6**, 198.
Jokipii, J. R. and Morfill, G. E.: 1985, *Astrophys. J.* **290**, L1.
Jones, F. C.: 1990a, *Astrophys. J.* **361**, 162.
Jones, F. C.: 1990b, in 'The Interstellar Disk-Halo Connection in Galaxies', *Proc. IAU Symp.* **144** (in press).
Jones, F. C. and Ellison, D. C.: 1987, *J. Geophys. Res.* **92**, 11205.
Kóta, J.: 1979, *Proc. 16th Int. Cosmic Ray Conf., Kyoto* **3**, 13.
Kan, J. R. and Swift, D. W.: 1983, *J. Geophys. Res.* **88**, 6919.
Kang, H. and Jones, T. W.: 1990, *Astrophys. J.* **353**, 149.
Kang, H. and Jones, T. W.: 1991, *Monthly Notices Roy. Astron. Soc.* (submitted).
Kantrowitz, A. R. and Petschek, H. E.: 1966, in W. B. Kunkel (ed.), *Plasma Physics in Theory and Applications*, McGraw-Hill, New York, p. 148.
Kazanas, D. and Ellison, D. C.: 1986a, *Astrophys. J.* **304**, 178.
Kazanas, D. and Ellison, D. C.: 1986b, *Nature* **319**, 380.
Kennel, C. F.: 1988, *J. Geophys. Res.* **93**, 8545.
Kennel, C. F. and Coroniti, F. V.: 1984, *Astrophys. J.* **283**, 694.
Kennel, C. F. and Petschek, H. E.: 1968, in R. Carovillano, J. F. McCray, and H. R. Radoski (eds.), *Physics of the Magnetosphere*, D. Reidel Publ. Co., Dordrecht, Holland, p. 485.
Kennel, C. F. and Sagdeev, R. Z.: 1967, *J. Geophys. Res.* **72**, 3303.
Kennel, C. F., Coroniti, F. V., Scarf, F. L., Livesey, W. A., Russell, C. T., Smith, E. J., Wenzel, K. P., and Scholer, M.: 1986, *J. Geophys. Res.* **91**, 11917.
Kennel, C. F., Edmiston, J. P., Scarf, F. L., Coroniti, F. V., Russell, C. T., Smith, E. J., Tsurutani, B. T., Scudder, J. D., Feldman, W. C., Anderson, R. R., Moser, F. S., and Temerin, M.: 1984, *J. Geophys. Res.* **89**, 5436.

Kirk, J. G.: 1988, Thesis for Dr. rer. nat. habil., Ludwig-Maximillians-Universität, München.
Kirk, J. G. and Heavens, A. F.: 1989, *Monthly Notices Roy. Astron. Soc.* **239**, 995.
Kirk, J. G. and Heavens, A. F.: 1990, *Proc. 21th Int. Cosmic Ray Conf., Adelaide* **4**, 93.
Kirk, J. G. and Schneider, P.: 1987a, *Astrophys. J.* **315**, 425.
Kirk, J. G. and Schneider, P.: 1987b, *Astrophys. J.* **322**, 256.
Kirk, J. G. and Schneider, P.: 1989, *Astron. Astrophys.* **217**, 344.
Krauss-Varban, D., Burgess, D., and Wu, C. S.: 1989, *J. Geophys. Res.* **94**, 15089.
Krymsky, G. F.: 1977, *Dokl. Akad. Nauk SSSR* **243**, 1306.
Krymsky, G. F.: 1981, *Izv. Akad. Nauk SSSR, Ser. Fiz.* **45**, 461 (in Russian).
Lagage, P. O. and Cesarsky, C. J.: 1983, *Astron. Astrophys.* **125**, 249.
Lee, M. A.: 1982, *J. Geophys. Res.* **87**, 5063.
Lee, M. A.: 1983, *J. Geophys. Res.* **88**, 6109.
Lee, M. A. and Ryan, J. M.: 1986, *Astrophys. J.* **303**, 829.
Lee, M. A., Skadron, G., and Fisk, L. A.: 1981, *Geophys. Res. Letters* **8**, 401.
Leroy, M. M.: 1984, *Adv. Space Res.* **4**, 231.
Leroy, M. M. and Winske, D.: 1983, *Ann. Geophys.* **1**, 527.
Leroy, M. M., Winske, D., Goodricht, C. C., Wu, C. S., and Papadopoulos, K.: 1982, *J. Geophys. Res.* **87**, 5081.
Lloyd-Evans, J., Coy, R. N., Lambert, A., Lapikens, J., Patel, M., Reid, R. J. O., and Watson, A. A.: 1983, *Nature* **305**, 784.
Lockwood, J. A., Debrunner, H., and Flückliger, E. O.: 1990a, *J. Geophys. Res.* **95**, 4187.
Lockwood, J. A., Debrunner, H., Flückliger, E. O., and Grädel, H.: 1990b, *Astrophys. J.* **355**, 287.
Lyu, L. H. and Kan, J. R.: 1990, *Geophys. Res. Letters* **17**, 1041.
Mandt, M. E. and Kan, J. R.: 1985, *J. Geophys. Res.* **90**, 115.
Mandt, M. E. and Kan, J. R.: 1988, *Geophys. Res. Letters* **15**, 1157.
Mandt, M. E. and Kan, J. R.: 1990, *J. Geophys. Res.* **95**, 6353.
Mandt, M. E., Kan, J. R., and Russell, C. T.: 1986, *J. Geophys. Res.* **91**, 8981.
Markiewicz, W. J., Drury, L. O'C., and Völk, H. J.: 1990, *Astron. Astrophys.* **236**, 487.
McKenzie, J. H. and Völk, H. J.: 1982, *Astron. Astrophys.* **116**, 191.
McKenzie, J. H. and Webb, G. M.: 1984, *J. Plasma Phys.* **31**, 275.
Mészáros, P. and Ostriker, J. P.: 1983, *Astrophys. J.* **273**, L59.
Miller, J. A. and Ramaty, R.: 1989, *Astrophys. J.* **344**, 973.
Möbius, E., Hovestadt, D., Klecker, B., Scholer, M., Ipavich, F. M., Carlson, C. W., and Lin, R. P.: 1986, *Geophys. Res. Letters* **13**, 1372.
Möbius, E., Scholer, M., Sckopke, N., Lühr, H., Paschmann, G., and Hovestadt, D.: 1987, *Geophys. Res. Letters* **14**, 681.
Ness, N. F., Scearce, C. S., and Seek, J. B.: 1964, *J. Geophys. Res.* **69**, 3531.
Ohsawa, Y. and Sakai, J.: 1987, *Astrophys. J.* **313**, 440.
Omidi, N. and Winske, D.: 1988, *Geophys. Res. Letters* **15**, 1303.
Omidi, N. and Winske, D.: 1990, *J. Geophys. Res.* **92**, 2281.
Onsager, T. G. and Thomsen, M. F.: 1991, *Rev. Geophys.* (submitted).
Onsager, T. G., Thomsen, M. F., Gosling, J. T., and Bame, S. J.: 1990, *J. Geophys. Res.* **95**, 2261.
Ostrowski, M.: 1988, *Monthly Notices Roy. Astron. Soc.* **233**, 257.
Papadopoulos, K.: 1988, *Astrophys. Space Sci.* **144**, 535.
Papadopoulos, K., Wagner, C. E., and Haber, I.: 1971, *Phys. Rev. Letters* **27**, 982.
Parker, E. N.: 1958a, *Phys. Rev.* **109**, 1328.
Parker, E. N.: 1958b, *Phys. Rev.* **110**, 1445.
Parker, E. N.: 1961, *J. Nucl. Energy* **2**, Part C, 146.
Paschmann, G., Sckopke, N., Asbridge, J. R., Bame, S. J., and Gosling, J. T.: 1980, *J. Geophys. Res.* **85**, 4689.
Paschmann, G., Sckopke, N., Papamastorakis, I., Asbridge, J. R., Bame, S. J., and Gosling, J. T.: 1981, *J. Geophys. Res.* **86**, 4355.
Peacock, J. A.: 1981, *Monthly Notices Roy. Astron. Soc.* **196**, 135.
Pesses, M. E.: 1979, *Particle Acceleration Mechanisms in Astrophysics*, AIP Conf. Proc. No. 56, p. 107.
Pesses, M. E., Jokipii, J. R., and Eichler, D.: 1981, *Astrophys. J.* **246**, L85.

Quest, K. B.: 1985, in B. T. Tsurutani and R. G. Stone (eds.), *Collisionless Shocks in the Heliosphere: Reviews of Current Research*, AGU Monograph, Vol. 35, AGU, Washington, D. C., p. 185.
Quest, K. B.: 1988, *J. Geophys. Res.* **93**, 9649.
Reames, D. V.: 1990, *Astrophys. J.* **358**, L63.
Rees, M. J. and Gunn, J. E.: 1974, *Monthly Notices Roy. Astron. Soc.* **167**, 1.
Reinhard, R., van Hes, P., Sanderson, T. R., Wenzel, K.-P., Smith, E. J., and Tsurutani, B. T.: 1983, *Proc. 18th Int. Cosmic Ray Conf., Bangalore* **3**, 160.
Reynolds, S. P.: 1988, in G. L. Verschuur and K. I. Kellerman (eds.), *Galactic and Extragalactic Radio Astronomy*, Springer-Verlag, New York, p. 439.
Samorski, M. and Stamm, W.: 1983, *Astrophys. J.* **268**, L17.
Sanderson, T. R., Reinhard, R., and Wenzel, K.-P.: 1983, *Proc. 18th Int. Cosmic Ray Conf., Bangalore* **3**, 156.
Schatzman, E.: 1963, *Ann. Astrophys.* **26**, 234.
Schneider, P. and Kirk, J. G.: 1987, *Astrophys. J.* **323**, L87.
Scholer, M.: 1985, in B. T. Tsurutani and R. G. Stone (eds.), *Collisionless Shocks in the Heliosphere: Reviews of Current Research*, AGU Monograph, Vol. 35, AGU, Washington, D.C., p. 287.
Scholer, M.: 1990, *Geophys. Res. Letters* **17**, 1821.
Scholer, M. and Terasawa, T.: 1990, *Geophys. Res. Letters* **17**, 119.
Scholer, M., Ipavich, F. M., Gloeckler, G., and Hovestadt, D.: 1980, *J. Geophys. Res.* **85**, 4602.
Scholer, M., Ipavich, F. M., Gloeckler, G., Hovestadt, D., and Klecker, B.: 1981, *J. Geophys. Res.* **86**, 1299.
Scudder, J. D., Burlaga, L. F., and Greenstadt, E. W.: 1984, *J. Geophys. Res.* **89**, 7545.
Shapiro, M. M.: 1990, *Proc. 21st Int. Cosmic Ray Conf., Adelaide* **4**, 8.
Sibeck, D. G., McEntire, R. W., Lui, A. T. Y., Krimigis, S. M., Zanetti, L. J., and Potemra, T. A.: 1987, *Geophys. Res. Letters* **14**, 1011.
Skilling, J.: 1975a, *Monthly Notices Roy. Astron. Soc.* **172**, 557.
Skilling, J.: 1975b, *Monthly Notices Roy. Astron. Soc.* **173**, 245.
Skilling, J.: 1975c, *Monthly Notices Roy. Astron. Soc.* **173**, 255.
Sonett, C. P. and Abrams, I. J.: 1963, *J. Geophys. Res.* **68**, 1233.
Sonnerup, B. U. O.: 1969, *J. Geophys. Res.* **74**, 1301.
Tan, L. C., Mason, G. M., Gloeckler, G., and Ipavich, F. M.: 1989, *J. Geophys. Res.* **94**, 6554.
Tan, L. C., Mason, G. M., Gloeckler, G., and Ipavich, F. M.: 1990, *Proc. 21st Int. Cosmic Ray Conf., Adelaide* **5**, 297.
Thomas, V. A.: 1989, *J. Geophys. Res.* **94**, 12009.
Thomas, V. A. and Brecht, S. H.: 1986, *Phys. Fluids* **29**, 2444.
Thomas, V. A. and Winske, D.: 1990, *Geophys. Res. Letters* **17**, 1247.
Thomas, V. A., Winske, D., and Omidi, N.: 1990, *J. Geophys. Res.* **95**, 18809.
Tidman, D. A. and Krall, N. A.: 1971, *Shock Waves in Collisionless Plasmas*, John Wiley and Sons, New York.
Toptyghin, I. N.: 1980, *Space Sci. Rev.* **26**, 157.
Tranquille, C., Richardson, I. G., Cowley, S. W. H., Sanderson, T. R., Wenzel, K.-P., and Hynds, R. J.: 1986, *Adv. Space Res.* **6**, 235.
Völk, H. J.: 1984, in Tran Than Van (ed.), *High Energy Astrophysics, Proc. 19th Rencontre de Moriond*, Editions Frontières, Gif-sur-Yvette, p. 281.
Völk, H. J.: 1987, *Proc. 20th Int. Cosmic Ray Conf., Moscow* **7**, 157.
Völk, H. J., Drury, L. O'C., and McKenzie, J. F.: 1984, *Astron. Astrophys.* **130**, 19.
Webb, G. M.: 1987, *Astrophys. J.* **319**, 215.
Wentzel, D. G.: 1968, *Astrophys. J.* **152**, 987.
Wentzel, D. G.: 1974, *Ann. Rev. Astron. Astrophys.* **12**, 71.
Winske, D.: 1985, *Space Sci. Rev.* **42**, 53.
Winske, D. and Leroy, M. M.: 1984, *J. Geophys. Res.* **89**, 2673.
Winske, D. and Quest, K. B.: 1988, *J. Geophys. Res.* **93**, 9681.
Winske, D., Omidi, N., Quest, K. B., and Thomas, V. A.: 1990, *J. Geophys. Res.* **95**, 18821.
Witzel, A., Schalinski, C. J., Johnston, K. J., Biermann, P. L., Krichbaum, T. P., Hummel, C. A., and Eckart, A.: 1988, *Astron. Astrophys.* **206**, 245.
Zachary, A.: 1987, 'Resonant Alfvén Wave Instabilities Driven by Streaming Fast Particles', Ph.D. thesis, Lawrence Livermore National Laboratory, University of California.
Zank, G. P.: 1989, *Astron. Astrophys.* **225**, 37.

Zank, G. P., Axford, W. I., and McKenzie, J. F.: 1990, *Astron. Astrophys.* **233**, 275.
Zank, G. P. and McKenzie, J. F.: 1985, *Proc. 19th Int. Cosmic Ray Conf., La Jolla* **3**, 111.
Zank, G. P. and McKenzie, J. F.: 1987, *J. Plasma Phys.* **37**, 347.
Zdziarski, A. A.: 1986, *Astrophys. J.* **305**, 45.